AUGUST 2019 M.Sc. in Mechanical Engineering ABUZER AÇIKGÖZ

REPUBLIC OF TURKEY

GAZİANTEP UNIVERSITY

GRADUATE SCHOOL OF NATURAL & APPLIED SCIENCES

BENDING STRESS ANALYSIS AND FATIGUE LIFE ESTIMATION OF INVOLUTE SPUR GEARS BY FINITE ELEMENT METHOD (FEM)

M.Sc. THESIS

IN

MECHANICAL ENGINEERING

BY

ABUZER AÇIKGÖZ

AUGUST 2019

BENDING STRESS ANALYSIS AND FATIGUE LIFE ESTIMATION OF INVOLUTE SPUR GEARS BY FINITE ELEMENT METHOD (FEM)

M.Sc. Thesis

in

Mechanical Engineering

Gaziantep University

Supervisor

Asst. Prof. Dr. Abdullah AKPOLAT

by

Abuzer AÇIKGÖZ

August 2019

REPUBLIC OF TURKEY
GAZİANTEP UNIVERSITY
GRADUATE SCHOOL OF NATURAL & APPLIED SCIENCES
MECHANICAL ENGINEERING

Name of the Thesis : Bending Stress Analysis and Fatigue Life Estimation of Involute Spur Gears by Finite Element Method (FEM)

Name of the Student : Abuzer AÇIKGÖZ

Exam Date : 19.08.2019

Approval of the Graduate School of Natural and Applied Sciences

Prof. Dr. A. Necmeddin YAZICI
Director

I certify that this thesis satisfies all the requirements as a thesis for the degree of Master of Science.

Prof. Dr. Mustafa GÜNAL
Head of Department

This is to certify that we have read this thesis and that in our consensus opinion it is fully adequate, in scope and quality, as a thesis for the degree of Master of Science.

Asst. Prof. Dr. Abdullah AKPOLAT
Supervisor

Examining Committee Members:	Signature
Assoc. Prof. Dr. Bülent AKTAŞ	....
Assoc. Prof. Dr. Ahmet ERKLİĞ	....
Asst. Prof. Dr. Abdullah AKPOLAT	....

I hereby declare that all information in this document has been obtained and presented in accordance with academic rules and ethical conduct. I also declare that, as required by these rules and conduct, I have fully cited and referenced all materials that are not original to this work.

Abuzer AÇIKGÖZ

ABSTRACT

BENDING STRESS ANALYSIS AND FATIGUE LIFE ESTIMATION OF INVOLUTE SPUR GEARS BY FINITE ELEMENT METHOD (FEM)

AÇIKGÖZ, Abuzer
M.Sc. in Mechanical Engineering
Supervisor: Asst. Prof. Dr. Abdullah AKPOLAT
August 2019
91 pages

The aim of this study is to perform fatigue analysis of spur gears depending on bending strength by using finite element method under static conditions. The change of stresses at the bottom of the tooth is an important parameter affecting the life of the gear. Several studies have been carried out for different gear types in relation to the bending of the gears in recent years. These studies are carried out with the analytical, experimental and finite element methods by using different parameters of the gears. Advanced computer technologies have provided significant convenience to designers and manufacturers in the analysis of machine elements such as gears which can affect many parameters. Assumptions and uncertainties in analytical methods, cost and time loss of experimental methods increase the importance of computer aided analysis. Computer aided finite element analysis with new developments gives very close results to the experimental studies. In this study, firstly, tooth root bending stress have been analysed under the parameters such as various load, rim thickness, teeth numbers, pressure angle, and module then compared with the ISO 6336-3:2006 (E) standards analytical calculations for same gear models. The effect of the parameters on number of cycle was investigated and fatigue strength of gears were analysed.

Key Words: Spur Gears, Bending Stress, FEM, Gear Bending Fatigue Strength.

ÖZET

EVOLVENT DÜZ DİŞLİ ÇARKLARDA SONLU ELEMANLAR METODUNU KULLANARAK EĞME GERİLMESİ ANALİZİ VE YORULMA ÖMRÜ TAHMİNİ

AÇIKGÖZ, Abuzer
Yüksek Lisans Tezi, Makine Mühendisliği
Tez Yöneticisi: Dr. Öğr. Üyesi Abdullah AKPOLAT
Ağustos 2019
91 sayfa

Bu çalışmanın amacı, düz dişlilerin statik koşullar altında eğilmeye bağlı yorulma analizini sonlu elemanlar yöntemi kullanarak gerçekleştirmektir. Dişli kök bölgelerinde oluşan gerilmeler dişlilerin ömrünü etkileyen önemli bir parametredir. Son yıllarda farklı dişli tiplerinin diş kökü gerilme davranışları ile ilgili birçok çalışma yapılmıştır. Yapılan bu çalışmalarda gerilme analizleri için analitik, deneysel ve sonlu elemanlar yöntemi kullanılarak farklı parametrelerin etkisi incelenmiştir. Günümüzde gelişmiş bilgisayar teknolojileri, birçok parametreden etkilenen dişliler gibi makine elemanlarının analizinde tasarımcılara ve üreticilere büyük kolaylık sağlamıştır. Analitik yöntemlerde kullanılan varsayımlar ve belirsizlikler, deneysel yöntemlerin oldukça maliyet ve zaman gerektirmesi, bilgisayar destekli analizin önemini arttırmaktadır. Bilgisayar destekli sonlu elemanlar analiz yöntemleri son yıllarda ciddi bir gelişim göstererek deneysel çalışmalara çok yakın sonuçlar vermektedir. Bu çalışmada dişlilerin diş kökünde oluşan gerilmeleri etkileyen dişli parametrelerini optimize ederek dişlilerin kullanım ömrünün arttırılması öngörüldü. Burada dişli kökünde gerilmeleri etkileyen; kuvvet, dişli cidar kalınlığı, diş sayısı, basınç acısı, modül, diş üstü yüksekliği, diş dibi kavisi yarıçapı ve diş genişliği gibi parametrelerin etkisi incelenmiştir ve elde edilen sonuçlar ISO 6336-3:2006 (E) standardında belirtilen hesaplama yöntemi ile elde edilen sonuçlar ile karşılaştırılmıştır. Daha sonra dişli geometrisinde etkili olan parametrelerin eğilmeye bağlı yorulma da cevrim sayılarına olan etkisi incelenmiştir.

Anahtar Kelimeler: Düz Dişliler, Eğilme Gerilmesi, SEY, Dişli Eğilme Yorulma Mukavemeti.

- To the two closest persons who encouraged me to reach what I am in now (My parents).

- To the person who was the cause of fulfilling this research (My dearest wife).

- To all those who contributed in fulfilling this research (My professors, brothers and friends).

ACKNOWLEDGEMENTS

I am pleased and honored to thank my supervisor, the example in knowledge and ethics, Assist. Prof. Dr. Abdullah AKPOLAT and I owe to him most sincerely respect and gratitude for all his help, support, patience and understanding.

I would like to present all the thanks, respect and honest good wishes to whom provided cooperation despite their tasks, dear Research Assist. Mr. Burak ŞAHİN, Research Assist. Mr. Gökhan DEMİRCAN and research assistants in Harran University Mechanical Engineering Department.

To the spirit of any beautiful meaning and the reason of every success whom all the words of thanks and love subsided before them, deepest heartfelt gratitude for my honorable Father (Şaban) and Mother (Beyhan).

Lovely thanks to the persons whom my life has no meaning without, my sisters and brothers. Warm thanks to who gave special regard, during my work especially my sweet son Abdullah and my wife Ayşe. I say thank you, to my friends, relatives, and my special friend who used all ways to support me.

TABLE OF CONTENTS

Page

LIST OF TABLES

LIST OF FIGURES

Page

LIST OF SYMBOLS

FEA	Finite Element Analysis
FEM	Finite Element Method
AGMA	American Gear Manufacturers Association
ISO	International Organization for Standardization
3D	Three Dimensions
2D	Two Dimensions
BEM	Boundary Element Method
a	Addendum
b	Dedendum
c	Clearance
F	Face width of a tooth
t	Circular thickness
m	Module
p_c	Circular pitch
P	Diametrical pitch
N	Number of teeth
d	Pitch diameter
h_t	Total depth
h_w	Working depth
ϕ	Pressure angle
w	Wear rate
H	Material hardness
σ	Contact normal stress
W^t	Transmitted tangential load
K_o	Overload factor
K_v	Dynamic factor
K_s	Size factor
K_H	Load distribution factor
E	Modulus of elasticity

Z_I	Geometry factor
m_N	Load sharing ratio
m_r	Gear ratio
N_P	Teeth number of pinion
N_G	Teeth number of gear
R	Pitch radius
ν	Poisson's ratio
w	Angular velocity
K_f	Friction factor
μ	Coefficient of friction
V_s	Sliding velocity
r_p	Pitch radii
r_b	Base radii

CHAPTER 1

INTRODUCTION

1.1 General Introduction

The transmission movement and power between machine elements or mechanical units are of great importance in engineering. For this purpose, various power transmission systems have been developed. In particular, systems such as belt-pulley mechanisms, chain-pulley mechanisms, gear systems and friction wheels appear as transmission elements that transmit power and movement between machines; they can also control the value of power, direction and speed. The power and motion transmission elements mentioned here have been used since ancient times. Power transmission elements have undergone many changes until today, especially after the industrial revolution. A variety of designs have emerged with the need for different power transmission systems. In this respect, the history of humankind has placed great importance on transmitting power and movement in order to do things more easily and efficiently. Very early times, gears made of wood and stone with primitive methods were used in fields such as agricultural activities and mills. In later stages, gear systems were also used to transfer water from rivers. Gear mechanisms, which are very important among power transmission elements, have undergone many changes in the historical process. Among the first examples of gear mechanisms and those used in today, there have been great improvements in size, efficiency, precision, functionality and many other features. It is almost impossible to come across an area where gears are not used today. Gears are used wide range from household appliances, automobiles to aircraft transmission elements. The reason why gear wheel mechanisms are preferred to friction mechanisms is that they have moment-free transmission and a more compact design. Modeling and simulation of physical behavior of gear wheels under various conditions has been the subject of numerous researches. There are many crucial properties designing a gear for a system in order to perform their function properly.

Initially conducted with simple strength models, these investigations continue with numerical methods with advances in computer technology. Numerical methods are preferred in solving complex geometry problems where analytical solution is difficult. Finite element method (FEM), boundary element method (BEM) and complex potential method are used in the analysis of gear wheels. The finite element method was developed in the 1950s for stress analysis of complex structures in aircraft-space technology. Nowadays, Finite element method (FEM) used from biomechanics to nuclear technology is widely utilized in many disciplines and different types of problems.

Rapidly growing industrial developments require precision, light, long-lasting and durable gears for the systems. The highest efficiency of the gears in the fields of use is a product of the work that lasts for years. The sole purpose of all these studies is to transmit energy with minimum loss and to keep the efficiency at the highest possible level. Particularly in aviation and transportation applications, there are great demands for light and efficient equipment [1]. In order to achieve this goal, the designer must understand the failure mechanism of the machine elements. The major factors limiting the gear life during torque transmission are surface wear due to friction and stresses on the gear stem due to bending. The amount of power lost in all gear directly affects machine failures and is also a major problem. The gear can fail in many different ways and there is no earlier indication until the total failure occurs, except for the rise noise stage and vibration. These undesirable factors are manifested in gear systems as in other machine elements and cause serious financial losses.

The gears are subjected to very different loading conditions depending on application areas. Particularly under variable loading conditions, gear materials must exhibit high elastic behavior and be very rigid. Depending on application areas, there are gears made of different materials such as plastic and metal. When designing a gear for industrial use, variables such as strength under static and dynamic loading, softness or hardness of movement, availability of equipment for thread cutting, lubrication capability, temperature and heat dissipation and service life must be taken into consideration. The production of spur gears for large loaded powertrain systems requires powerful and precise analysis methods that provide information on the magnitude of both contact and bending stresses that can be applied as quickly as possible. It is the top priority of the designers that these analysis methods should give fast and realistic results. In recent years, the finite element method is sufficient for designers to provide this information, but the creation of these geometries is quite complex and long in analysis programs. Therefore, computer-aided drawing programs are used to create geometries faster. Today, SOLIDWORKS, CATIA, Pro Engineer and many other programs are used for this purpose. In addition to commercially used programs, it is used in many homemade programs directed towards a specific purpose.

While analyzing this situation, the commands followed in ANSYS and the procedures and steps followed in the analysis will be discussed in detail in the fourth section. The graphs and tables obtained as a result of the latest analyzes were examined and the appropriateness of the selected input parameters, their effects on the gear geometry, the stress and fatigue life of the gear were interpreted and the most appropriate parameters were determined from the selected values.

1.2 Background

The gears are highly sensitive to changes in stresses acting on them during operation. Fatigue failures are the most common type of failure due to the cyclic loading nature of the gears. There are two types: contact fatigue caused by friction of gear surfaces and fatigue formed at the bottom due to bending. In particular, it is possible to minimize fatigue damage at the bottom of the tooth and extend the life of the gear with new approaches. According to reliable statistics, breaks represent approximately 60% of all gear damage. They are classified as:

- The teeth root fatigue fractures, representing almost 33% of all gear damages,
- Teeth root fractures because of overloads, representing about 20% of all gear damages,
- Tooth tip corner fracture, formed by improper assembly or operation, represents about 5%,
- Other breakages are mostly gear rim failures, rarely hub or spoke fractures, represents about 2% of all of the gear damages. [3]

Active tooth flank damage constitutes approximately 40% of all gear damages. These types of damage are categorized as:

- Pitting – 14% periodicity of occurrence among all of the gear damage,
- Wear and scuffing – 20% frequency of case,
- Plastic deformation – 6% frequency of incident,
- Micro-pitting. [3]

All these types of failures are described with more details in next chapters.

1.3 Research Objective

In the literature review section, studies carried out by many researchers were included. Many articles and thesis studies on this subject have been conducted. These studies mostly focused on gear bending stresses. Researchers focused on the different type of gear model bending stress analysis including a variety of gear parameters. It is very rare in literature bending fatigue analysis of spur gears conduct by finite element method. The main objective of this study is fatigue analysis based on gear parameters of spur gears.

Those who design gears are constantly surprised that some gears run better and outlast would be expected from the design formulas, while others prematurely fail even when they are operated within the design limits of the transmitted load. Gear designers need to be able to examine the various causes of gear wear and failure. New gear designs must be based on both textbook logic and experience if the perfect job is to be done. [4]

It is very important to do the proper analysis while studying gear wear and failure. The cause of failure is often quite different from the quantity of transmitted load. An incorrect analysis can lead a designer to produce a new gearset bigger than it should to be, and yet the new set may still fail because the real cause of trouble is remaining uncorrected. [4]

The main target of this study is to detect the estimated life of gear due to bending fatigue for different type of spur gears. Bending fatigue analysis of spur gears was investigated by using the finite element method. Analyses of spur gears were achieved by changing some parameters of the gear such as force, rim thickness, number of teeth, pressure angle, module, addendum, tool tip radius, profile shift face width, and gear ratio.

1.4 Organization of the Thesis

This thesis includes six chapters, which present the bending fatigue analysis of the spur gears under different parameters.

Chapter 1 shows detailed information along with a general introduction, background and the research objectives. At the end, organization of the thesis are briefly described.

Chapter 2 is a literature review on related studies performed.

Chapter 3 indicates concise information about gear design, gear types, basic gear nomenclature, gear manufacturing methods and fail classification in the gears. And it covers the basic methods which are used to predict bending fatigue failures.

Chapter 4 consists detailed information about the methodology of bending fatigue analysis of spur gear with the finite element for different parameters as follows;

1- Forces
2- Rim thickness
3- Teeth Number
4- Pressure angle
5- Module
6- Addendum
7- Tool tip radius coefficient
8- Face width

Chapter 5 presents the results of the FE analysis of bending fatigue of spur gears with different parameters. It shows the optimum design according to results collected.

Chapter 6 provides an overview and discuss the results and it also provides a set of recommendations for future work

CHAPTER 2

LITERATURE SURVEY

2.1 Introduction

In previous studies on gears, improvements in power and motion transmission have been achieved by using different analysis methods. Especially by changing the gear parameters, the best gear combinations have been tried to be revealed. These combinations were analyzed by using different methods. As a result of these studies, researchers have developed many new gear models used in the industry. Researchers especially use theoretical, numerical and experimental methods in studies. Time and cost are important parameters in analysis methods. The cost and time differences in analysis methods have recently led researchers to use the finite element method instead of analytical and experimental methods

2.2 Literature Review

The literature overview based on bending fatigue of gear, analysis methods and theoretical technique is presented below:

2.2.1 Literature Based on Analytical Calculation of Bending Fatigue

Fernandez, P. J. L. [5] worked on bending fatigue errors with real case studies and revealed that such fatigue would be practice. The structure of the cracks due to bending was summarized under headings. 1) Fatigue fractures occur at the bottom of the tooth on the active side. 2) Breaks occur at the midpoint of the tooth end at normal loading, and at the point of maximum stress in case of misalignment. 3) The fracture path is L-shaped and moves from the passive side of the tooth towards the bottom, where fracture occurs. 4) Cracked tooth breaks due to instant load discharges caused by a few more teeth break.

Rey, G. G. [6] gave an effective procedure, formulas and information to estimate the value of the expected fatigue life in the case of a steel cylindrical gear with high cycles. Load capacity of cylindrical gears was calculated according to AGMA 2105-D04 standard. Based on this study, stress cycle factors were considered as the strength life properties of gear materials. It also used the factors Z_n and Y_n to set the required number of processes and fatigue limit stresses. The process was determined by considering the pitting resistance and bending resistance of the spur and helical gears. The results here indicated the amount of cycle that the gears could operate safely, and therefore the estimated life values were given.

Kramberger, J. et al. [7] examined the fatigue life of the thin rim gears in the truck gearbox; both crack initiation and crack propagation were evaluated together. Fatigue analyzes of gears were performed on different surface quality and different rim thickness. The number of cycles corresponding to the first fatigue damage was determined. Then the rim thickness of the tooth crack propagation path and remaining life calculations were made. According to the results, the value of critical rim thickness was determined as 1.5*m. Rim thickness of a gear was bigger than 1.5*m, the estimated crack would spread neither through the tooth nor through the rim of the gear. It was concluded that these gear applications make vehicles safer. This recommended model allows you to determine the entire service life under given service times, appropriate fatigue material parameters, and predicted crack growth path.

Fadhil, B. M. [8] investigated the effects of pressure angle at different rim thicknesses on crack initiation and propagation path. In this study, finite element method was used to simulate the initiation and progression of the crack formed at the bottom of the gear. The stress concentration factor was calculated and used to determine the direction of crack propagation and the fatigue life was calculated. The results of this study were compared with previous experimental studies where 3 different pressure angles and three different rim thickness values were used. FRANC2D and ABAQUS were used to simulate the effects of these variables. Fatigue life was calculated with simplified Paris equation. The results showed that gear pressure angle had significant effects on fatigue life depending on rim thickness.

Zhang, X. et al. [9] analyzed the fatigue crack growth in gears with ANSYS and FRANC3D finite element codes, numerical simulation was applied and related fatigue tests were performed. During simulation, the location of the maximum stress induced by external forces was determined by the ANSYS software, and the results obtained were then imported into FRANC3D to analyze crack propagation. The results analyzed were used into the finite element analysis program to find the stress and stress intensity factor. As a result of the researches, crack mode I was dominant during crack growth and it was found that the crack length increased with the increase in the stress intensity factor.

Podrug, S. et al. [10] was established a numerical model to predict the growth of fatigue crack in the tooth root of the gear. In this model, the effect of changing the position of the applied force and the size of the gear was investigated during the operation of a real gear. The stress cycle at the toothed root was made more realistic in this way. The effect of rim thickness on the crack propagation at the bottom of gears was analyzed. In numerical calculations, the crack closure effect was also regarded, and the idea of partial crack closure revealed an analytical version for crack closure due to plasticity. The model was significantly different from some previously published simplified models. This model was used to determine fatigue crack growth in a real gear made of carbide and milled steel 14CiNiMo13-4, where the required material parameters were previously determined by appropriate test specimens. The results of the analysis in this work showed significant differences in loading conditions, prediction of the crack propagation life and the crack path in a tooth root.

Zhou, C. et al. [11] presented a work related to analytical solutions to calculate bending and contact strength for spiral bevel gears that were verified by ISO gear standard and finite element method. The bending strength was calculated depending on Lewis cantilever beam approximation, utilizing the modified normal force and the friction component. The modified normal force was derived at the highest point of single tooth contact (HPSTC) in the conventional equivalent gear. The bending stress in the analytical solution was 14.67% bigger than calculated one according to ISO 10,300–1 2001 gear standard as friction coefficient reached 0.20. Both theoretical and FEM analysis showed that friction had an important effect on load capacity of the gears, and it exerted stronger influence on the bending strength. The developed analytical solution could be well applied to the determination of load capacity of spiral bevel gears, especially under harsh working conditions or in the demand for higher performance.

Hotait, M. A., & Kahraman, [12] found a method for calculating bending fatigue life of hypoid gears. This method was used in a previously developed finite element-based stress analysis model formed at the root of hypoid gear. In this study, face-milled and face-hobbed hypoid gears were used to create multi-axis stress time history in root fillet regions. In this study, comparison was made with uniaxial fatigue models in order to reveal the necessity of multi-axis fatigue models. The model was performed with a sample milled hypoid gear set from an industrial application to demonstrate its effect on key cutting tool parameters on various misalignments as well as the resulting tooth bending lifetime. At the end, the multiaxial version was used to analyze the effect of misalignments and the blade side radius at the teeth bending fatigue lifetime of hypoid gears. Each one indicated a significant impact at the sturdiness of the example hypoid gear.

Kumar, P. et al. [13] proposed a work to predict fatigue failure (contact and bending) initiation on spur gear with respect to American Gear manufacturing Association (AGMA) design methods. The particular bending and contact fatigue initiation of spur gear tooth profile was investigated by using AGMA equations. Their particular result showed that bending fatigue life of through hardened gear was better compared to case hardened gear. The highest chance of contact/bending fatigue failure occured in single tooth contact area and the contact fatigue life was less than bending fatigue life.

2.2.2 Literature Based on the Experimental Analysis of Bending Fatigue

Handschuh, R. F. et al. [14] were conducted a series of experimental studies to determine the bending fatigue behavior of AISI 9310 steel gears. Stresses in the fillet region of the gears were determined by linear elastic finite element model. In the test procedure, single-tooth bending method was used to obtain crack initiation and propagation. This method was used in fatigue analysis of spur gears. In this method, gears were connected to the test device with the dedicated gear test fixture. The highest point of single tooth contact was selected for the load application point. In this study, the experiments were conducted ranging from 1/4 cycle to thousands of cycles. The relationship of stress and cycles for crack initiation was found to be semi logarithmic. In the case of crack propagation, the relationship between stress and cycle number was linear. It was concluded that the applied loads were directly related to crack propagation. Very high loads crack initiation and propagation times showed similar relationships. However, at low loads, the crack initiation cycle was considerably lower than the crack propagation cycle.

Gasparini, G. et al. [15] conducted a relevant study. They obtained data on the fatigue limit of four different test groups in their study. Curves obtained from these tests were analyzed together with the results obtained from Agusta-Westland experience and other sources and it was observed that they were the most appropriate one. Very high cycle results confirmed the predictions based on the previously tested data's for both fatigue limit and curve shapes. Gear test scheme and gear during test as shown Figure 2.1.

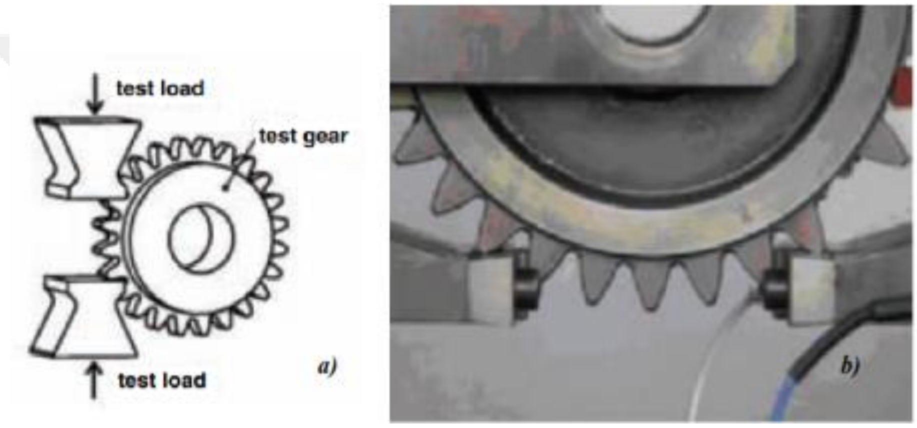

Figure 2.1 a) Test scheme without supporting the gear blank **b)** Gear specimen during test

The developed test procedure was standardized for new materials, new processes and new models. The Agusta-Westland approach was an appropriate standard for evaluating, comparing and defining test results. Edoardo, C. et al. [16] performed their experimental studies in 5 different gear test groups. Bending fatigue tests were performed in 2 different case-hardened steels and 3 different nitrided gear steels frequently used in industry. Considering the tests to be standard, all gears were produced according to the same geometric design and using the same machining technique. Single Tooth Bending Fatigue (STBF) tests were used to determine fatigue limits of the materials and S-N diagrams were created. In addition, the resistance of the gear materials under high loads was analyzed. The test specimen mounted clamping system Figure 2.2-a and gear test specimen mounted test rig Figure 2.2-b given below. The performance of case-carburized steels with the best fatigue resistance and the lowest fatigue resistance nitriting steels were very close to each other. These results were similar to previous studies. The worst fatigue capacity formed in the carburizing steel grade nitrided. However, the results did not change significantly when steel carburized with the same steel type. Contrary to what is generally accepted, S-N graphs of nitrided steels were not very different from carburized steels. Only nitride steels had better performance under very high loads.

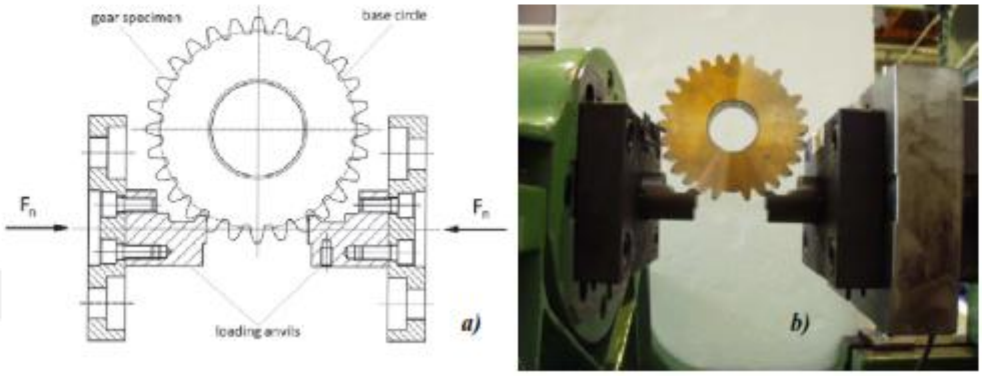

Figure 2.2 a) Gear specimen mounted on the test rig. **b)** Gear specimen mounted in the clamping system.

Gorla, C., et al. [17] conducted a bending fatigue analysis of gears. Useful data were obtained, and the results were discussed. The data obtained in this study could be used by many gear designers and it could be used in new model gearbox designs the present test fixture as seen Figure 2.3. The researchers did not obtain enough data about the contact fatigue analysis, but it was expected to be an example of comparative studies. The results of two innovative gear materials were analyzed, test results and applied heat treatments were evaluated. Jamasko steel was found to be suitable for large size applications. These applications could be used in wind turbine gearboxes. The use of these air-hardenable steels with low treatment distortion could significantly reduce costs and contribute to environmental sustainability.

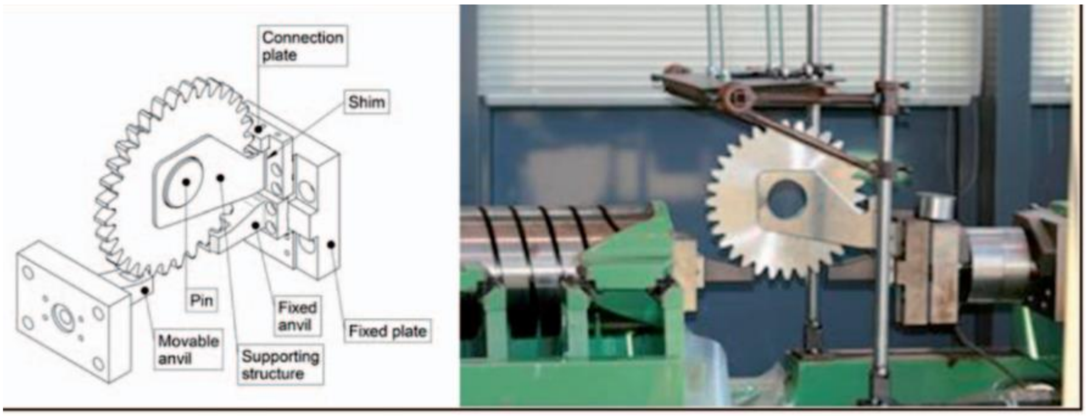

Figure 2.3 Bending fatigue test apparatus: on the left a 3D schema and part nomenclature; on the right gear mounted on the test rig

Glodez, S. et al. [18] conducted a series of experimental tests on the spur gears used in the gearboxes, the most basic requirements of the industry. The effects of different load distributions of the gears along the tooth width on the interpretation of crack growth at the root of the gears were analyzed with a suitable experimental design as shown Figure 2.4. These results were evaluated by using statistical analysis methods. When all these results were evaluated together, it was found that different load distributions along the tooth width had significant effects on crack growth and hence the service life of the gear.

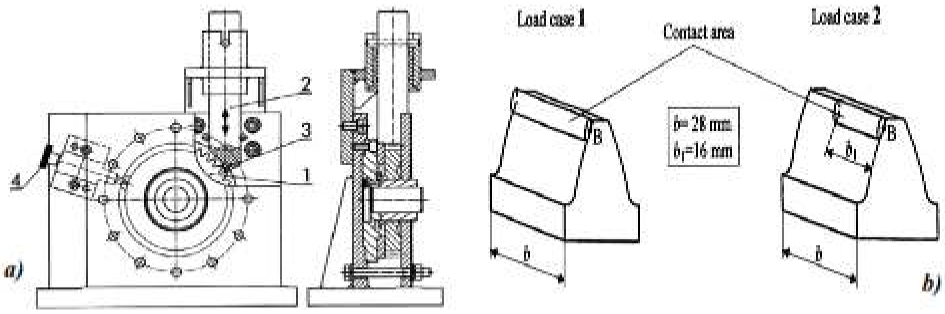

Figure 2.4 a) Gear holding device (1-gear, 2- shoe, 3-roller, 4- positioner) b) Two load cases of different load distributions along the tooth width

Since the fatigue crack progression in the tests provided a three-dimensional experimental analysis, it could be used to provide calibration for similar analyzes.

2.2.3 Literature Based on Finite Element Method

Kramberger, J. et al. [19] found a computational model to determine the bending-related service life of a real spur gear made of 42CrMo4. The fatigue life that caused the gear to break in the modeling was divided into two parts as crack initiation and crack propagation period. The number of stress cycles required for the initiation of fatigue cracking was calculated by finite element method. The crack propagation at the bottom of the gear was simulated by using a FEM method based on computer program using linear elastic fracture mechanics principles. The Paris equation was used to simulate fatigue crack growth. As a result, almost the entire service life was spent at the crack start at low stress levels close to the fatigue limit. This is a very important factor in determining the service life of gears. Because in practice, the gears often operate at loads close to the fatigue limit.

Jyothirmaia, S. et al. [20] designed helical gears and analyzed various performance criteria by using finite element method and analytical approaches. The theoretical analysis of the helical gears was evaluated according to AGMA standards. Three different helical gears; single, herringbone and crossed helical gear systems were evaluated. The results obtained from the developed FEA model showed quite similar features to the analytical approach. Crossed helical gear performance gave the best values in terms of stress at low speeds and low loads. In contrast, herringbone and single helical gear systems were used for optimum speed and load values. The low stress observed in the case of single helical gear showed that it could be used at high speeds and heavy loads.

Lewicki, D. G. et al. [21] showed that robust gear designs should be made considering the beginning of the crack as well as the path of crack advancement. Consequently, they tried to determine the effect of load on crack propagation in moving gear teeth. They made two-dimensional analysis of involute spur gear and three-dimensional analysis of spiral-bevel pinion gear using finite element and boundary element method. They compared the results of the studies with experimental results. The obtained results were confirmed by the theory developed in predicting toothed crack propagation paths based on Erdogan and Sikh criteria. Calculated stress intensity factors and mixed mode crack angle estimation techniques were used in crack simulation for two-dimensional analysis. This simulation could be used in a simple static analysis where the tooth load was placed at the highest point of the single tooth contact. Crack simulation in three-dimensional analysis could be used for a simple static analysis. The tooth load was placed at the point where the single tooth contact was highest, as long as the crack did not approach the contact area on the tooth

Vučkovića, K. et al. [22] investigated the effects of friction on the case carburized steel spur gear fatigue test on fatigue life and the location of the crack initiation zone. The crack initiation area was estimated by using the strain life approach considering the residual stress effects, surface quality and mean stress. Fatigue life inferences were made in this area. Two different load models were evaluated in these applications. In the first case, the test tooth, which represented the commonly used principle of operation, was loaded through the actuating arm. In the second case, the test tooth supported the reaction through the fixed anvil. In both cases, the loads on the tested gears were applied when they touched the highest point of the single tooth contact. This study showed that friction significantly affected tooth bending fatigue life and crack starting point. Therefore, the second load model could be proposed as an effective alternative in reducing the effect of friction on tooth bending life and eliminating the effect of friction on the location of the crack start zone.

Song, D. et al. [23] were made a study to determine the bending fatigue that occurred at the root of the gear and contact fatigue on the gear surface. 3D finite element method was used for the theoretical assembling straight bevel gear pair analysis. Fatigue failures in driving gears are most common in engineering machines. Bending fatigue failure is also one of the most important problems for driving gears for straight bevel gear pairs. The maximum bending stress took place at the load applied highest point of single tooth contact and contact fatigue stress was in the district of the pitch line for gears. Maximum bending fatigue stress and maximum contact fatigue stress increased with increasing operating torque in gears. Also driving pinion gear stress was higher than driven gear stress.

Cura, F. et al. [24] studied on thin rim thickness gears need to be designed very precisely. It should be ensured that the cracks, in the tooth root are spread out safely, otherwise devastating results may occur. The important parameters are the design geometry of the gear wheel and the starting point of the crack. For special gear geometry configurations, there are many effective parameters such as centrifugal load on the crack propagation path. This research activity was carried out by using numerical models and extended finite element method was used in addition to traditional 2D and 3D finite element models. It was thought that the stress area in the tooth root fillet and near the fracture evaluated the crack starting point and explained the direction of propagation. The results showed that the crack start point and crack propagation path were strongly influenced by the presence of centrifugal load. This impact was primarily evident in the uncertainty area of the backup ratio.

Zhang, D. et al. [25] investigated the causes of bending fatigue failures in micro straight bevel gear of a lubrication pump. Firstly, the causes of fatigue damage in gear roots were investigated. At this stage, macroscopically inspection, geometrical examination, fractography investigation and other necessary metallurgical investigations were made. In all these analyzes, failure analysis table was established on the causes of fatigue. Then finite element analysis was performed to evaluate these factors. As a result of all these investigations, it was determined that stress concentrations exceeding the critical stress level in the gear fillet region caused failure. It was concluded that the main factor that increased the stress intensity in these regions was processing errors. This naturally reduced the service life of the gears. In addition, it was seen that the excessive wear of the gears was caused by poor connection and misalignment.

Kramberger J. et al. [26] performed 3D analyzes of gears with complex geometry. The initial crack growth at the tooth root of the gear was modeled for thin rim gears. The effects of different web arrangements on fatigue life were investigated with comparison between gears in the presence and absence of web. In these analyzes, crack propagation was simulated with linear elastic fracture mechanics principles using boundary element method. The results of the simulation showed that the crack and gear edge reinforcement projected on the web spreads faster than non-reinforced gears. However, an asymmetric transmission type was more disadvantageous than the symmetric type, since it could lead to a more dangerous breaking mode. The application demonstrated that the three-dimensional numerical approach could be a very influential tool in the analysis of thin rimed gears.

Ghaffari, M. A. et al. [26] was performed 3D FEA in order to investigate both fatigue crack initiation and crack propagation in gear teeth. A linear elastic fracture mechanics approach was used to model mixed-mode fatigue crack propagation. Two different load conditions were used, the first was applied along the face width and the second was applied partially to the surface. Different fatigue crack propagation was occurred under these two different loading conditions. The main purpose of this study was to increase fatigue crack life with boron / epoxy patches. As a result, epoxy patches increased the fatigue life.

Rad, A. A. et al. [27] simulated fatigue crack propagation in helical gear root by using linear elastic fracture mechanics. Simulation was carried out to obtain crack growth and propagation path with expanded FEM. The fatigue life of the gear was calculated by using Paris equation. This method significantly reduced the modeling time compared to previous studies. Meshing step that caused ultimate bending stress in the root was pointed out by using this analysis results. A semi-elliptical crack was occurred at the area of maximum Von Mises stress at the tooth root. In the final case, the stress intensity factor reached a critical level in the gradually extended surface crack. The service life was designed with 295×104 for the gear, and the final shape of crack growth was obtained.

2.3 Summary of Literature Review

In this section, a comprehensive literature review about tooth bending stress and bending fatigue life estimations was completed. Previous studies were analyzed according to the analysis method of bending fatigue. In this analysis, the effects of gear geometry, different loading conditions, and the effects of surface quality of the gears were examined. Mostly one or two parameters were the subject of research. In recent years, with the effect of advanced computer technologies, significant increases have been observed in the studies on the finite element method. There is a close relationship between bending fatigue life and gear geometry. Especially gear geometry designs are developed to increase the service life. In order to achieve this, prominent studies aim at reducing stresses in the toothed root regions. In many studies, gear tooth root fatigue and surface fatigue are evaluated together. The aim of this study is to investigate the effect of bending fatigue on the life span of gears by changing the effective parameters of gear geometry.

CHAPTER 3

THEORY

3.1 Gear Design

The main purpose of the gear is to transfer movement from the shaft to the next. Gears can be classified differently depending on the state of the transmission type being considered, for example, a rotary or linear transmission. Four examples are most commonly used in industry (spur, helical, bevel, and worm gears).

The standard cutting tool for Gears is symmetrical when the gears are symmetrical and the cutter according to the Y-axis. The Threaded symmetry of a tooth contains the profile selection of the same pressure angles, consisting of two, e.g., $\phi_d = \phi_c$. D and C are used on the drive and coast side, respectively. If there is any inaccuracy or error in the gear, the motion is incorrectly transferred (the motion is not transmitted correctly). Also, if errors in the gears are critical, this can destroy or gradually damage parts in the gear box. In addition, if the fails in the gears are serious, this can destroy or damage parts in the gear box. So, it becomes necessary to know the subject of gear. In order for the gear to be better accepted, some information must be obtained about the gear design and the gear tooth movement system.

3.2 Gear Types

There are a wide variety of gear types, and each of them serves a variety of functions. To understand gears, it is desirable to classify more important species. The relationship of shaft axes to which the gears are mounted is one approach. Shafts may be intersecting, non-intersecting, parallel, and non-parallel as in the Table 3.1

Table 3.1 Types of gears in common use

Parallel axes	Intersecting axes	Nonintersecting and nonparallel axes
Spur external Spur internal Helical external Helical internal	Straight bevel Zerol bevel Spiral bevel Face gear	Crossed helical Single-enveloping worm Double-enveloping worm Hypoid Spiroid

3.2.1 Types of Gears that Operate on Parallel Shafts

3.2.1.1 Spur Gear

Spur gears are used to convey movement, either parallel shafts or between a shaft and rack. Spur gear teeth are radial and are evenly spaced on the outer periphery and parallel to the shaft in the process of being mounted. The touching of mating teeth of a spur gear is in a flat line parallel to a tangent plane to the pitched cylinders of the gears (pitched cylinder is thought as an imaginary cylinder in a gear rolled without sliding in a pitch cylinder or another gears' pitch plane).
One of the simplest and common types of gears is spur gear. It holds its teeth parallel to the axis of shaft and it is used to transmit power and rotational motion for parallel shafts while there is only uniform torque and speed. They have a high degree of efficiency and superior sensitivity. Involute profile allows for high production tolerances for the easiest tooth to be removed. Spur gears usually have an axially aligned contact line, and the load is classified as equal in the width of the gear to the tooth. The types of spur gears are shown in Figure 3.1.

(a) (b) (c)

Figure 3.1 Types of spur gear (a) external spur gear (b) internal spur gear (c) rack and pinion gears

3.2.1.2 Helical Gears

The purpose of use of helical gears shown in Figure 3.2. is to convey the motion between a shaft and a rack, or the motion between parallel and diagonal shafts, by interlocking the teeth that extend along a helix in a way that angles to the shaft axis. In this respect, the match of teeth event occurs in such a way that the number of two or more teeth constantly touches each other. This allows for smoother movement than the one occurring in spur gears. However, axial thrust is produced by helical gears unlike flat gears, which gives cause for an insignificant loss of power.

The gears from which the helical gears are made consist of teeth cut at an angle to the upper part and gears which make a helical angle to the axis of rotation. Helical and spur gears are used in similar areas and are used to transfer torque and motion between shafts that are parallel or cross each other . However, the helical gears tend to be softer and less noisy than spur gears, due to the gradual incorporation of the teeth in the meshing stage. Additionally, the sloping tooth implements thrust and radial loads that are not present in the spur gear. Two helical gears (herringbone gears) may be attached side by side to terminate the resulting axial thrust, to prevent axial thrust occurring in this sense.

Figure 3.2 Types of helical gear

3.2.1.3 Herringbone Gears

Double helix (Herringbone) gear wheels shown in Figure 3.3. have the same characteristics as the helical gear wheel, but because of the opposite helix, the axial forces balance each other so that no axial force occurs. If there is rifling between the right and left helix , this gear is called double helix. In herringbone gears, where there are no grooves, oil compression occurs at high speeds causing noise at the ends where the helices join. At the same time, the temperature increases at high speeds. Another benefit of the groove is that it minimizes tooth breakage due to axial load.

Figure 3.3. Herringbone gear

3.2.1.4 Internal Gears

In internal gear mechanisms, the spur gear wheel grasps the hoop gear, which is threaded to its inner side, so that both gears rotate in the same direction. In internal gear mechanisms, since two concave and convex surfaces are in contact with each other, it is better for them to lean against each other than the convex wheel mechanisms. Therefore, the surface pressure is lower, the strength is higher, the grip rate is greater. They can form like spur and helical teeth. Planetary mechanisms, elastic couplings, brake drums are the various areas in which these gears are used. Figure 3.4. also shows the internal gear.

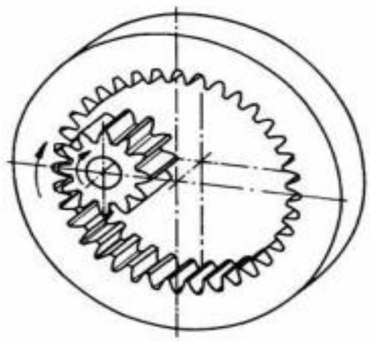

Figure 3.4 Internal gear.

3.2.2 Types of Gears that Operate on Intersecting Shafts

3.2.2.1 Bevel Gears

Conical gears are used where power and motion transmission must be transmitted in a 90º angle. They have two tapers that roll without sliding over each other during rotation. Although the intersection angle may be $\delta < 90°$, $\delta = 90°$, $\delta > 90°$, in practice the most common case is δ=90. Conical gears are produced in two ways, straight and helically. If the teeth pass through the center of the gear, they are called straight bevel gear, and if the teeth are not straight, they are called helical bevel gear.

3.2.2.1.1 Straight Bevel Gears

Such gears are similar to spur gears in that there is linear contact between the teeth. The thickness of the tooth is greater at the base of the taper than at the top of the taper. The suppression force is formed from the top of the taper downwards under load. The shaft angle is usually 90 º. Bevel gears are more commonly used at low speeds. At high speeds, dynamic forces increase and the grip rate decreases. Figure 3.5. also shows bevel gears.

Figure 3.5 Straigth bevel gears

3.2.2.1.2 Spiral Bevel Gears

The gear pair is a gear that can be used at higher speeds than straight bevel gears, which can work properly as other gears come into contact. One advantage over straight bevel gears is that it operates more quietly. Different types of helical curves can be used for such gears. Spiral bevel gears are also capable of carrying more load than their counterparts. Spiral bevel gears are generally preferred over straight bevel gears when speeds are greater than 300 m/min (1000 sfm) and especially for very small gears. If speeds are higher than 300 m/min (1000 sfm) and especially if very small gears are to be used, spiral bevel gears are generally preferred to straigth conical gears. Spiral bevel gear is shown in Figure 3.6.

Figure 3.6 Spiral bevel gears

3.2.2.1.3 Zero Bevel Gears

The zero bevel gears are gears with a zero spiral angle and are curvedtooth. Since their teeth are not oblique, they have a different structure than spiral bevel gears. They are preferred in areas where Spiral bevel gears are used and have a slightly greater tooth strength than the straigth one.

3.2.2.2 Face Gears

The face gears are so named because the top of the gear cuts the teeth. They are not normally retained as bevel gears but are more similar than other species when thought of as functional. Spur pinion and face gear are both mounted on shafts that intersect with 90° angle. Pinion bearings mostly carry radial load, while Gear bearings have both print and radial payload. Pinion bearings often transport radial load, but gear bearings can transport both thrust and radial load. The terminology is shown in Figure 3.7. The pinion can be made of helix, but it is usually made of spur which goes with a face gear.

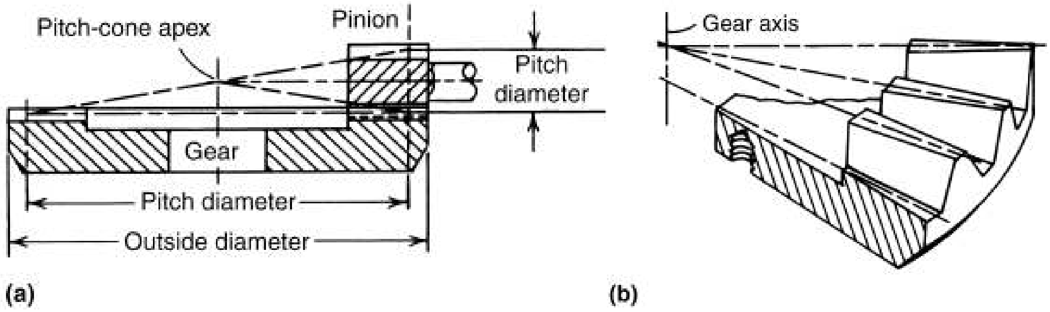

Figure 3.7 Face gear terminology. (a) Cross-sectional view showing gear and pinion positions. (b) Relationship of gear teeth to gear axis

3.2.3 Gears that Operate on Nonparallel and Nonintersecting Shafts

3.2.3.1 Worm Gears

Worm gears are a special case of bevel gears that transmit motion between the opposite shafts with a cross-angle of 90° between them. The contact between the teeth is not spotless, since they are linear, they can transport larger loads than bevel gears and provide greater cycle proportions. It consists of a threaded wheel that is rotated by a single or multi-mouth screw. In general, they are noiseless and non-pulsing mechanisms that can transmit very large power compared to their volume. Operating yields range from 40-90%. As the cycle rate of the mechanism increases, its yields decrease. The direction of rotation of the worm gear teeth also depends on left or right hand cutting. In general worm gearing is more effective when the gear ratio of the two shafts is high. Basically, higher speeds are needed to achieve better efficiency in worm gears. Figure 3.8. also shows the worm mechanism.

Figure 3.8 Worm gears

3.2.3.2 Crossed-Helical Gears

Crossed-helical gears have members that are cylindrical and also called non-enveloping worm gears. There is a movement between mating teeth. This is called wedging effect and it causes slipping on tooth flanks. These gears, which have a low carrying capacity, are used where the shafts need to turn angled at each other.

3.2.3.3 Hypoid Gears

Hypoid gears generally resemble spiral bevel gears. An important difference is that the pinion axis of the hypoid gear pair is slightly away from the gear axis. But it has a significant difference, which is that the pinion axis of the hypoid gear pair is slightly away from the gear axis. This feature is quite advantageous for many designs. Hypoid gears work smoother and quieter than spiral bevel gears where they work and are slightly stronger.

3.2.3.4 Spiroid Gears

Spiroid gears resembles a worm and are from a tapered pinion , and a gear element with a facial gear whose teeth are tilted longitudinally. It has a curved helical angle in its teeth but is not a true helical helical spiral. High gear ratio in compact arrangements, low cost when mass-produced and good load carrying capacity make these gears attractive among researchers.

3.3 Basic Gear Nomenclature

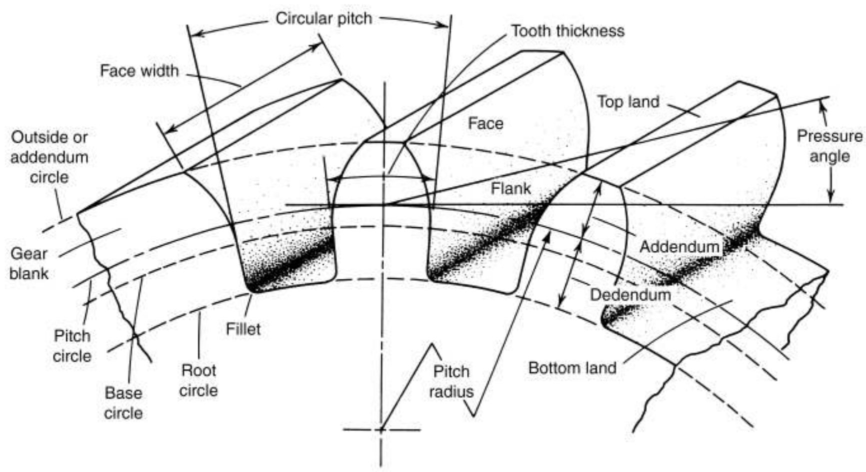

Figure 3.9 Gear terminology

Basic gear nomenclature as given Figure 3.9 explained.

Main gear: gear with a greater number of teeth in a gear pair.

Pinion gear: gear with a smaller number of teeth in a gear pair.

Base Diameter (Dp, Dg): It is the diameter in which the working gear pair transmits force and motion to each other. All gear calculations are based on this diameter.

Center Distance (C): the distance between the main gear center and the pinion gear center.

Base circle: The diameter at which the involute curve forming the tooth profile begins. This diameter is less than a certain number of teeth, while the number of teeth is greater than the diameter of the bottom of the tooth.

Involute: The curve that forms the tooth profile.

Root circle: The circle that passes through the bottom teeth.

Circular pitch: The environmental pitch measured through circle.

Addendum: The radial distance between pitch circle and the addendum circle.

Dedendum: The radial distance between the pitch circle and the root circle.

Whole depth: The summation of addendum and dedendum.

Working depth: The sum of the addendum of one tooth and the addendum of the other tooth in the tooth pair.

Clearance: The gap between the top of one tooth and the bottom of the tooth in the gear pair.

Backlash: The space behind when the tooth touches to the other in the socket.

Circular pitch: The distance that sees the peripheral pitch.

Tooth thickness: Peripheral tooth thickness.

Module: The value of the pitch diameter divided by the number of teeth.

Diametral pitch: The value used in the American Association of Gear Manufacturers (AGMA) standards and used instead of the module parameter in metric system.

Pitch point: The point at which the teeth transfer motion to each other on the pitch diameter.

Pressure angle: The angle between the tangent and the line of motion drawn from the point where the circles touch each other.

Face of a tooth: The length of the tooth surface area outside the pitch surface.

As it is explained main gear parameters above also in Figure 3.10 indicates the gear pair working parameters.

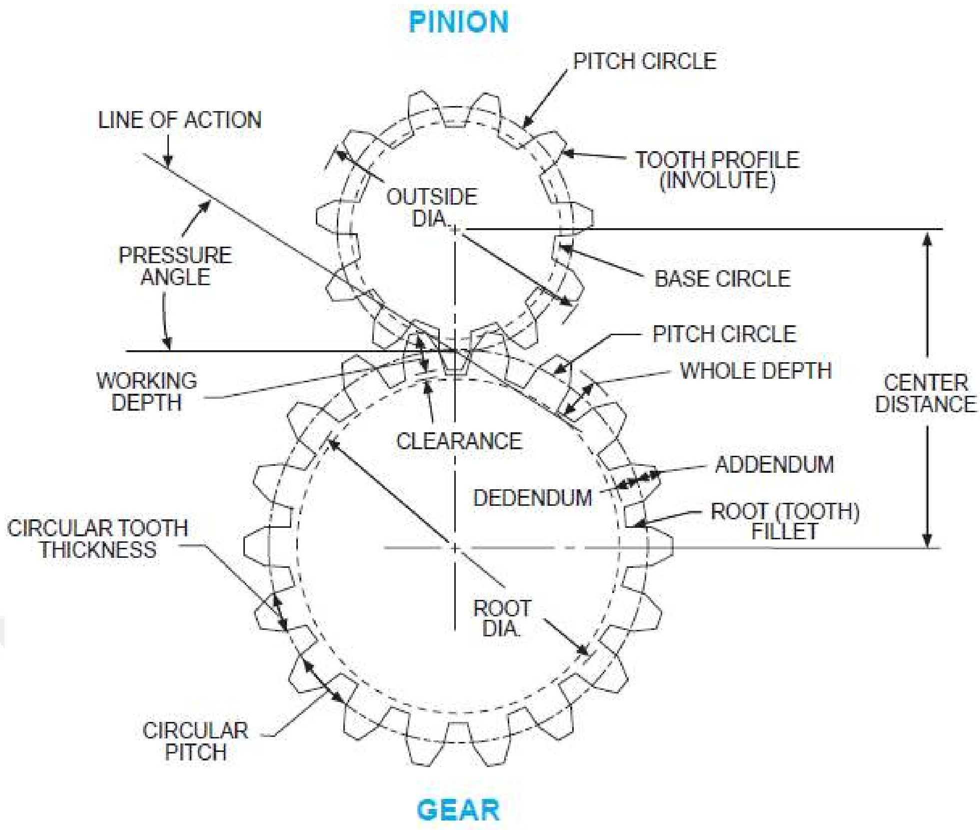

Figure 3.10. Gear and pinion terminology

3.4 Types of Failures in Gear Tooth

Gears can fail for very different reasons. Various loads and frictional heating of the gears working in contact with each other result in various failures. And this leads to an increase in noise and vibrations, resulting in reduced performance. Each type of failure that occurs in the gears leaves characteristic clues in the gear teeth, and if these clues are examined in detail it is possible to reveal the cause of the failure.

3.4.1 Classification of Gear Failure Modes

Failure analysts have categorized gear failures in different ways. Various gear modes are classified by the American gear Manufacturers Association (AGMA) under wide range of categories of wear, scuffing, contact fatigue, cracking, bending fatigue, fracture, and plastic deformation[29].

Errichello [30] examined gear failures by splitting them into two broad groups as seen Table 3.2:

• Lubrication-related failures

• Nonlubrication-related failures

In general, the gears malfunction after the tooth stress overcomes the confidence limit. When a failure occurs, the cost of replacement or rehabilitation as well as the cost lost during the downtime of the system in which the machines stop is quite high. Therefore, the different types of problems that may occur in the gear should be analyzed very well. Not all engineering areas are needed to successfully design the gears. Gear design is a synthesis process in which gear geometry, materials, heat treatment, production methods, and lubrication are chosen to meet the requirements of an application. For gear design; materials, gear geometry, production methods and heat treatment should be selected properly. And the designer should design the gear set with wear resistance, sufficient power and scuffing resistance.

Table 3.2 Types of failures [31]

Nonlubrication-related failures	
Overload	**Bending Fatigue**
Brittle fracture	Low cycle fatigue (≤1000 cycle to failure
Ductile fracture	High cycle fatigue (≥1000 cycle to fatigue
Plastic deformation	
Cold flow	
Hot flow	
Indentation	
Rolling	
Brushing	
Peening	
Brinelling	
Rippling	
Ridging	
Bending (yielding)	
Tip to root interference	

Lubrication-related failures		
Hertzian fatigue	**Wear**	**Scuffing**
Pitting	Adhesion	Scoring
Initial	Normal	Galling
Superficial	Running-in	Seizing
Destructive	Mild	Welding
Spalling	Moderate	Smearing
Micro pitting	Severe	Initial
Frosting	Excessive	Moderate
Gray staining	Abrasion	Destructive
Peeling	Scoring	
Subcase fatigue (case crushing)	Scratching	
Plowing	Cutting	
	Plowing	
	Gouging	
	Corrosion	
	Fretting corrosion	
	Electrical discharge damage	
	Polishing(burnishing)	

Fatigue is the biggest type of failure in the gears. Also, micro-pitting, which causes wear, is a type of fatigue failure. The gears are malfunctioned by one or more of the following forms: bending fatigue, wear, pitting, scuffing or micro-pitting. Pitting and micro-pitting depend on surface contact stresses. The main feature of these specimens is the loss of material on the flank surface, but the damage location is characteristic of each kind. These types of failures are shown in Figure 3.11.

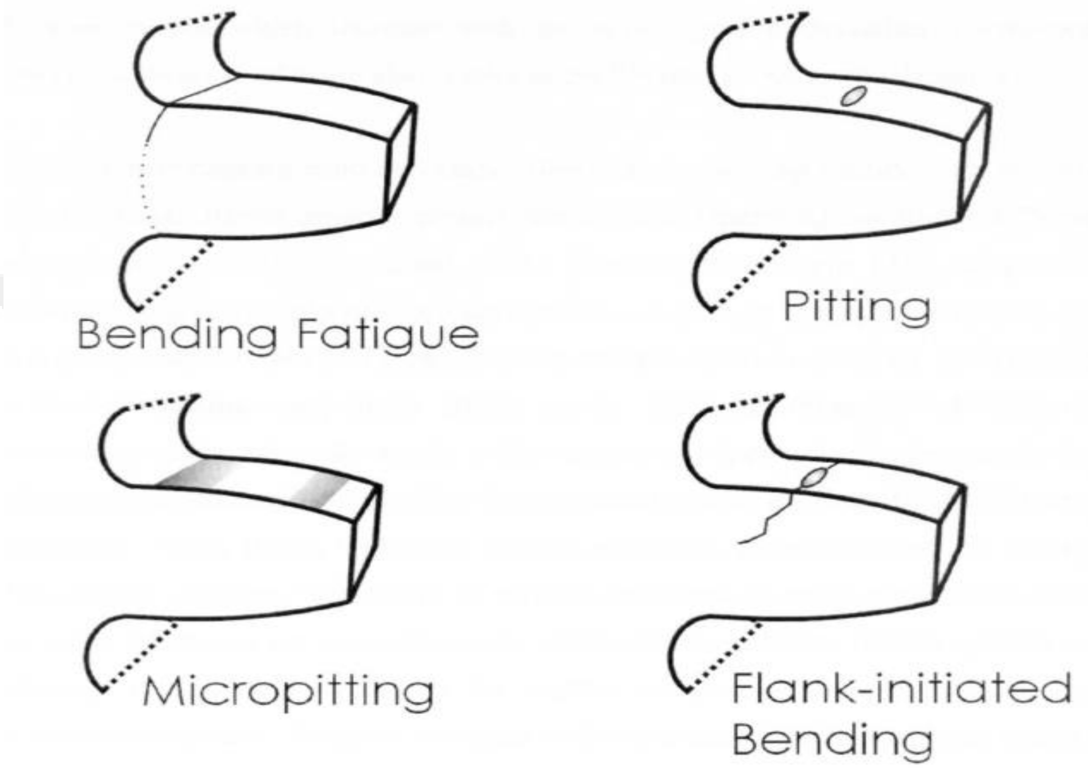

Figure 3.11 Various failure types in gears

The failure types of gears can be categorized as follows: Bending Fatigue, Pitting, Spalling, Wear, Plastic flow, fracture, process related.

3.4.1.1 Pitting

A surface fatigue is a type of damage, that can occurs shortly after the gear wheel begins operating and can be seen in three ways as given below:

Initial pitting: It is caused by high stress caused by the rough surface of the new gears. It develops in a very short time, reaches a maximum degree and loses its effect by polishing and. It usually occurs within a narrow area located just above or slightly below the rolling point. No precautions are required for initial pitting for most of the fully hardened gears used in industry.

Progressive pitting: It usually starts in the area below the rolling line. The pits increase in size and number until the surface is damaged. At the beginning of the study, the progressive pitting is approximately as dense as the initial pitting. Progressive pitting is usually caused by excessive stresses caused by surface roughness, where the initial pitting cannot be alleviated. If the hardness of the tooth surface is below a certain value, this deterioration is inevitable.

Normal pitting: In fully loaded, fully hardened toothed gears, the normal pitting occurring under the rolling circle. As a result of ongoing work, the pit boundaries wear so that no further pits appear.

3.4.1.2 Spalling

Spalling is a term used to describe the sizeable area left behind when a part of the gear surface breaks. It occurs as a combination of large pits overlapping or intertwined in a single point in fully hardened gears and soft white materials. Practically the same as progressive pitting. It occurs in completely hardened gear and in soft materials as a combination of overlapping of large pits, practically the same as progressive pitting. Spalling is revealed by high contact stresses with the addition of rough, rupture-free areas of the outer surface. In surface hardened gears, internal stresses caused by surface and sub-surface faults and incorrect heat treatments also cause spalling.

3.4.1.3 Wear

Wear is the undesired rupture of material on friction surfaces. In this way, the surfaces lose their initial shape, the gaps between the parts become larger and consequently the maximum sensitivity decreases, and noise and vibration signals occur. In general, wear is the result of physical and chemical changes in contact surfaces under external influences. The types of wear that occur in gears generally vary depending on the operating conditions. However, wear is mainly caused by insufficient or no oil film between the two contacting tooth surfaces. As a result of insufficient oil film between the two surfaces, direct contact occurs between the two tooth surfaces and wear begin. Abrasion damage can be divided into two classes as abrasive and adhesive wear.

Abrasion wear: It is also referred as cutting wear. Abrasion is the type of wear that occurs as a result of dirt and burrs coming from casting or worn particles coming from teeth or bearings or sliding particles of filter. The best way to avoid such wear is by detecting and cleaning the position and amount of these foreign particles in the oil with various imaging or sensing devices. The best way to avoid such wear is by detecting and cleaning the foreign particles in the oil with various imaging or sensing devices.

Adhesion wear: It is the most common wear mechanism and is based on the formation of micro-welding zones as a result of high mechanical stresses on the contact surfaces of the elements. There is a large difference between the actual contact surface size and the geometric contact surface size, depending on the surface roughness and the amount of loading. The fact that the actual contact surface is small allows the stresses at the contact points to yield stress even at small loads, and even above them.

3.4.1.4 Plastic Flow

The plastic flow is the undesired cold forming due to high contact pressures between the co-operating tooth surfaces and rolling and sliding events. It is a type of damage that occurs as a result of the deformation of surface and subsurface material by flowing. Although it is generally seen in soft materials, it can also occur on cemented toothed surfaces under heavy load.

3.4.1.5 Fracture

Fractures in gears are more dangerous and riskier than many types of damage. This can have very dangerous consequences, especially in a helicopter, elevator or crane. Therefore, in working conditions where human life is at risk, the safety coefficient for fracture in gears is considered high. The forces that push the teeth of the impeller to bend cause the highest stresses in the arches of the tooth root and at the intersection of the tooth root and the tooth profile. A gear is subjected to tensile stresses on the contact side and compression stresses on the opposite side. If the tensile stress occurring in the critical areas is allowed to exceed the strength limit of the gear material, fatigue cracks eventually form and progress with the work until the tooth is removed from the impeller body.

3.4.1.6 Process Related

Pinion and small gear wheels are generally made of solid material or welded to the shaft. If the quantity is high, the production is performed by forging. After production, surface hardening is performed to increase the abrasion resistance of gear surfaces.

When the gears go through these manufacturing processes, some damage may occur. These damages are cracks during hardening and cracks during grinding.

3.4.1.7 Fatigue Failures

Fatigue failure comes about because of cracking under repeated stresses and smaller value than ultimate tensile strength. This type of failure:

- Ordinarily relies on the quantity of repetitions of imputed stress range
- Does not happen beneath some stress magnitude called as fatigue limit
- Is considerably occurred by grooves, discontinuities of surfaces and imperfections of sub surfaces that will diminish the amplitudes of stress
- Is expanded considerably by rising the average tensile stress that is about loading cycle

Three phases are considered as fatigue failure that must be examined intently: the beginning of the fracture, the propagation under progressive loops of loading, and the last one, rupture part when the expanding crack that weakened the area. Most consideration is dedicated to the first stage. The second level is encountered to decide the heading of the propagation. It clarifies the idea that a fatigue crack will pursue the weak resistance point through the metal. The final rupture might be by tension or a shear force, yet in either case, the dimension of the rupture territory can be utilized to estimate stress magnitude that had been performed to the area.

3.4.1.7.1 Bending Fatigue

Fatigue failure occurs at values much lower than the ultimate tensile strength as a result of cracking under repeated stresses. This type of failure depends on the number of repeat of the stress rather than the total time and It does not occur under certain stress amplitudes called fatigue limits. Increasing the average bending stress also increases fatigue failures. There are three stages for fatigue failure. The first one is the origin of the fracture. The second one is the progression under stress loading cycles. And the third one is the final fracture of the piece when the spreading crack sufficiently weakens the section.

The beginning of failures type of bending fatigue ordinarily is surface defects of the root fillet or embodiment of nonmetallic materials close to the surface. Cracks gradually proceed around the starting point until they achieve the crucial dimension for the case material at the standard level of stress. For solidified high carbon material normally utilized for gears, when the crack achieves this crucial size, it blows up the case. When this happen, the tooth rigidity is diminished, and dynamic load increments occur. This delivers a promptly distinguishable increment in noise and vibration and symbolizes the failure.

As mentioned previously, the most prevalent method of fatigue failure in gearing is bending fatigue. There are many variants of this failure mode, but by first displaying the classical failure, the differences can be better understood. The classical failure of bending fatigue is that which happens and progresses in the region intended to receive the peak stress of bending.
Five circumstances make Figure 3.12 an ideal fatigue failure in the bending of the tooth:

- The beginning is on the root radius surface of the loaded tooth side
- The beginning is between the ends of the tooth at the midpoint where the standard load is anticipated
- First one of the teeth failed, and the fracture proceeded slowly towards the point of zero stress at the root, which during the transition moved to a point below the reverse root radius and then proceeded to that radius
- Because the fracture proceeded, the tooth distorted at each period till the load was continuously grabbed by the upper corner of the next tooth, which (because it was now overloaded) quickly began a failure in a certain region of tooth bending fatigue.
- Specifications of the material and metallurgical features

Figure 3.12 Spiral bevel pinion displaying the typical fatigue of the tooth bending.

Using photo elastic models, the rudiments of classical bending fatigue can be explored. Once the crack is launched at the root radius and progresses towards the point of zero stress (Fig.3.13), the point runs away from the leading edge of crack's and moves horizontally until it reaches a place below the reverse root. The smallest residual distance to the root at that moment is outward, and the point ends there. Meanwhile, because the damaged tooth is deflected, the load has been picked up by the top of the nearby tooth. The first tooth load was now relieved, enabling for a slower development owing to reduced cyclic stress. It is now only a matter of how long until a crack in the same position is initiated by the next tooth. For many reasons, variants from the typical bending fatigue occur.

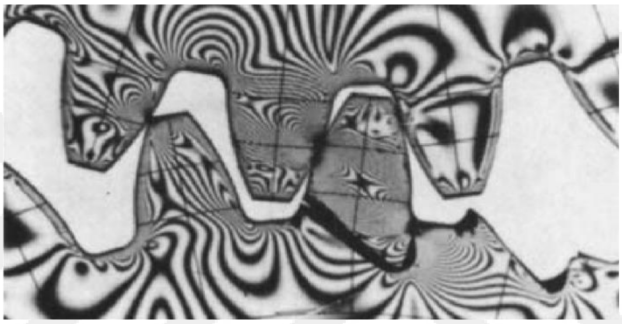

Figure 3.13 Mating teeth photo elastic research shows the zero-stress point change during crack propagation until the final fracture hits the reverse root radius.

The bending fatigue of a spur gear tooth located at the start of the loaded side (Fig. 3.14) along the surface of the root radius but about a third away from the opening can be called a classic failure. And therefore, the peak loads applied were in the same region. This, then, is the region intended for ordinary bending fatigue initiation point. The proceeding was to the bore straightly, which was the least resistance's shortest direction.

Figure 3.14 Tooth-bending fatigue from the root radius, loaded side, one-third from the open end.

Fig. 3.15 shows a spur-gear tooth's bending fatigue meeting all but one of the requirements for a traditional failure. The beginning was at one end and not the mid-length of the tooth. There might have been many factors for this initiation stage; in this case, the sections had been twisted by a serious shock load until a temporary overload at the end of the tooth was applied, causing a crack to form. The crack became an elevated concentration of stress from which propagation of fatigue continued.

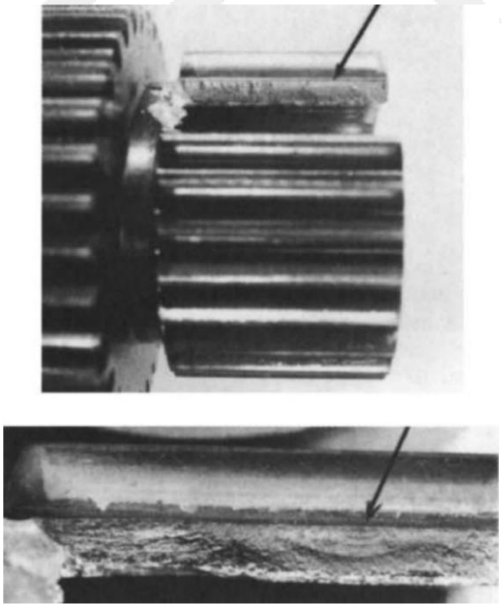

Figure 3.15 The failure of spur pinion. Tooth-bending fatigue with beginnings on one end of the tooth at the root radius of the loaded side.

Fig. 3.16 shows an illustration of bending fatigue that did not comply with conventional circumstances. Crack formation was on the case/core border at a nonmetallic incorporation; it did not originate on the surface. Subsequent propagation was to the surface through the situation as well as to the zero-stress point through the center.

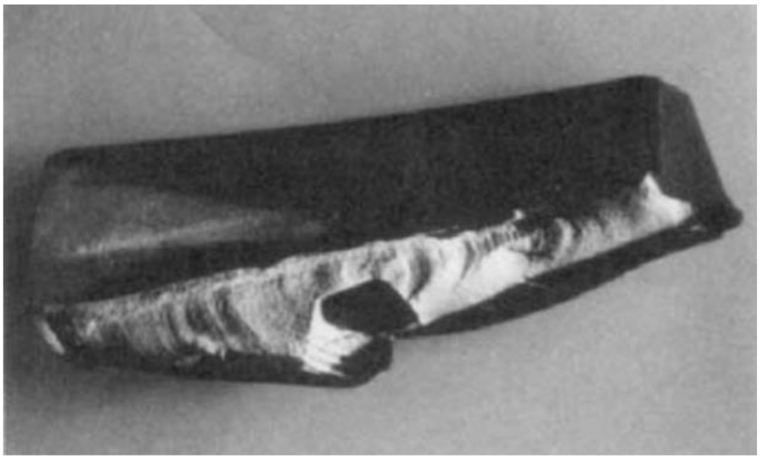

Figure 3.16 The failure of spur pinion. Tooth-bending fatigue is in the root radius at the mid-length of the tooth, but the origin is in the case/core transformation at an inclusion.

Another instance of non-conforming bending fatigue is shown in Fig 3.17. At the root radius and mid length, failure occurred, but the beginning was not on the ground. The beginning was at the top of a tapped bolt hole which was inserted from the rear side of the equipment and ended up from the root radius below 6.4 mm (0.25 in.)

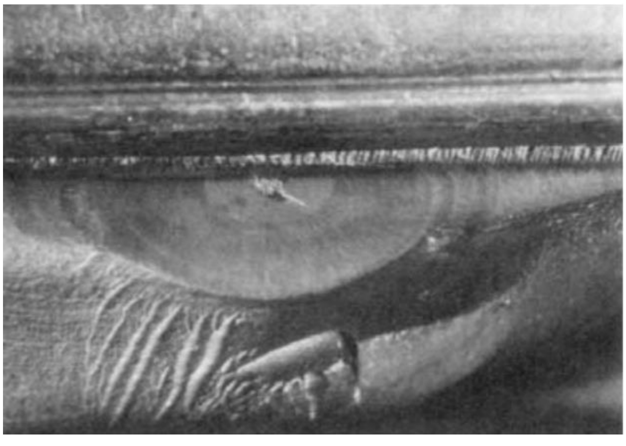

Figure 3.17 Tooth failure of a spiral bevel gear.

"Gear Tribology and Lubrication," non-lubricated failures include both types of failure overload and fatigue bending were shown in Table 3.3.

Table 3.3 Gear failure modes proposed by Alban

Failure Mode	Type of Failure
Fatigue	Pitting, spalling, tooth bending, thermal fatigue and rolling contact
Impact	Tooth bending, tooth chipping, tooth shear, torsional shear and case crushing,
Wear	Abrasive, adhesive
Stress rupture	Internal, external

3.4.1.7.2 Contact Fatigue

Contact fatigue is indeed the surface cracking that is subjected to repeated Hertzian stresses generated under controlled circumstances of rolling and sliding load. In relation to cracking, microstructural modifications, including alterations in retained austenite, martensite morphology and residual stress may lead in contact fatigue.

The tangential forces and heat gradient induced by friction change the size and distribution of stresses in and below the contact region when sliding is implemented on rolling. The differentiating shear stress rises in magnitude and sliding forces move closer to the surface. The onset of contact-fatigue cracks of gear teeth, which are exposed to substantial quantities of sliding close to the pitch line, is therefore discovered to be in the ground material. These cracks continue to spread to the ground at a shallow angle, resulting in pits when secondary cracks connect the cracks to the ground. If pitting is serious, the tooth's bending resistance may be reduced to the stage where fracturing may happen. It has been acknowledged that there are several significantly distinct types of contact-fatigue damage, but the factors controlling each type's nucleation and propagation are partly understood. The contact fatigue of hardened steel was the topic of comprehensive studies using empirical and testing techniques, and papers revealed a wide variety in the contact fatigue strength of comparable products when tested in conjunction with rolling under various circumstances of contact geometry, velocity, lubrication, temperature, and sliding. Though the origin of fatigue and the places of the roots are somewhat distinct, these are real fractures of fatigue created by the roots of shear stress owing to contact stress among two flat surfaces.

The nomenclature used by the gear sector to define the fracture appearance of failed parts of contact fatigue is listed in Table 3.4.

Table 3.4 List of terminology for contact fatigue used to define the various fatigue processes

Category	Fatigue mechanisms
Macroscale	
Macro pitting	Pitting Spalling Fatigue wear Initial pitting Scabbing Destructive pitting Shelling
Subcase fatigue	Case crushing
Microscale	
Micro pitting	Frosting Microspalling Glazing Surface distress Gray staining Peeling

CHAPTER 4

METHODOLOGY

4.1 Introduction

The analysis of gear wheels by classical methods is difficult. Therefore, it is necessary to use numerical based solution methods. The package programs used to implement numerical based solution methods could analyze the behavior of the modeled systems under different loading conditions in a short time. This enables the product to be prepared before the production to see the errors that may occur and to take precautions against these errors. In this way, a wide range of benefits could be achieved in terms of time, cost and perfect products [32]. The latest and most important numerical solution method, Finite Element Method was used as a solution technique in this thesis.

4.2 Brief History of Finite Element Method

Because of human mental limitations, the behavior of the complex environment and creatures is incomprehensible. Therefore, it is a natural method followed by engineers, scientists, and even economists to divide systems into components or elements whose behavior can be easily understood, and then rebuild the original system [33].

The problems that cannot be analyzed as a whole can be divided into pieces and after each part is solved in itself, combining the solutions leads researchers to the right result. Shortly, this method is needed to solve the original problem by analyzing from unit to whole system. Over the years, this method has developed and continues to develop [34]. The finite element method is a numerical procedure used in the solution of differential equations in physics and engineering. In the first half of the 1950s, Ritz Courant obtained approximate solutions in vibration analysis using the methods of numerical analysis and variation and became one of the first applicators of the finite element method. This method was developed in the 50's in order to perform stress analysis of complex structures in aircraft and space industry [35]. After Courant, M. J.

Turner, R.W. Clough, H.C. Martin and L.C. Topp published an article on the problems of stiffness and deflection of complex structures.

These publications encouraged other researchers and resulted in the discussion of the application of the method about structural and solid mechanics in various articles. The common idea of these articles about finite elements can be expressed as follows. Any continuous quantity, such as temperature, pressure and displacement, is considered to be a model consisting of a finite number of parts and a family of fragmentary continuous functions defined on these parts. Since 1960, it has been developing rapidly, and the studies made with the finite element method, which has gained a rightful place in practice, have increased day by day. Thousands of articles and numerous books have been published and various conferences have been organized [36]. These systems, which were very expensive with mainframe computer applications in the 1970s, were used mostly by aviation, automotive, defense and nuclear industries. In the 1980s, pre- and post-processors were developed with the help of microcomputers. With the help of super computers from the 1990s to today, it is possible to obtain acceptable solutions for the problem. Particularly complex problems could be solved. With the developed finite element method package programs, it is easy to see the data of the problem that is desired to be solved and to analyze and evaluate the results in the computer environment [37].

Software packages of this method was initially limited and used for special purpose. However, nowadays, modeling and analysis can be done easily with general-purpose finite element software. Among the most widely used Finite Element method package programs on the market today are ANSYS, NASTRAN, COSMOSWORKS and ABAQUS.

4.3 Review of Finite Element Method

Engineering problems are generally mathematical models of physical situations. Finite element method (FEM) is a numerical solution method that presents an acceptable approach to different engineering problems. The mathematical basis of these numerical solution methods is well known. In addition, efficient and precise usage of these methods is possible with the production of advanced computers. Physical problems are mathematically modeled as differential equations, integral equations or integro-differential equations. These modeled problems are solved by using analytical and numerical methods. Analytical solution methods can be used in the form of solving the main equation by using known solution techniques without any approach. Today, due to changing material properties (e.g. composite materials), complex geometry and complex boundary conditions, only few problems can be solved by analytical solution methods. These solutions take a lot of time. Therefore, it is inevitable to use numerical solution methods. If the analytical solution of the given problem is possible, this solution should, be preferred. Finite element method (FEM), boundary element method (BEM), finite difference (FD) methods are numerical solution methods. FEM is the most widely used and most common method of numerical solution. FEM was developed by engineers rather than mathematicians and was first applied to stress analysis problems. In all these problems, it is desirable to calculate a size area. In stress analysis, this value is the displacement area or the stress area in stress analysis; temperature area or heat flow in heat analysis; the flow function or velocity potential function in fluid analysis. The maximum value of the area or the largest gradient of field is of particular importance in practice. In FEM, the structure is divided into several elements whose behavior is already determined. The elements are reassembled at points called "nod". In this way, a set of algebraic equations is obtained. In stress analysis, these equations are equilibrium equations in nodes. Depending on the problem under investigation, hundreds or even thousands of equations are obtained. The solution of this equation necessitates the use of advanced computers [38].

4.4 Tools and Workflow

In the initial stages of the software development, all nodes forming the problem geometry were determined one by one and then the elements were created. This was extremely troublesome, and the possibility of errors occurred was a great deal. With the development of CAD models in finite element package programs, great convenience in the pre-processor phase was provided.

There are 3 major steps in this study;

- Forming the gear geometry,
- Solid modeling of the gear,
- Determination of boundary conditions and analysis.

Three programs were used in the implementation and analysis of this method; these programs are software used in gear modeling, Solid Works, and ANSYS.

Firstly, a homemade software developed by Şahin, B. [39] and Şahin, B. et al. [40] was used to create gear geometries. In the geometry obtained from this software, nods are very close to each other in the X and Y coordinate system depending on the data entered to program. The trochoid portions of tooth profiles are transferred to the Solid Works program with the point of the coordinate system (0, 0, 0), the center of the gear as shown in Figure 4.1.

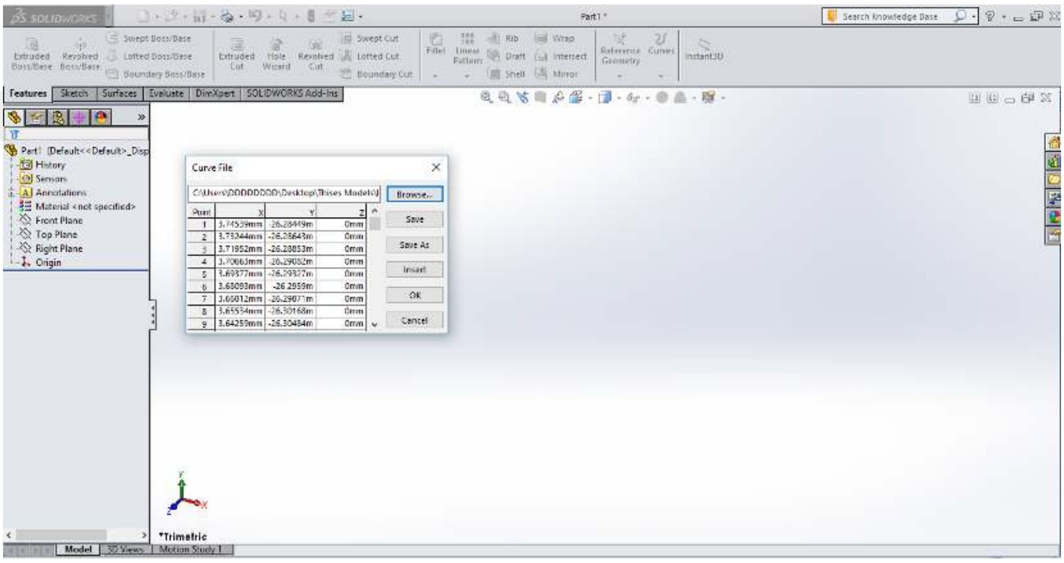

Figure 4.1 Inserting coordinates of tooth profiles.

Right and left sides of trochoid portions of tooth profiles are obtained separately and joined together to form a tooth in the solid works program as shown in Figure 4.2.

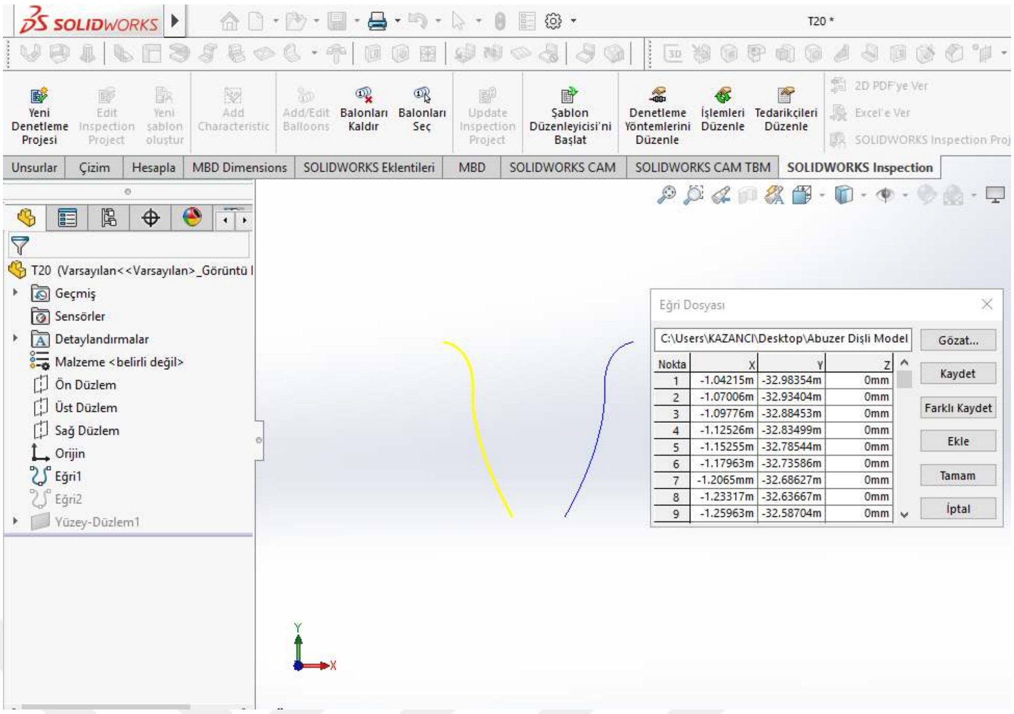

Figure 4.2 Tooth profiles in SOLIDWORK space.

Gear models are created in the solidwork program and a 2D model of a complete gear was modeled as given in Figure 4.3.

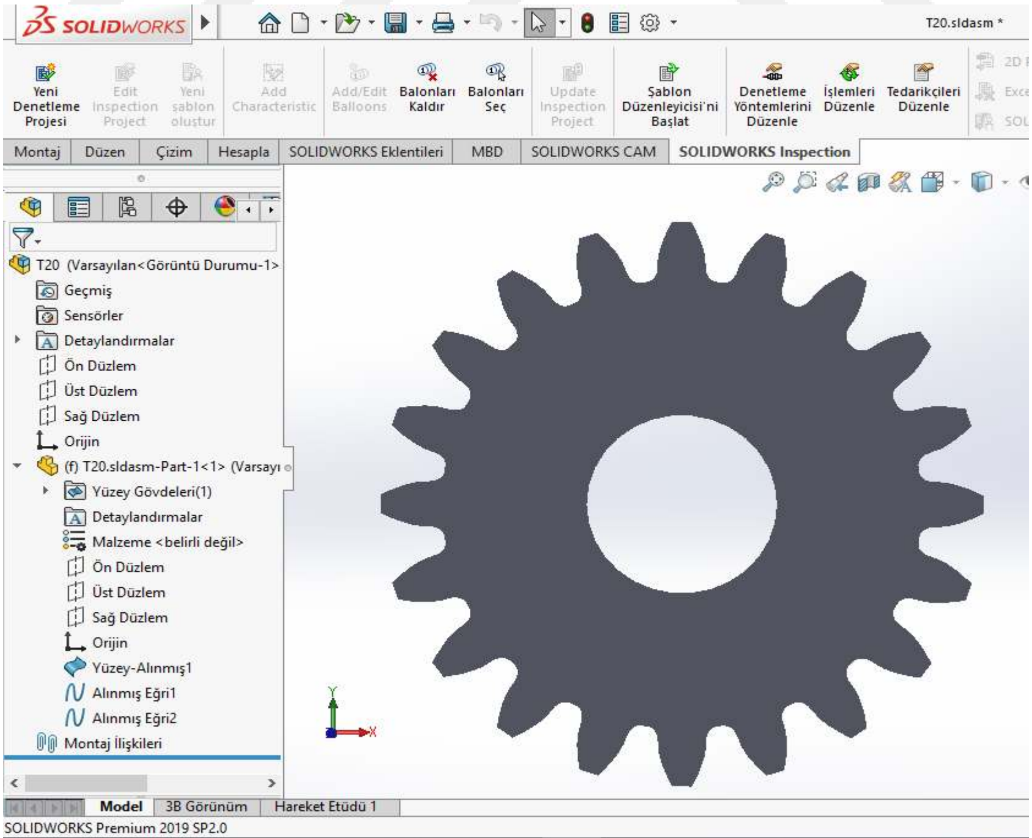

Figure 4.3 Drawing of gear models

A 2D solid model was created in the Solid Works program and the gear was transferred to ANSYS for analysis.

In the ANSYS finite element package program, analyzes are performed in various modules. In this study, ANSYS workbench static structure module is performed. The following steps are generally followed in the creation of the module and analysis as shown in Figure 4.4. The Workbench option is opened from the main menu of the ANSYS commercial package program.

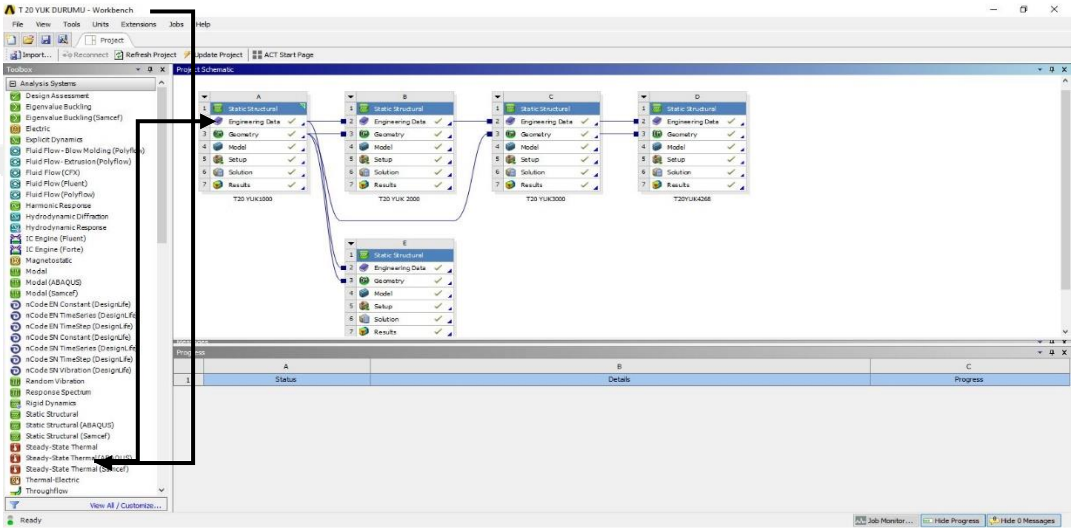

Figure 4.4 ANSYS Workbench Static structure module

The Workbench option includes modules for using in various analyzes. Static structure option is selected for gear bending fatigue analysis among these options. For this, the path of ***ANSYS 18.1>Workbench> Static Structure*** is followed as shown in Figure 4.5. After selecting the module, the geometry modeled in SolidWorks is opened.

Figure 4.5 Static Structure main menu

For the modeled geometry, material properties are defined in the Engineering Data menu. ANSYS package program enables to user a wide materials library. However, users can also manually define material properties. In this thesis, structural steel is used as a material as shown in Figure 4.6.

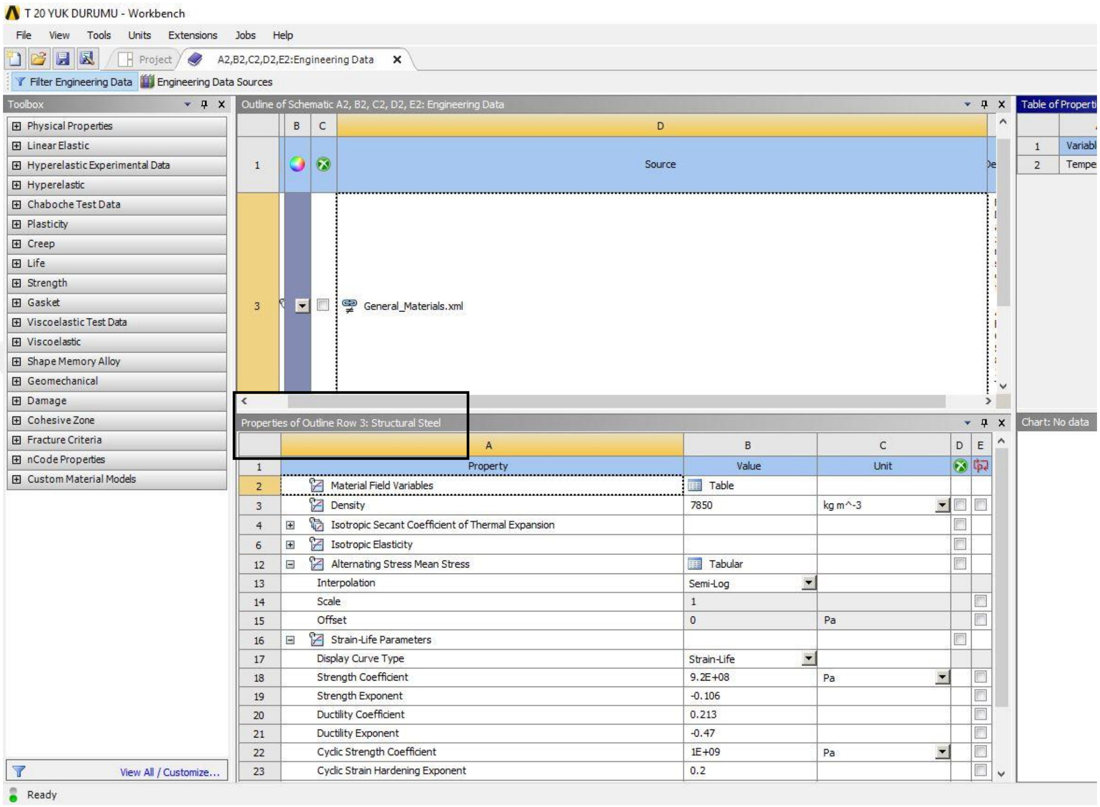

Figure 4.6 Material selection menu

In addition, some commands must be set for fatigue life analysis under the Engineering Data menu. Semi-log graphs are used for data obtained from fatigue life studies. Also strain life method is used to obtain fatigue life graphs as shown in Figure 4.7.

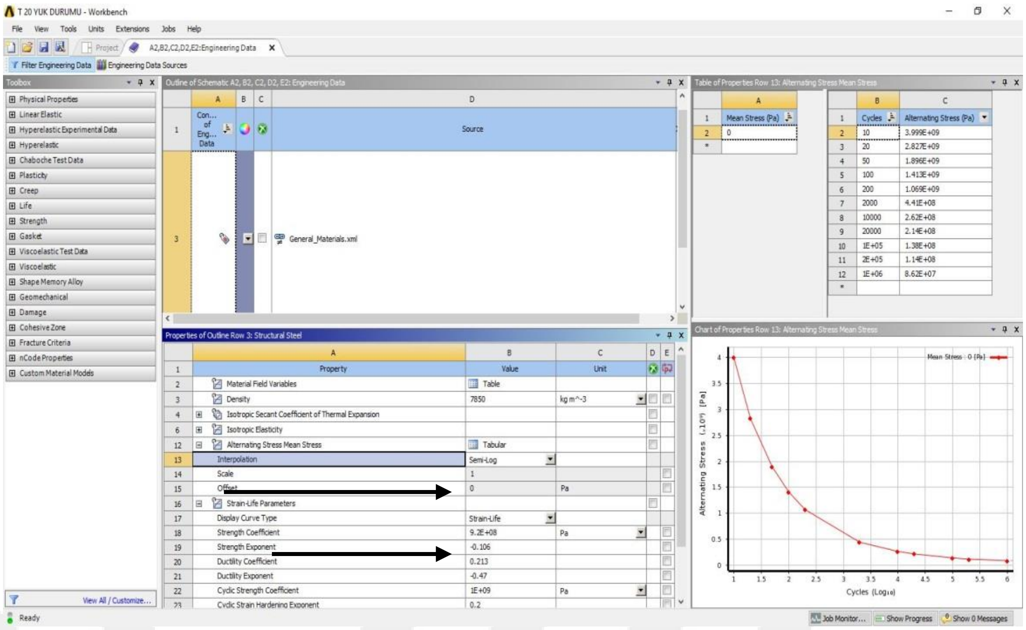

Figure 4.7 Graphs command

Following the determination of the material properties, the geometry modeled in the Solid Works program is opened. In order to define various parameters in relation to the analysis, ***"Edit Geometry in Design Modeler"*** is accessed from the menu. At this stage, the application point of the load is determined on the geometry. The load is applied to the highest point of single tooth contact (HPSTC). The coordinates of these points for all gear models are available as an output from the homemade gear modeler software. Following the ***Design Modeler-Tools-Face Split*** commands, a circle passing through the HPSTC for the load application point is added as shown in Figure 4.8.

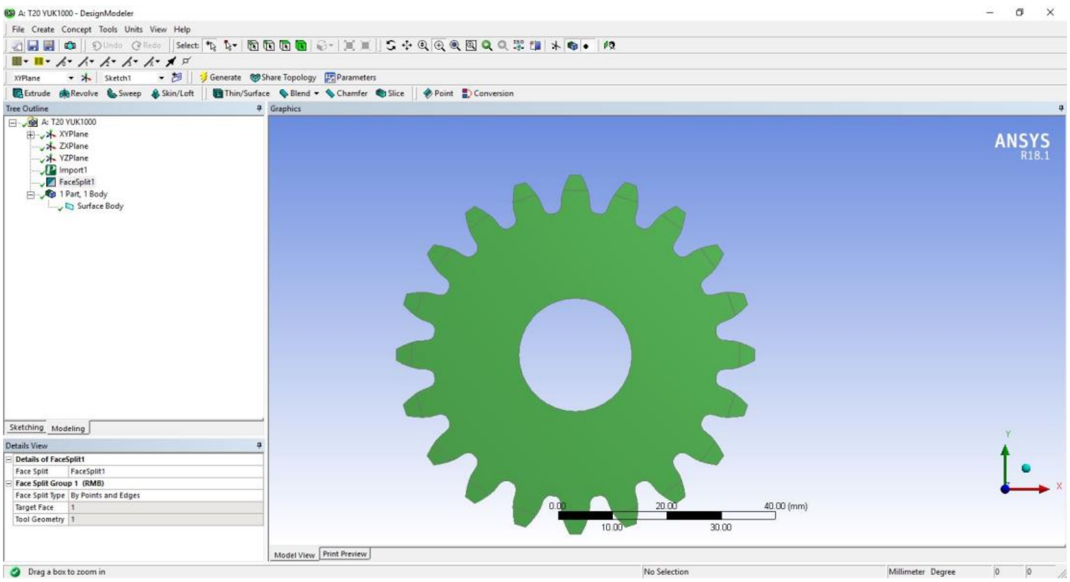

Figure 4.8 Design modeler face split

After all these operations, analysis of the gear geometry is completed via ***Static Structure*** > ***Model*** > ***Edit*** command. At this stage of the program, the ANSYS Mechanical menu is opened as shown in Figure 4.9.

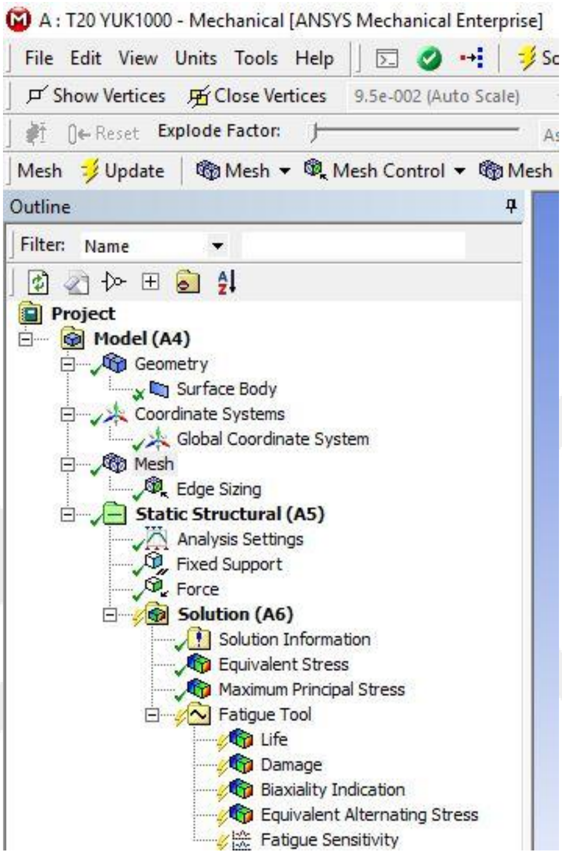

Figure 4.9 ANSYS Mechanical menu

When the geometry in the subheading of the model section is placed at the point (0.0.0) in the coordinate system, the first thing to be done here is the mesh operation. In order to perform the analysis of the formed models, that is to achieve the finite element solution, the model must be divided into a finite number of elements. In FEM, mesh is a subject that requires expertise. The element size generated in 2D and 3D geometries significantly changes the stress values and thus fatigue life cycle. In order to obtain the correct result, the area or volume should be divided into elements in a very good way. In finite elements, the solution can be one, two or three-dimensional. However, the shapes of the elements used may be as shown in Figure 4.10. Although the boundaries of the finite element are generally precisely selected, curved bounded finite elements can be used in some problems.

In order to reduce time, different size of mesh can be defined in analysis regions of the geometries. In this study, in order to shorten the processing time, a mesh of 0.1 mm size with the linear mesh command on the analyzed gear tooth is defined as shown in Figure 4.11. The remaining part of the gear circle is defined as fine mesh from the mesh options defined in the program. Dividing the region into more elements where the stress intensity is greater is crucial for the accuracy of the result. Figure 4.11. shows the regions where the intensity of stress is high and they are divided into more elements. When dividing geometry meshes, attention should be paid to dividing the meshes into four-sided meshes and dividing the opposite sides of the meshes into equal numbers. This is very important to obtain a model that leads the analysis to the correct result.

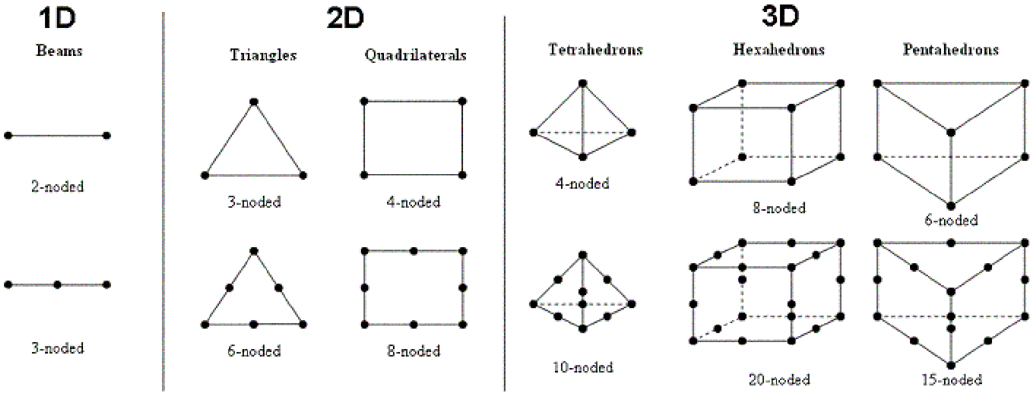

Figure 4.10 ANSYS element shape

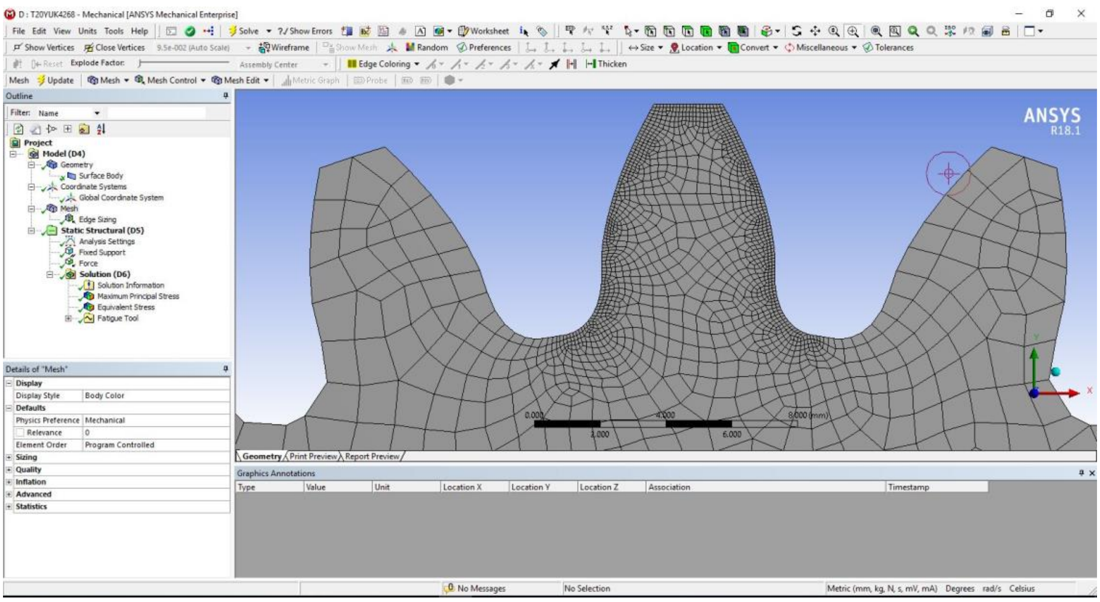

Figure 4.11 Mesh distribution of gear

Static Structure > Insert > Fixed Support steps are followed, and the fixed support option is added to the solution. In this menu, the gear is fixed to the shaft hole part as shown in Figure 4.12. By fixing the gear geometry, stresses can be obtained under the applied load.

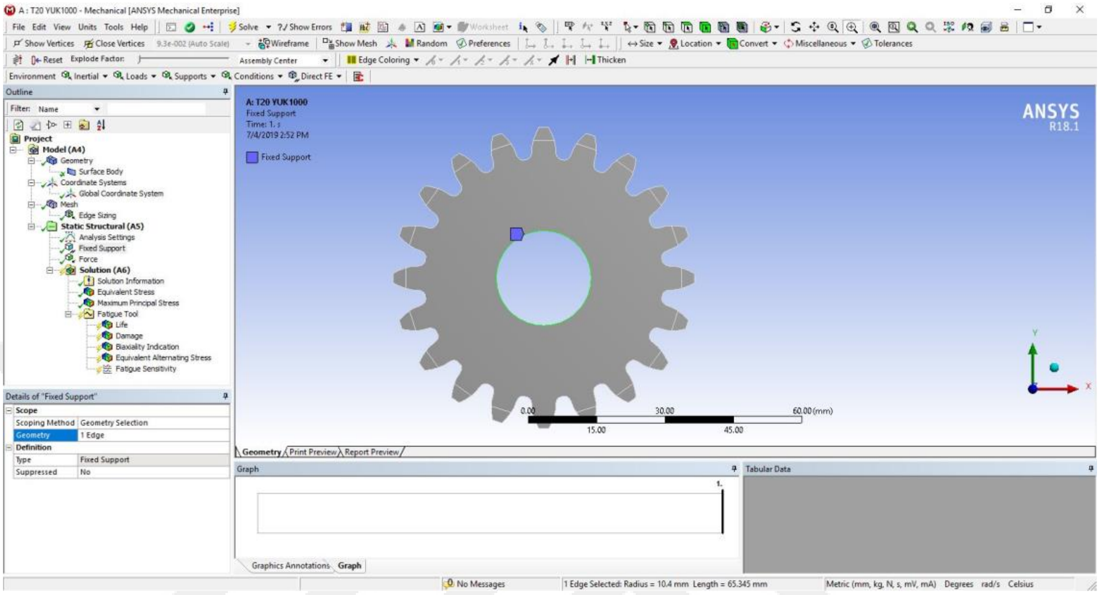

Figure 4.12 Fixed support

Static Structure > Insert > Force steps are followed to apply force to any part of the geometry. In this thesis, 2D analysis is performed and load is applied to HPSTC. The magnitudes of the load in the X and Y coordinates are entered. The total load applied to the surface normally as shown in Figure 4.13.

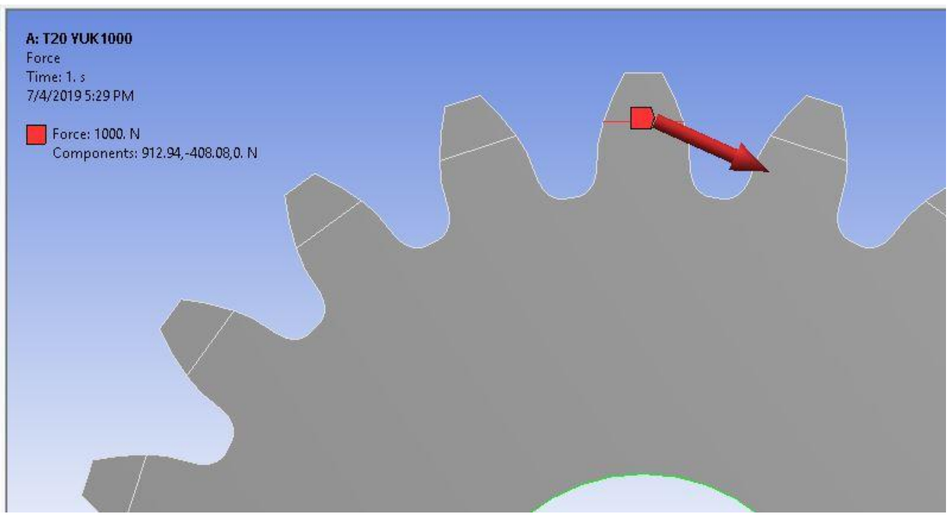

Figure 4.13 Applied load to tooth surface

At this stage, the tools to be analyzed are defined. Firstly, tools for calculating stresses are added.

Tools are added via ***Solution > Insert > Stress Equivalent (Von Misses) Stress and Solution > Insert > Maximum Principle Stress.*** As a result of the solution, it is sufficient to click the relevant menu for stress distributions on the geometry as shown in Figure 4.14 and Figure 4.15.

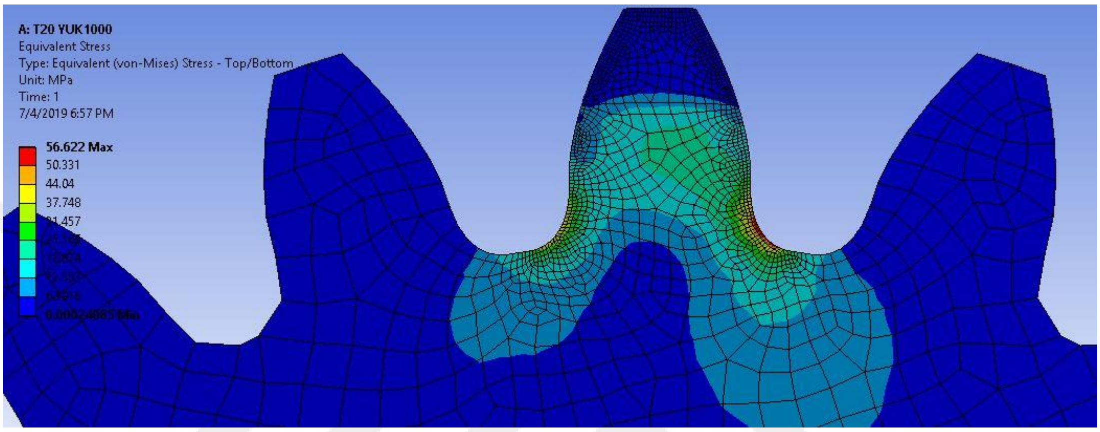

Figure 4.14 Equivalent (von-misses) stress distribution.

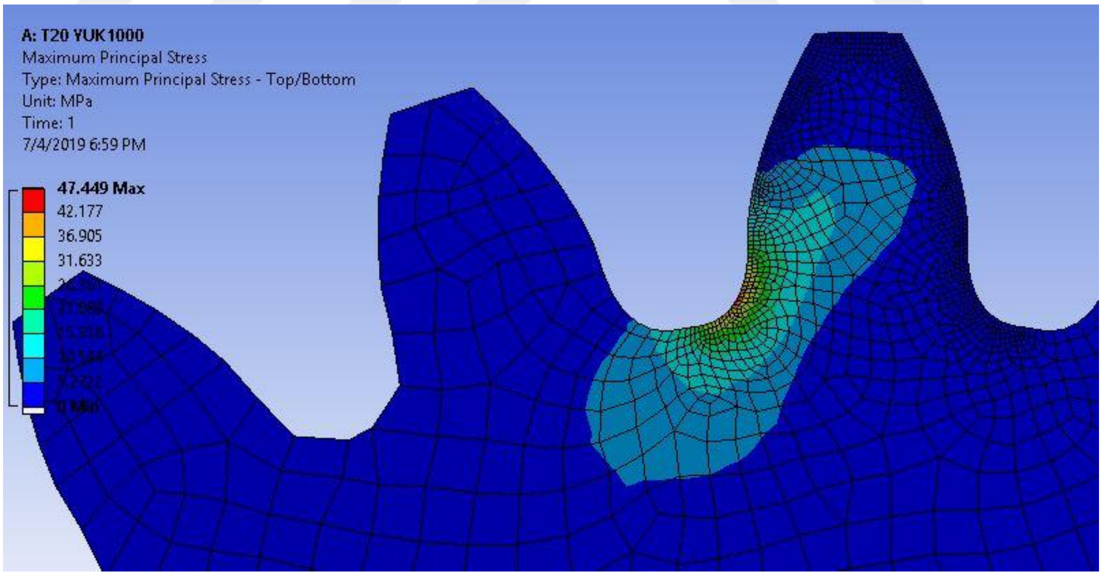

Figure 4.15 Maximum principle stress distribution.

Finally, ***Solution > Insert > Fatigue > Fatigue Tool*** added to main menu. Life menus are added inside the fatigue tool. The results regarding the fatigue life of the geometry under applied load are given in Figure 4.16.

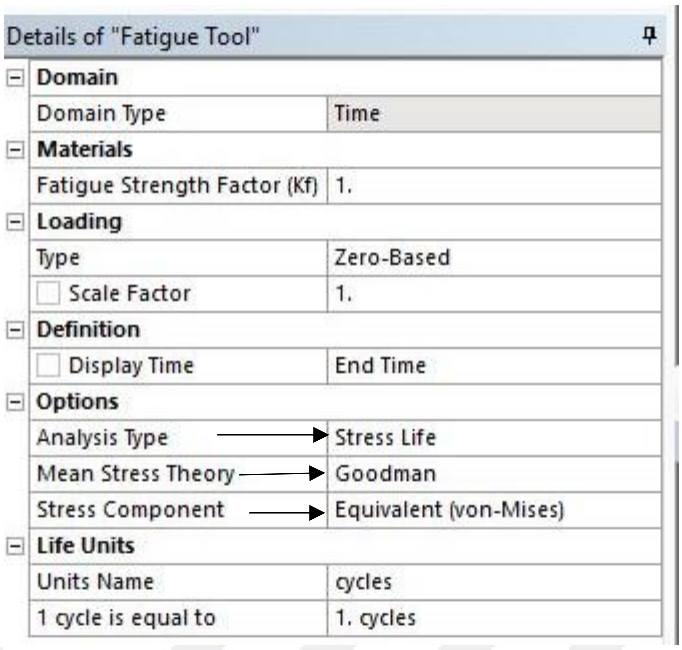

Figure 4.16 ANSYS Workbench Fatigue Tool Menu

The fatigue life estimation menus analysis completed according to the stress life methods. Goodman Mean Stress Theory used for life estimations. As a result of ISO based tooth root stress comparison to Maximum Principal Stress and Equivalent (Von-Misses) stress the Equivalent (Von-Misses) stress is closer to ISO based tooth root stress distributions.

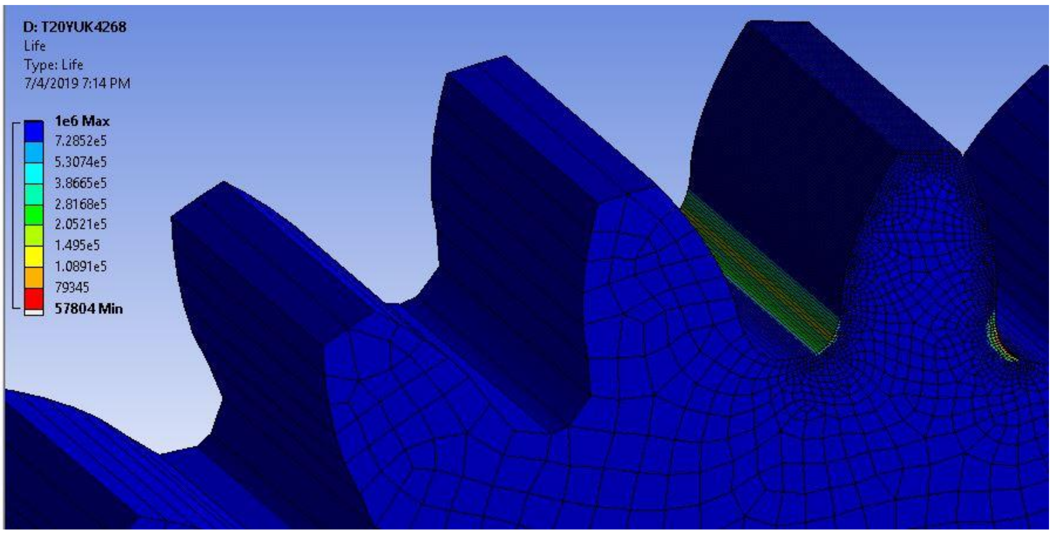

Figure 4.17 Fatigue life

CHAPTER 5

CASE STUDIES BENDING STRESS

In Chapter 4, the processes and follow-up steps in the formation of the model developed for bending stress by finite element method are discussed in detail. Although this method used in the analysis of tooth root stresses gives the best results within the boundary conditions determined within itself, it should be compared with the results obtained by analytical or experimental methods. In this study, the finite element analysis has been compared with the analytical results obtained from ISO 6336-: 2006 (E) standard.

The bending stress of the tooth root as defined by the ISO 6336-3:2006 (E) standard can be defined either by experimental methods or numerical analysis (method A) or by an estimated analytical technique (method B). Method B is suitable for calculating the stress of the tooth root in cylindrical gear pairs, but also in pulsator experiments with a specified load application level according to this standard.

For single tooth bending fatigue (STBF) testing, the execution of Method B, as it is, involves the definition of a virtual gear mating with the sample of the test equipment. The virtual mating gear should be constructed in such a way that the gear specimen's highest point of single tooth connect (HPSTC) in matching up with the virtual gear coincides with the specified pulsator test application level. Nevertheless, calculating the tooth root stress utilizing method B is also possible without any need to define a virtual mating gear, just modifying only the equations described in the standard ISO based on a basic geometric analysis. Here, for the comfort of the reader is provided a short synthesis of the calculation method suited for symmetrical pulsator tests.

The bending stress of tooth root, σ_F, is the same as the nominal tooth root pressure, σ_{F0}, multiplied by the overload factors, K_A, K_V, K_{Fa}, $K_{F\beta}$ and Eqn. 5.1 is given below:

$$\sigma_F = {\sigma_{F0}}/{K_A * K_V * K_{F\alpha} * K_{F\beta}} \tag{5.1}$$

Therefore, the real tooth root bending stress, σ_F, coincides in this situation with the nominal tooth root bending pressure, σ_{F0} calculated as a fundamental stress multiplied by a number of stress correction variables, Eqn. 5.2 is given as follows:

$$\sigma_F \equiv \sigma_{F0} = \frac{F_N \cos\alpha}{bm} Y_F * Y_S * Y_\beta * Y_B * Y_{DT} \tag{5.2}$$

The fundamental stress is equivalent to the proportion of the tangential load, which is the force acting normally on the F_n tooth profile (i.e. the test load for pulsator experiments) multiplied by the pressure angle's cosine divided by product of the the gear module m and the face width b. The specimens being tested, the spur gears with a full-body framework, the rim thickness factor, Y_B and the helix angle factor, Y_β, are equivalent to unity along with the profound tooth factor, Y_{DT}, as meshing is not repeated. It is necessary to calculate the tooth shape factor, Y_F, and the stress concentration factor, Y_S, taking into account the geometry of the root fillet and the load entry point according to the ISO standard Eqn. 5.3-5:

$$Y_F = \frac{(6h_{Fp}/m)\cos\alpha_{Fp}}{({S_F}/{m})^2 \cos\alpha} \tag{5.3}$$

$$Y_s = (1.2 + 0,13L) q_s^{\left[\frac{1}{1,21+\frac{2.3}{l}}\right]} \tag{5.4}$$

With

$$l = \frac{S_F}{h_{Fp}} \; and \; q_s = \frac{S_F}{2\rho_F} \tag{5.5}$$

The quantities to be established are, therefore, the thickness of the crucial section, S_F, the curvature radius of the tooth root filet profile in the critical section, ρ_F, the bending arm of the load applied, h_{Fp}, and the angle between both the load applied and the tooth axis, α_{Fp}. These components can be calculated following the conventional ISO method since it is necessary to determine the last two components, h_{Fp} and α_{Fp}, for the pulsator test application point. The ISO calculation method needs certain additional geometric components to be determined starting from the measurements of the fundamental rack profile of the finished tooth defined in accordance with Eqn. 5.6-11:

$$E = \frac{\pi}{4} m - h_{Fp} \tan\alpha + \frac{s_{pr}}{\cos\alpha} - (1 - \sin\alpha)\frac{\rho_{fP}}{\cos\alpha} \tag{5.6}$$

$$G = \frac{\rho_{fP}}{m} - \frac{h_{fP}}{m} + x \tag{5.7}$$

$$h = \frac{2}{z}\left(\frac{\pi}{2} - \frac{E}{m}\right) + \frac{\pi}{3} \tag{5.8}$$

$$\theta = \frac{2G}{z}\tan\theta - h \tag{5.9}$$

The angle *h* is determined to solve iteratively the earlier specified transcendental equation beginning with an original *p/6* value. The radius of curvature of the tooth root fillet profile and the thickness of the critical section can be defined with the ISO standard equations, since the critical cross-section does not depend on the point of load application given Figure 5.1:

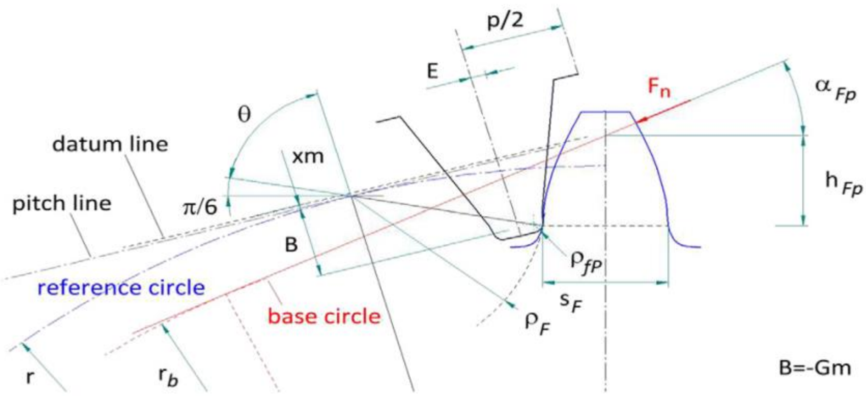

Figure 5.1 Generating rack profile on producing the 30^0 tangent point at the tooth root fillet.

$$\frac{s_F}{m} = z\sin\left(\frac{\pi}{3} - \theta\right) + \sqrt{3}\left(\frac{G}{\cos\theta} - \frac{\rho_{fP}}{m}\right) \tag{5.10}$$

$$\frac{\rho_F}{m} = \frac{\rho_{fP}}{m} + \frac{2G^2}{\cos\theta(z\cos\theta^2 - 2G)} \tag{5.11}$$

The *αFp* angle, in other words, the angle between the perpendicular line to the tooth axis loaded and the applied force action line and the amount of teeth spanned by the two anvils is indicated by *n* as follows in Eqn. 5.12:

$$\alpha_{FP} = (n-1)\frac{p_b}{d_b} = (n-1)\frac{\pi}{z} \tag{5.12}$$

The bending lever arm, h_{Fp}, can be calculated as the distinction between the load direction intersection point lengths and the gear axis critical cross section. The calculation can be done using the following equation based on fundamental geometric relationships given in Eqn. 5.13:

$$\frac{h_{Fp}}{m} = \left[\frac{z}{2}\frac{\cos\alpha}{\cos\alpha_{Fp}}\right] - \left[\frac{z}{2}\cos\left(\frac{\pi}{3} - \theta\right) + \left(\frac{G}{\cos\theta} - \frac{\rho_{fP}}{m}\right)\sin\left(\frac{\pi}{6}\right)\right] \tag{5.13}$$

In addition, the basic considerations for modeling and establishing boundary conditions as well as the case studies are as follows.

In the case of spur gears, the tooth is symmetrical with respect to the radial axis (tooth centerline). As the tooth form does not change in the width direction and theoretically, it can be assumed that the force distribution across the tooth width is uniform, the teeth can be modeled as two-dimensional (2D) bodies [41]. Modeling of a two dimensional problem as plane stress or plane strain determines the thickness according to the cross section of the plane.

It is most unfavorable to apply the force to the highest point of single tooth contact (HPSTC). In fact, depending on the coupling ratio, the tooth force is shared with the other gear following one another. If the teeth are not manufactured sensitively to provide load sharing, it can be said that the tooth force can have a full effect on the tooth tip. Theoretically, the point of application of the load that provides the maximum tension at the bottom of the tooth is the tooth tip. However, in practical approaches, the highest stress of the tooth root occurs at the highest point of single tooth contact (HPSTC). In this part of the study, stress and fatigue life analyzes are performed under different gear parameters by finite element method.

5.1 Effect of Force

Firstly, the effect of the applied load on tooth root stresses are investigated. The gear geometry modeled in 2D is in the same boundary conditions, specifications and parameters is determined for the effect of force change. The gear model analyzed in this case is given in Table 5.1.

Table 5.1 Spur gear characteristic for applied forces

GEAR PROPERTIES	CASE I					
Forces (N)	1000	2000	3000	4268	6000	8000
Rim Thickness	2*h					
Teeth Number	20					
Press. Angle (°)	20					
Module (mm)	3					
Addendum (a)	1.0*m					
Dedendum	1.25*m					
Tool Tip Radius Coefficient	0.3					
Face Width (mm)	20					

Gear tooth root bending stress result according to ANSYS Workbench (18.1) and ISO 6336- :2006 (E), given Table 5.2. FEM results and ISO analytical calculation results were found to be very close for each load value. As can be seen in Figure 5.1, where these results are compared, the variation of stresses is similar.

Table 5.2 Stress values of gear for applied forces

Case 1(Effect of Force)						
Applied Force	1000	2000	3000	4268	6000	8000
Equivalent (von-Mises) Stress (MPa)	52.105	103.08	156.33	222.18	312.57	412.76
Maximum Principal Stress (MPa)	52.885	108.88	158.97	225.73	317.32	431.05
ISO Bending Stress (MPa)	50.40	100.80	151.20	215.11	302.04	403.20

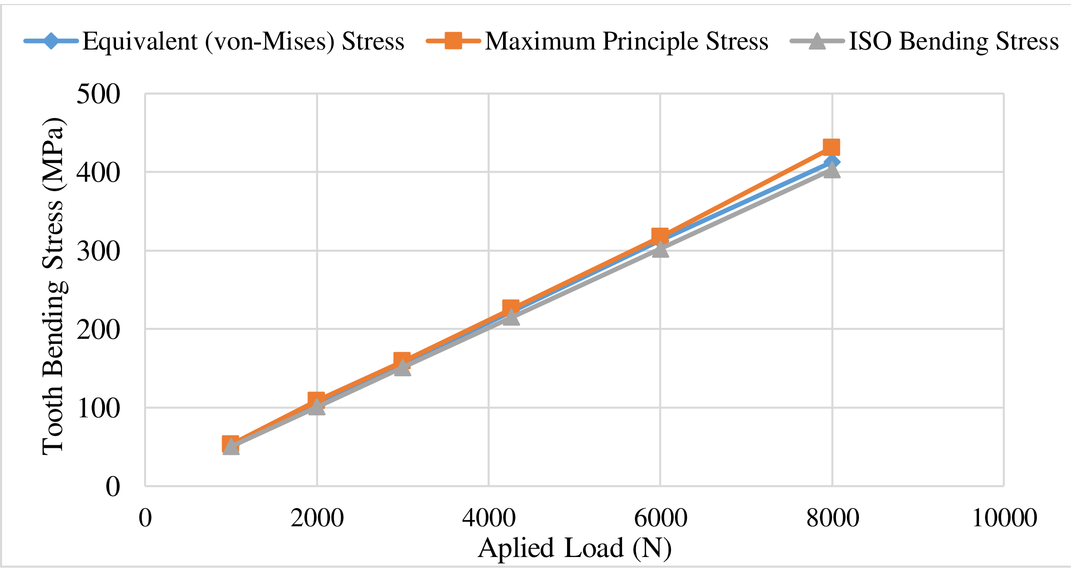

Figure 5.2 Tooth Bending Stress for different forces.

The values obtained in ANSYS Workbench (18.1) screenshots are given in Figure 5.2. When FEM results are analyzed, it is seen that Equivalent (von-Mises) stress values are closer to ISO stress values than Maximum principle stress value.

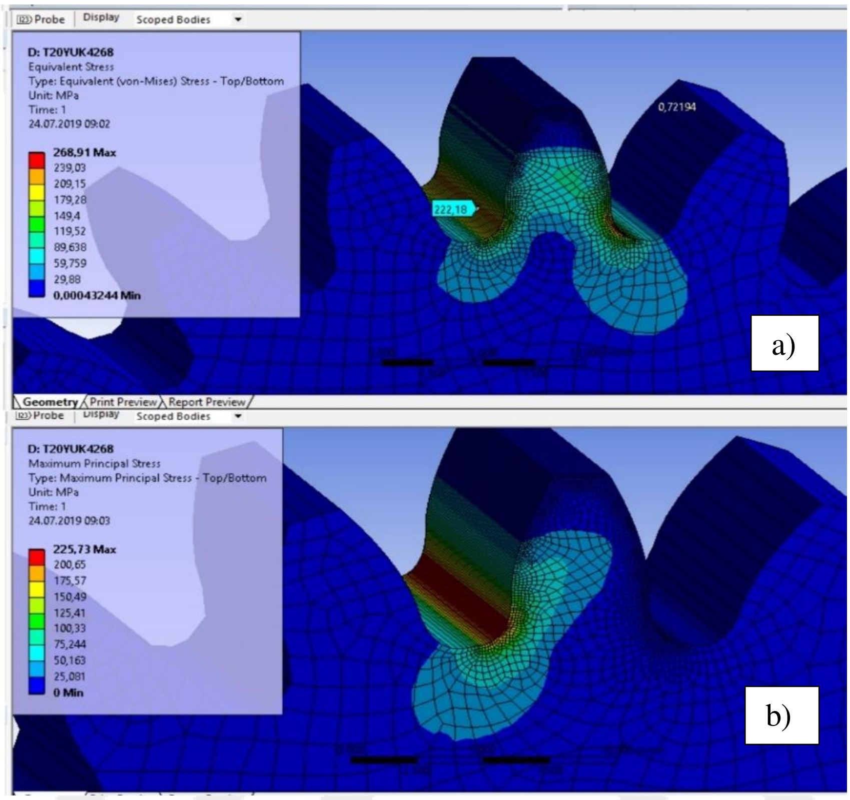

Figure 5.3 Stress distribution on gear tooth root. a) Equivalent (von-Mises) stress b) Maximum Principle Stress

5.2 Effect of Rim Thickness

Gear rim thickness, which is one of the most important parameters in gear design, has been the subject of many studies. The main theme of this work is the thin rim thickness gears shown in Figure 5.4., but there are some limitations here. The most important of these limitations is fatigue life due to bending. In addition, considering the crack initiation and propagation phase, which forms the fatigue life of a tooth, the crack propagation life is short and can cause unexpected fractures. Therefore, fatigue errors due to insufficient rim thickness are frequently encountered even if many effective parameters are made properly in the formation of gear geometry. The effect of rim thickness is shown in Table 5.4.

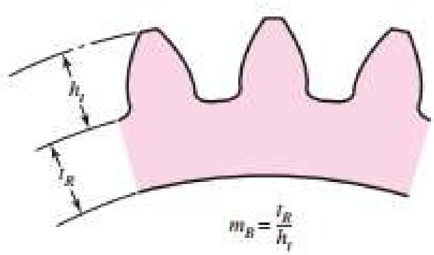

Figure 5.4 Ratio of rim thickness to the tooth height [50].

Table 5.3 Spur gear characteristic for various rim thicknesses

GEAR PROPERTIES	CASE II (Rim Thickness)		
Forces (N)	4268		
Rim Thickness	1*h	1.5*h	2*h
Teeth Number	20		
Press. Angle (°)	20		
Module (m)	3		
Addendum (ha)	1.0*m		
Dedendum	1.25*m		
Tool Tip Radius Coefficient	0.3		
Face Width (mm)	20		

In this case, gear tooth models with various rim thicknesses (1*h, 1.5*h, 2*h) were analyzed as given in Table 5.3. It is seen in Table 5.4., that at lowest bending stresses occurred in 2*h models. As can be seen from the Figure 5.5, ISO formulations have no direct effect on various rim thickness stress calculations. In the ISO standards, the calculation of the stress of the gears is made an assumption. That is seen in Table 5.4 stress is calculated on the model assuming that there is no shaft hole in the gear.

Table 5.4 Stress values of gear for different rim thickness

Case 2 (Load 4268)			
Rim Thickness	1.0*h	1.5*m	2.0*h
Equivalent (von-Mises) Stress	231.88	223.38	222.18
Maximum Principle Stress	247.82	234.79	225.73
ISO Bending Stress	231.20	231.20	231.20

However, in the analysis made with the finite element method, the stresses in the tooth root decreased with increasing rim thickness as seen Figure 5.5. In FEM analyzes, when the size of the shaft hole is reduced too much stresses are concentrated in this section because of the shaft hole is used as fixed support. The counter colored photo taken from Ansys shows the Equivalent (von-Mises) Stress and Maximum Principle Stress as seen Figure 5.6

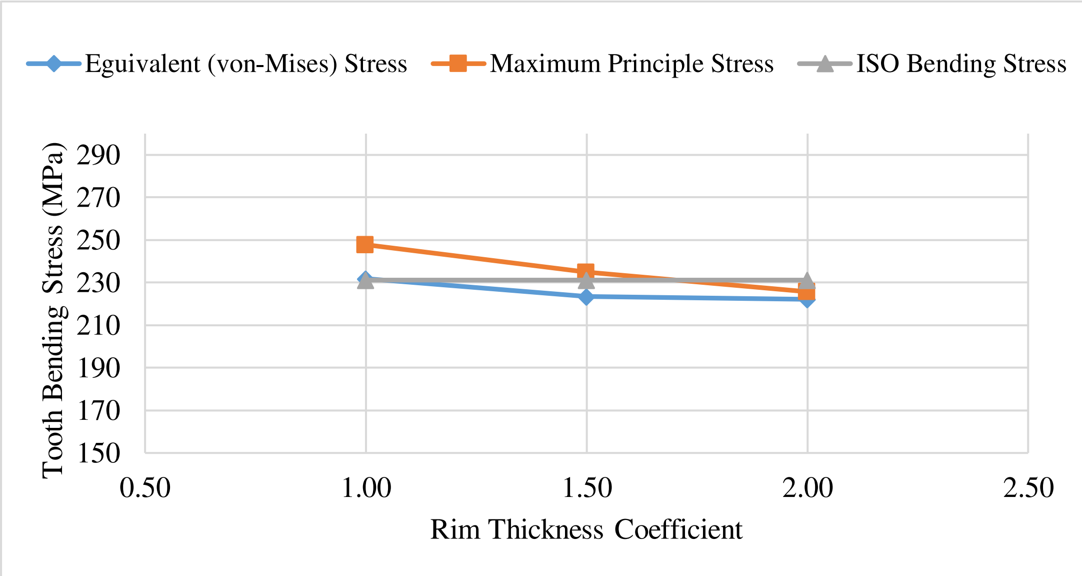

Figure 5.5 Tooth Bending Stress for different rim thicknesses

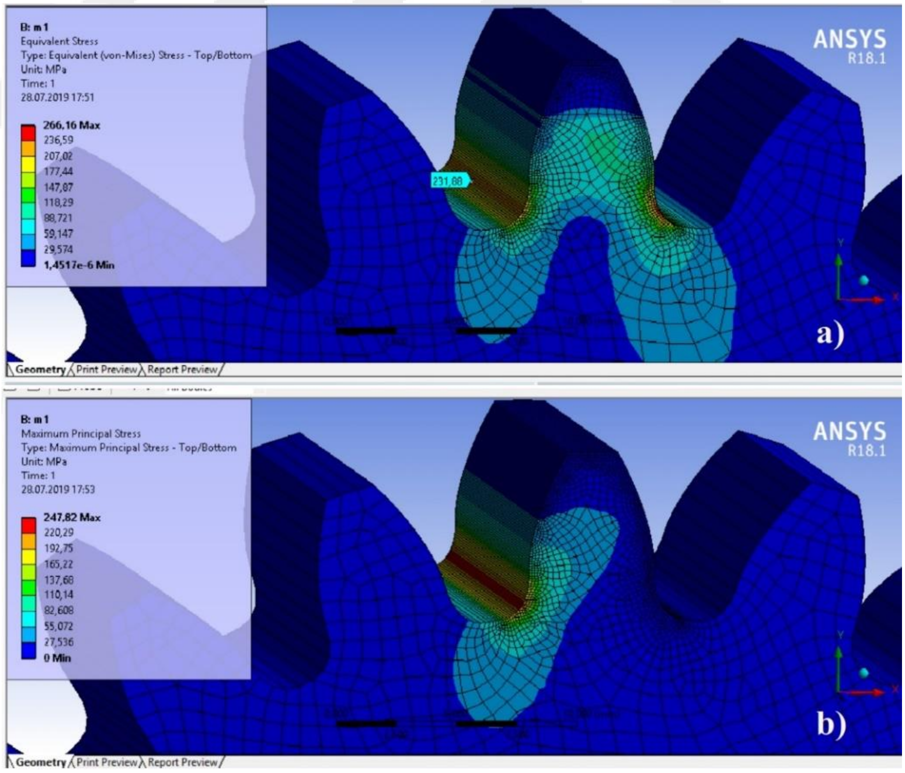

Figure 5.6 Stress distribution on gear tooth root. a) Equivalent (von-Mises) stress, b) Maximum Principle Stress

5.3 Effect of Number of Teeth

At this stage, the effect of the teeth number on tooth root stress is investigated. In order to do that, six different model with variable number of teeth are created and all the other gear parameters are same as seen in Table 5.5.

Table 5.5 Spur gear characteristics for different teeth numbers

GEAR PROPERTIES	CASE III (Teeth Number)					
Forces (N)	4268					
Rim Thickness	2*h					
Teeth Number	20	40	60	80	100	120
Press. Angle (°)	20					
Module (m)	3					
Addendum (ha)	1.0*m					
Dedendum	1.25*m					
Tool Tip Radius Coefficient	0.3					
Face Width (mm)	20					

In this part of the study, the effects of the number of teeth on tooth root stresses were analyzed and compared with ISO stress values, results are given Table 5.6. The increment in the number of teeth, increase the gear size because of the gear module is kept constant, therefore the toot root stresses are reduced.

As can be seen from Figure 5.7, the number of teeth 80, 100 and 120 slightly changed tooth root stresses. The reduction in ISO stress values was much more limited.

Table 5.6 Stress values of gear for different teeth numbers

Case III (Teeth Number)						
Teeth Number	20	40	60	80	100	120
Equivalent (von-Mises) Stress	222.18	195.34	172.98	172.72	168.91	168.50
Maximum Principle Stress	225.73	204.20	181.08	183.54	177.3	176.66
ISO Bending Stress	215.11	184.69	177.90	175.69	175.64	175.34

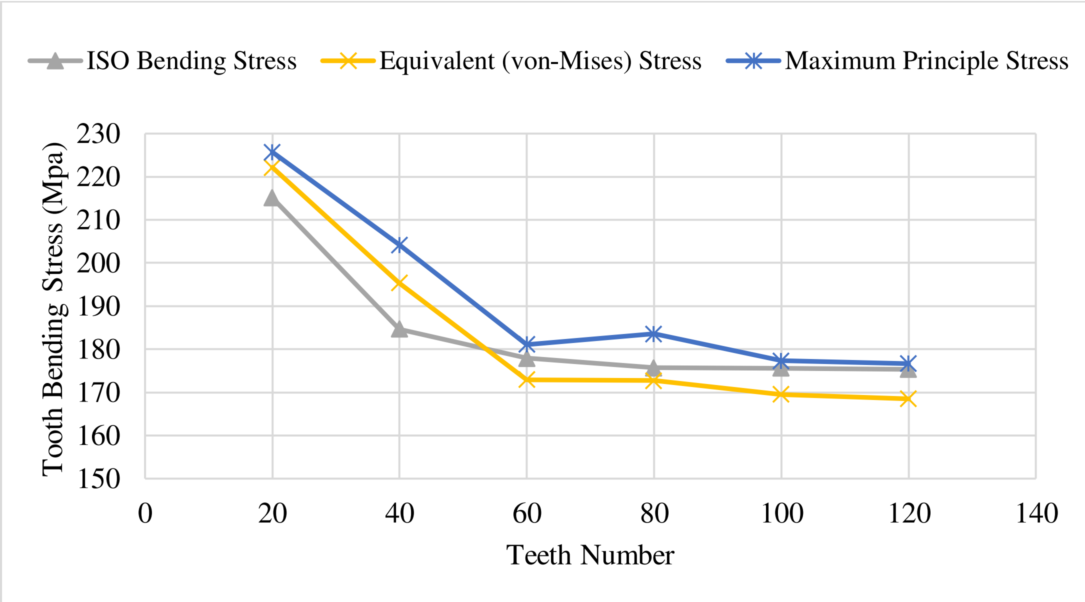

Figure 5.7 Tooth Bending Stress for teeth number

Ansys Workbench screenshots with Maximum Principle stress and Equivalent (von-Mises) stresses are given in Figure 5.8.

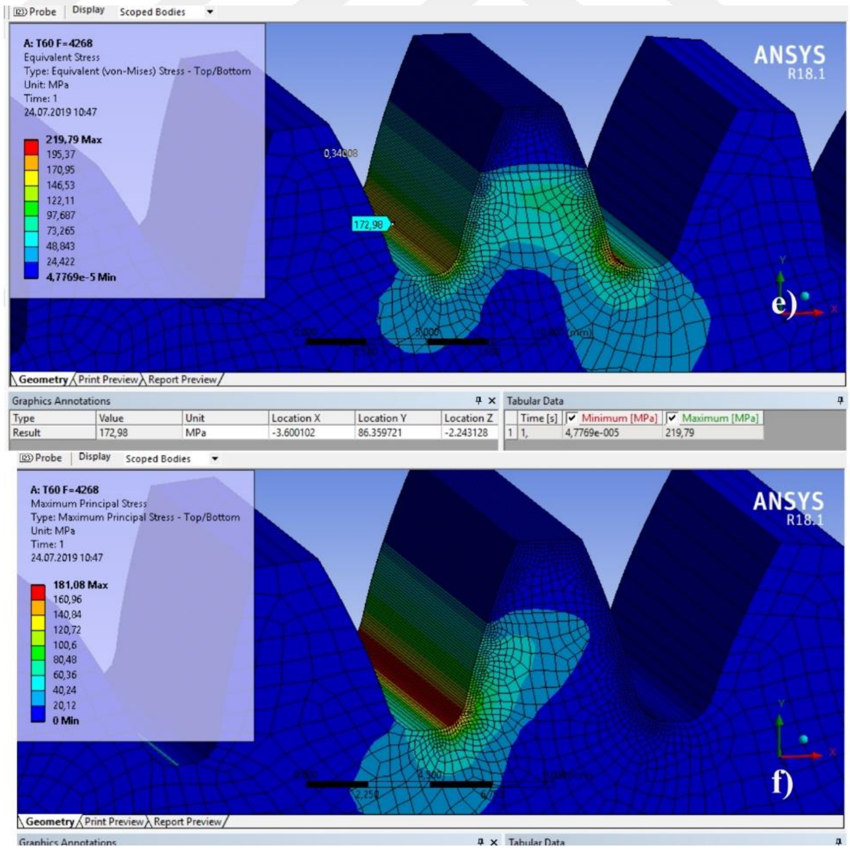

Figure 5.8 Stress distributions on gear tooth root. a) Equivalent (von-Mises) stress, b) Maximum Principle Stress

5.4 Effect of Pressure Angle

At this stage, the effects of the pressure angle on the tooth root stresses are investigated. Four different pressure angles are compared and all other parameters of gear kept same, as given in Table 5.7.

Table 5.7 Spur gear characteristic for different pressure angles

GEAR PROPERTIES	CASE IV			
Force (N)	4268			
Rim Thickness (mm)	2*h			
Teeth Number	20			
Pressure Angle (°)	18	20	22.5	25
Module (mm)	3.0			
Addendum (mm)	1.0*m			
Dedendum (mm)	1.25*m			
Tool Tip Radius Coefficient	0.3			
Face Width (mm)	20			

Gear models with different pressure angles were analyzed with the aspect of gear tooth root stresses. Table 5.8 shows FEM stress result comparison with ISO analytical calculated stresses. The changes in pressure angle effects on tooth root stresses. As can be given in Figure 5.9, about 10 % decrease in stress values was observed an increase of pressure angle from 18° to 25°.

Table 5.8 Stress values of gear for different pressure angles

Case 3 (Load 4268)				
Pressure Angle	18	20	22.5	25
Equivalent (von-Mises) Stress	230.67	222.18	218.43	205.03
Maximum Principle Stress	236.00	225.73	228.99	220.50
ISO Bending Stress	223.95	215.11	204.94	194.90

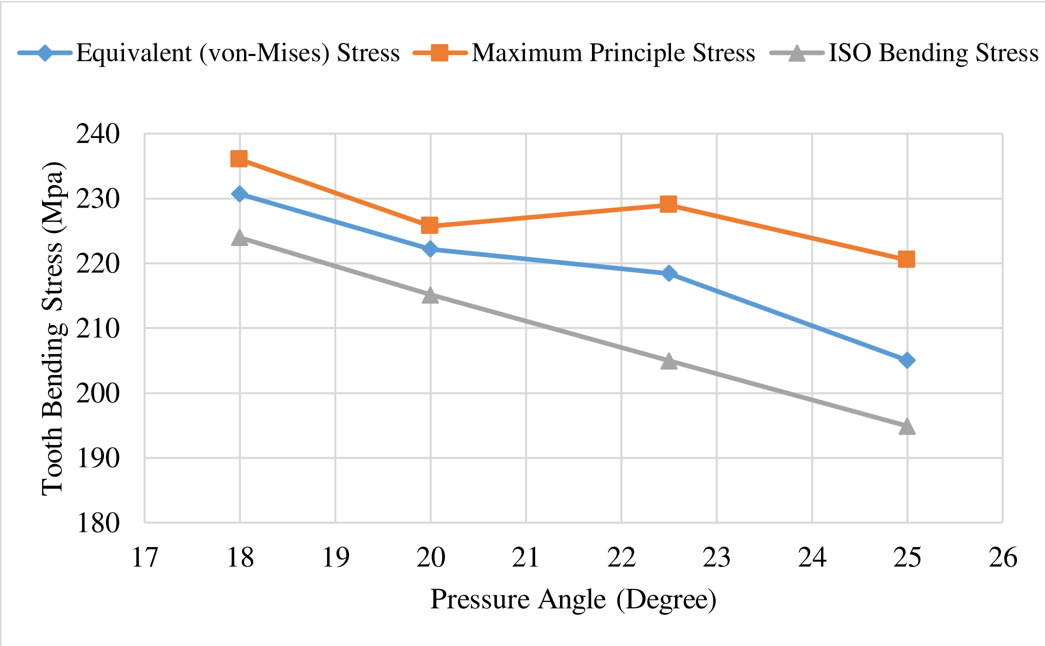

Figure 5.9 Tooth Bending Stress for different pressure angles

The counter colored photo taken from Ansys shows the Equivalent (von-Mises) Stress and Maximum Principle Stress as seen Figure 5.10

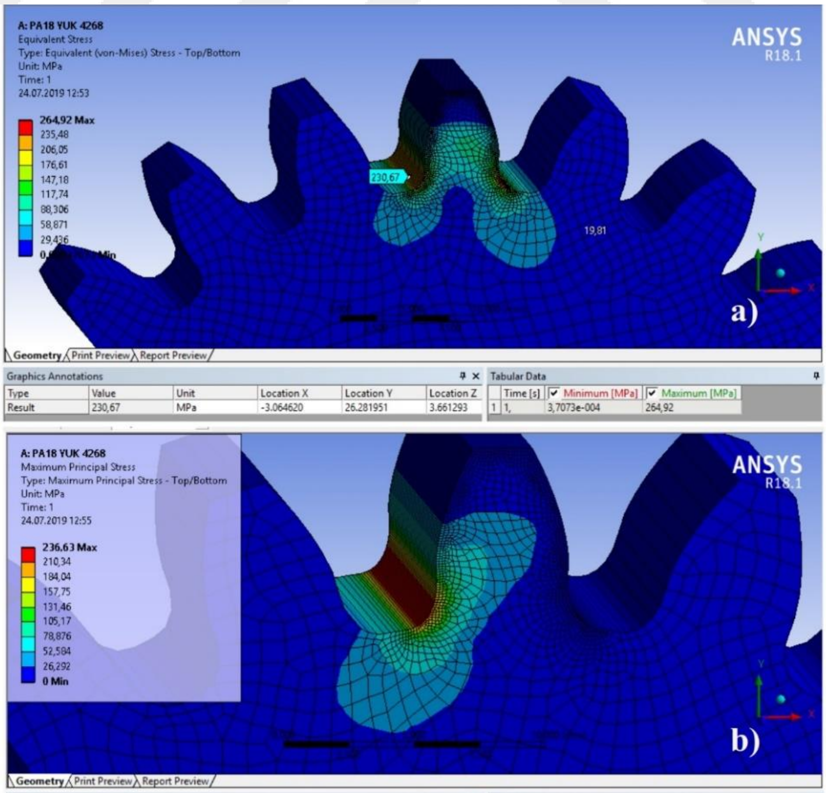

Figure 5.10 Stress distribution on gear tooth root. a) Equivalent (von-Mises) stress, b) Maximum Principle Stress

5.5 Effect of Module

In this case all the gear parameters are kept same, and the different gear module shown in Table 5.9. (1, 2, 3, 4, 5, 6) is analyzed with respect to module of gear effect the tooth root stress.

Table 5.9 Spur gear characteristic for different modules

GEAR PROPERTIES	CASE V					
Module (mm)	1	2	3	4	5	6
Teeth Number	20					
Pressure Angle (°)	20					
Rim Thickness (mm)	2*h					
Tool Tip Radius Coefficient	0.3					
Addendum (mm)	1.0*m					
Dedendum (mm)	1.25*m					
Face Width (mm)	20					
Force (N)	4268					

Table 5.10 Stress values of gear for different modules

Case 5 (Load 4268)						
Module	1	2	3	4	5	6
Equivalent (von-Mises) Stress	526.32	311.02	222.18	171.88	144.38	121.1
Maximum Principle Stress	565.96	333.69	225.73	174.37	147.17	121.94
ISO Bending Stress	645.33	322.67	215.11	161.33	129.07	107.56

As can be seen in Table 5.10, the module is a highly effective parameter in gear root stresses. As the gear module increases, root stresses decreased as seen Figure 5.9. The main reason for this is that the size of the gears increases with the increase in the module value provided that the number of teeth is constant.

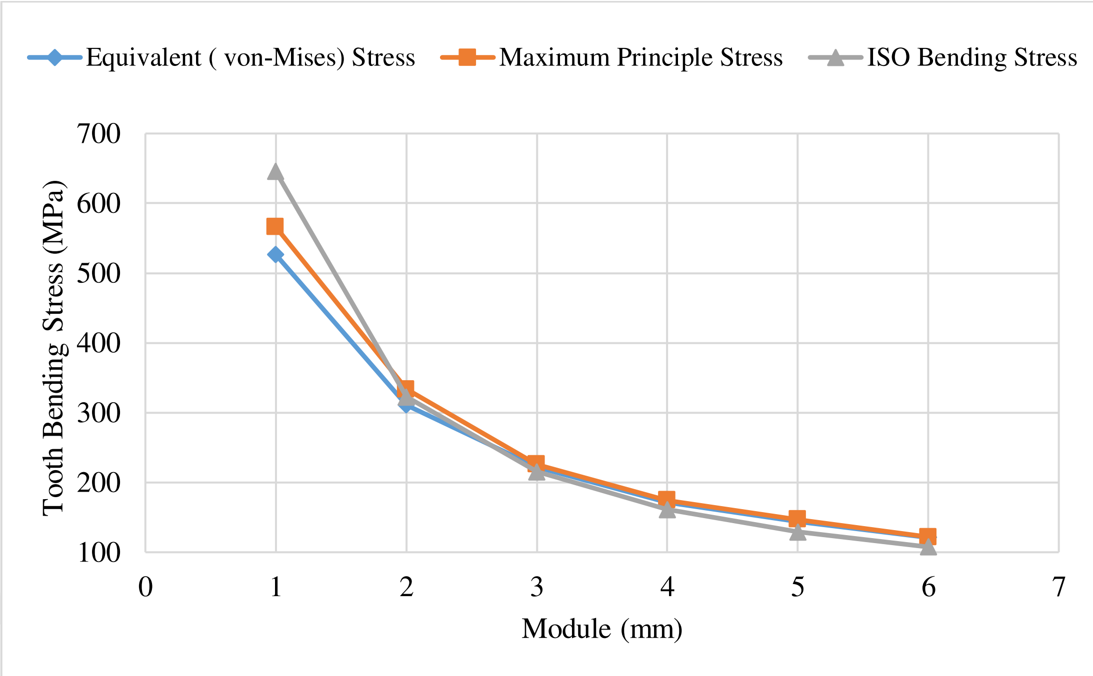

Figure 5.11 Tooth Bending Stress for different modules

The counter colored photo taken from Ansys shows the Equivalent (von-Mises) Stress and Maximum Principle Stress as seen Figure 5.12

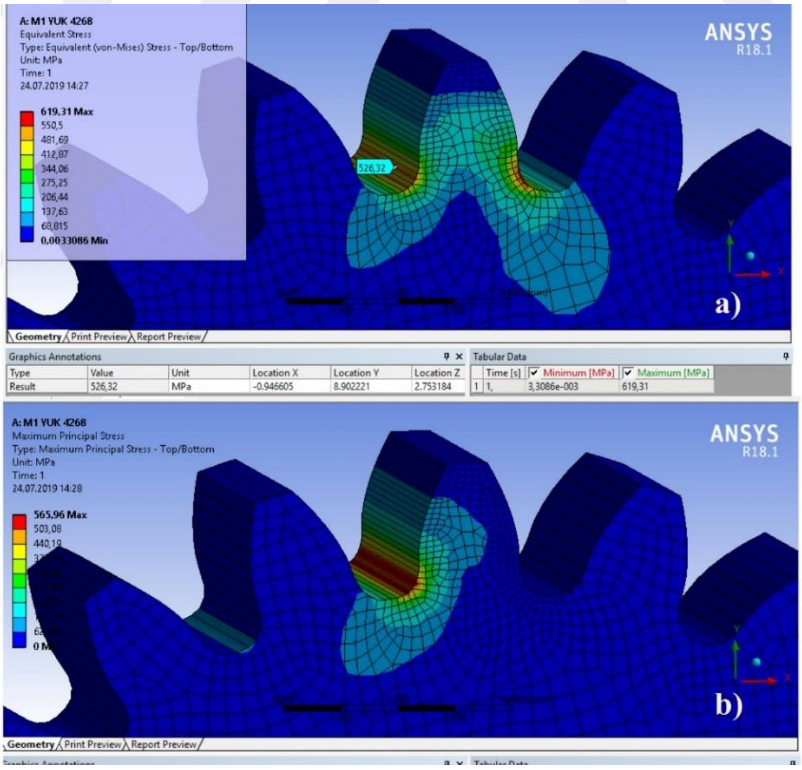

Figure 5.12 Stress distributions on gear tooth root. a) Equivalent (von-Mises) stress, b) Maximum Principle Stress

5.6 Effect of Addendum

Addendum is one of the most important parameters in the modeling of gear wheels. The modeling of addendum and dedendum should be considered together. Typically, 1.25*m Dedendum is used when 1*m addendum is used in designs. In this study the standard uses of model is considered as a base. Beside this, the effects of different models are analyzed. Specifications of gear models are shown in Table 5.11.

Table 5.11 Spur gear characteristic for different addendum values

GEAR PROPERTIES	CASE VI			
Module (mm)	3.0			
Teeth Number	20			
Pressure Angle (°)	20			
Rim Thickness (mm)	2*h			
Tool Tip Radius Coefficient	0.3			
Addendum (mm)	1.0*m	1.1*m	1.2*m	1.3*m
Dedendum (mm)	1.4*m			
Face Width (mm)	20			
Force (N)	4268			

Table 5.12 Stress values of gear for different addendum values

Case 6 (Load 4268)				
Addendum	1.0	1.1	1.2	1.3
Dedendum	1.4	1.4	1.4	1.4
Equivalent (von-Mises) Stress	242.56	232.56	219.34	224.53
Maximum Principle Stress	256.97	249.02	234.31	233.31
ISO Bending Stress	224.57	216.66	209.34	202.59

In this analyzes made here, it was observed that the stress level decreased with the increase of addendum as seen Table 5.12. One of the main reasons for this is that the value of the horizontal component of the force acting on the surface decreases with the extension of the addendum. Stress change was more limited in the analysis performed in FEM compared to the ISO stress value shown in Figure 5.13 clearly.

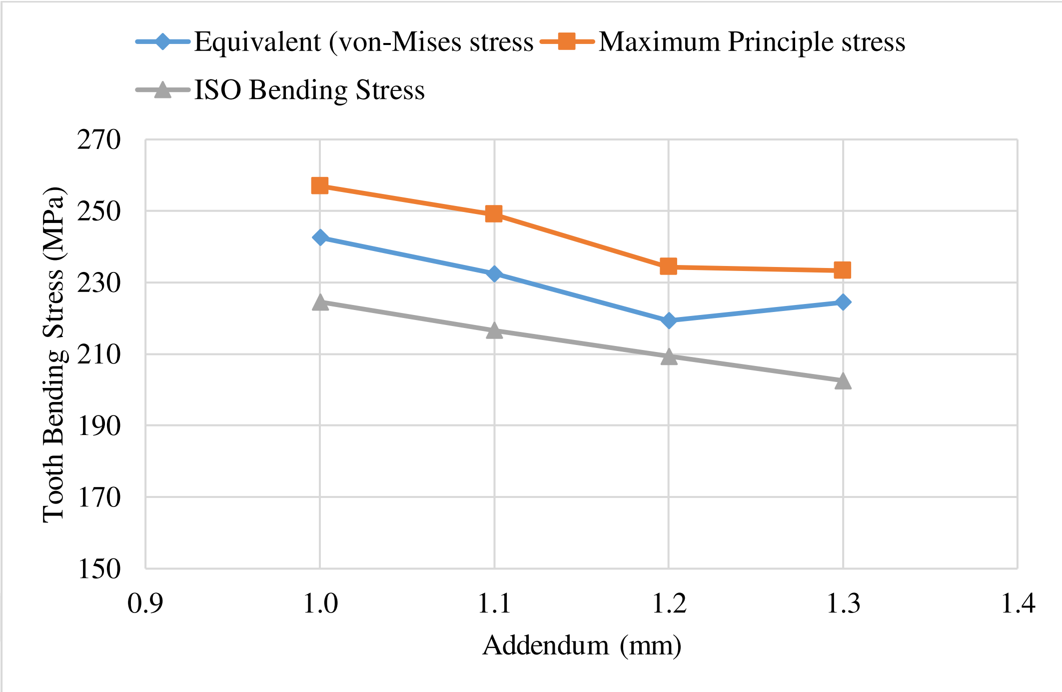

Figure 5.13 Tooth Bending Stress for different addendum values

The counter colored photo taken from Ansys shows the Equivalent (von-Mises) Stress and Maximum Principle Stress as seen Figure 5.14.

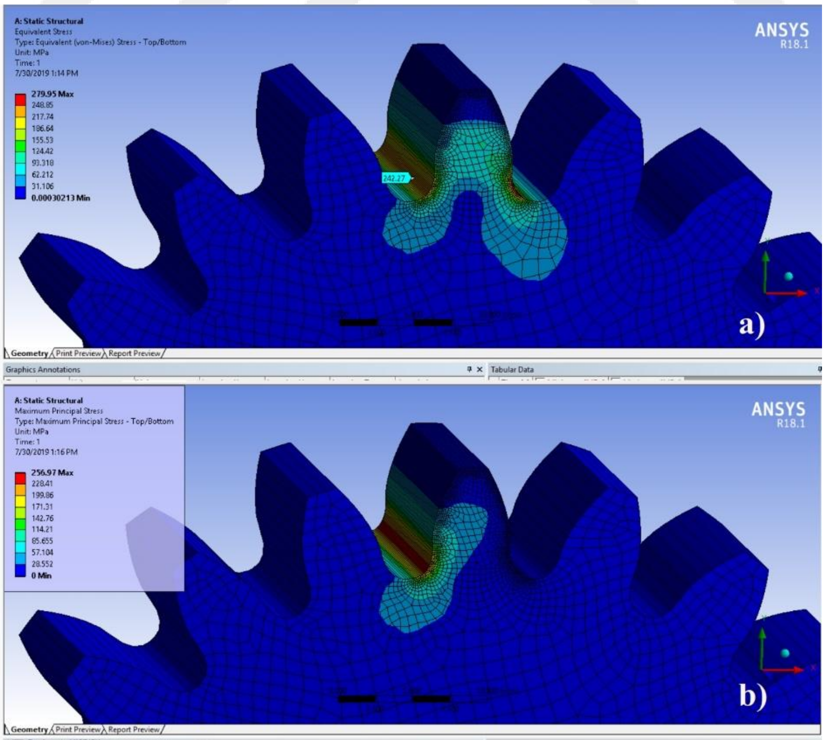

Figure 5.14 Stress distributions on gear tooth root. a) Equivalent (von-Mises) stress, b) Maximum Principle Stress

5.7 Effect of Tool Tip Radius

The modelled shape and minimum radius of gear tooth root fillet curvature depend on the design and type of the cutting tool. As well as the shape and radius of the root fillet, smoothness between the root area and the active profile of a tooth can have a significant impact on its strength. Tool tip radius coefficient has a big effect on the tooth root stress. The gear specifications are given 5.13.

Table 5.13 Spur gear characteristic for different tool tip radius coefficients

GEAR PROPERTIES	CASE VII				
Module (mm)	3.0				
Teeth Number	20				
Pressure Angle (°)	20				
Rim Thickness (mm)	2*h				
Tool Tip Radius Coefficient	0.1*m	0.2*m	0.3*m	0.38*m	0.47*m
Addendum (mm)	1.0*m				
Dedendum (mm)	1.25*m				
Face Width (mm)	20				
Force (N)	4268				

As shown in Table 5.14, the tool tip radius coefficient has changed the root stresses of the gears considerably. The tool type radius coefficient used here is 0.38, which is the maximum value that can be used in the design of gears in ISO standards. However, Akpolat and Şahin [52] showed in their study that tool tip radius coefficient could be used safely up to 0.47.

Table 5.14 Stress values of gear for different tool tip radius coefficients

Case 7 (Load 4268)					
Tool Tip Radius Coefficient	0.1	0.2	0.3	0.38	0.47
Equivalent (von-Mises) Stress	253.85	230.16	222.18	219.44	206.65
Maximum Principle Stress	272.9	248.33	225.78	229.06	210.81
ISO Bending Stress	248.92	231.20	215.11	203.38	190.86

The ISO stress value showed a linear decrease as the tool tip radius coefficient value increased. However, it is seen in Figure 5.15 that there are slight fluctuations especially in maximum principle stress value.

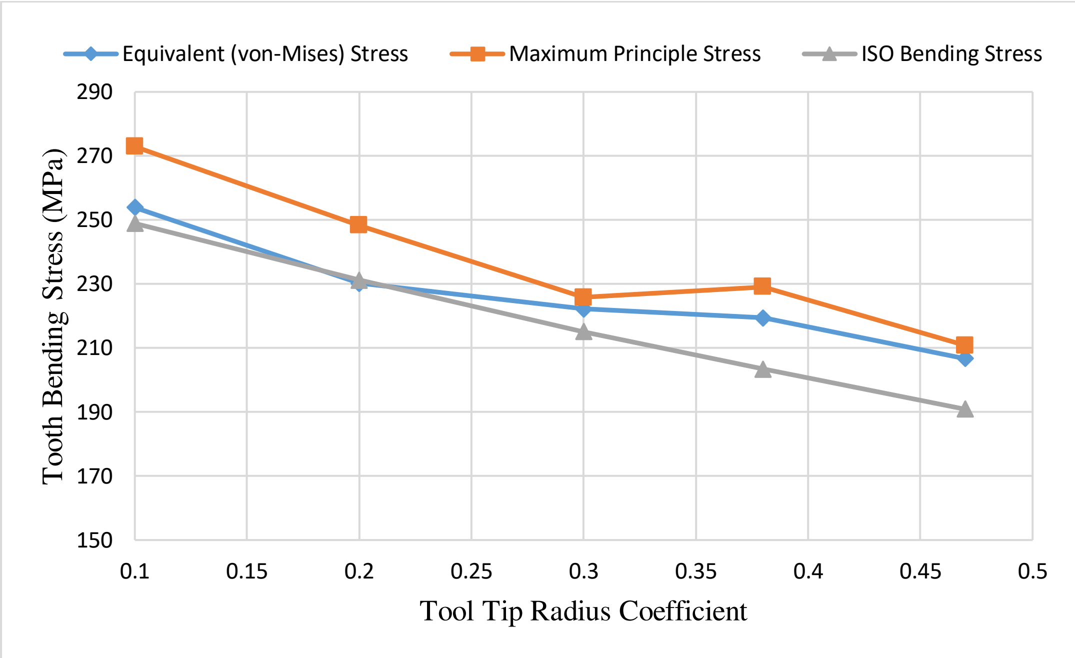

Figure 5.15 Tooth Bending Stress for different tool tip radius coefficients

The counter colored photo taken from Ansys shows the Equivalent (von-Mises) Stress and Maximum Principle Stress as seen Figure 5.16

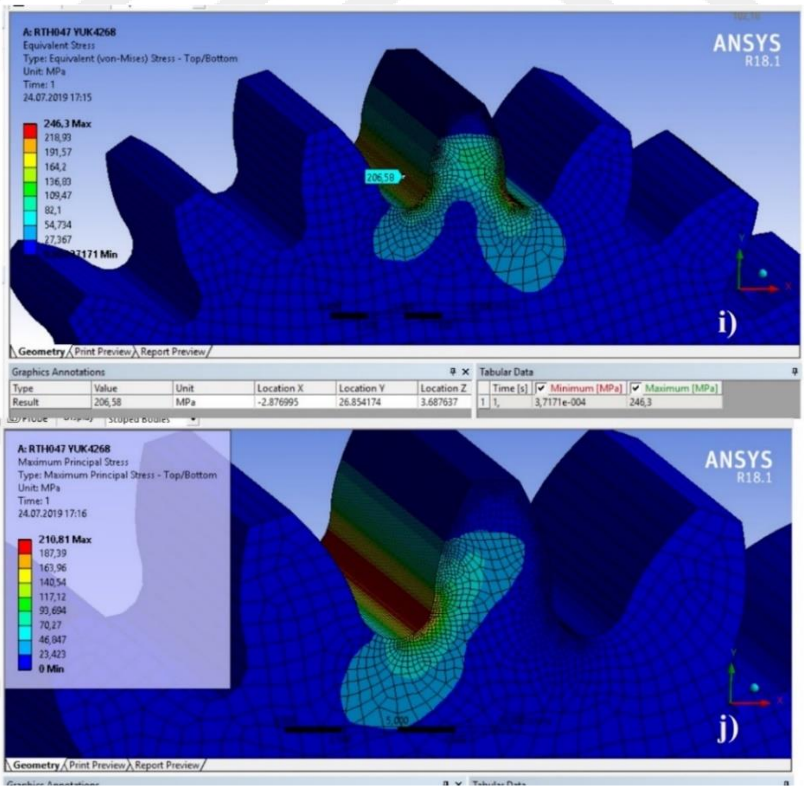

Figure 5.16 Stress distributions on gear tooth root. a) Equivalent (von-Mises) stress, b) Maximum Principle Stress

5.8 Effect of Face Width

At this stage, the effects of face width are investigated. It should be noted that although analyzes are made in 2D, the face width is also accepted as a variable parameter. The solution of the models in the new generation finite element analysis systems is possible with this method. The situation directly effects to the results that have been evaluated, and the other gear parameters are the same as given Table 5.15.

Table 5.15 Spur gear characteristic for different face width values

GEAR PROPERTIES	CASE VIII					
Module (mm)	3.0					
Teeth Number	20					
Pressure Angle (°)	20					
Rim Thickness (mm)	2*h					
Tool Tip Radius Coefficient	0.3*m					
Addendum (mm)	1.0*m					
Dedendum (mm)	1.25*m					
Face Width (mm)	10	20	30	40	50	60
Force (N)	4268					

As the face width increases, the bending stress in the spur gears decreases because the force acting on the unit area decreases. ISO stress values and FEM values are very close to each other as seen Figure 5.17. In gears with small face widths, the stress values obtained with FEM are larger, whereas with the increases face width the ISO stress values are greater than FEM stress values as seen Table 5.16.

Table 5.16 Stress values of gear for different face width values

Case 8 (Load 4268)						
Face Width	10	20	30	40	50	60
Equivalent (von-Mises) Stress	465.43	222.18	141.5	101.36	77.666	62.13
Maximum Principle Stress	481.24	225.73	147.65	107.02	83.621	67.635
ISO Bending Stress	430.42	215.11	143.41	107.56	86.04	71.70

The counter colored photo taken from Ansys shows the Equivalent (von-Mises) Stress and Maximum Principle Stress as seen Figure 5.18.

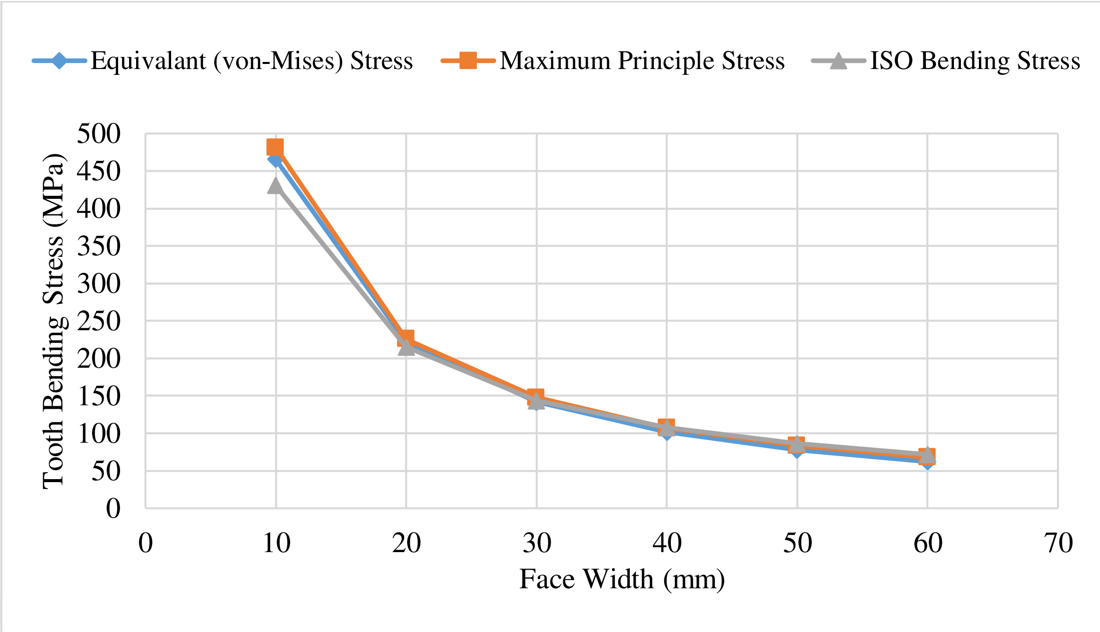

Figure 5.17 Tooth Bending Stress for face width

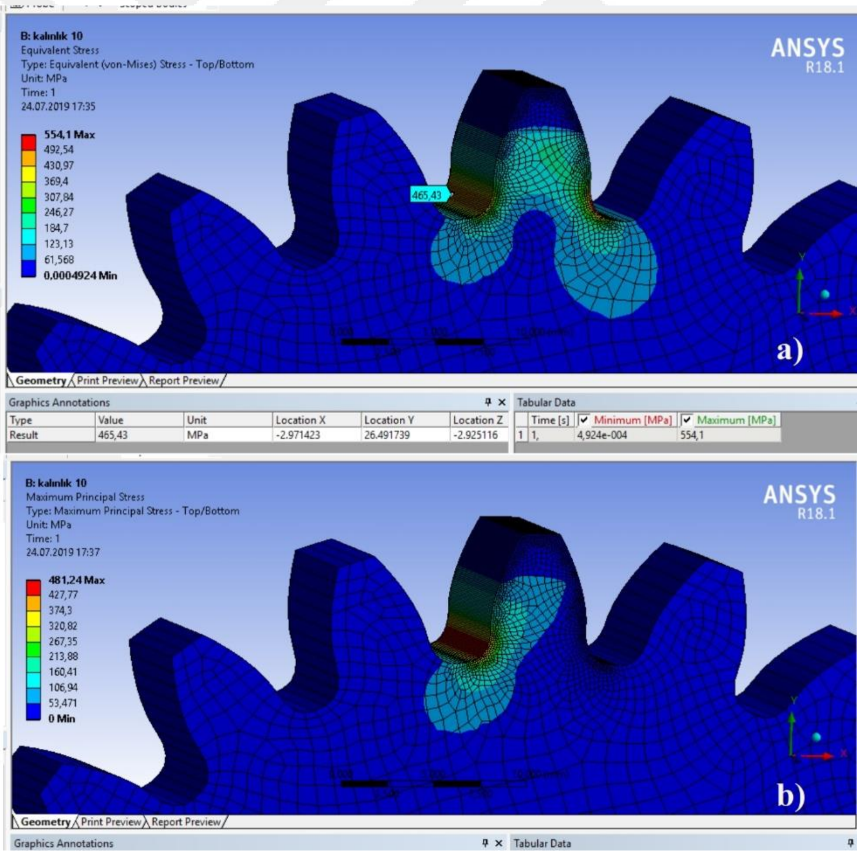

Figure 5.18 Stress distributions on gear tooth root. a) Equivalent (von-Mises) stress, b) Maximum Principle Stress

CHAPTER 6

BENDING FATIGUE CASE STUDY

In this part of the study, in order to confirm the accuracy of life values obtained with FEM, an approach was made using the data of the experimental study in the literature. Conrado et all. "A comparison of bending fatigue strength of carburized and nitrided gears for industrial applications" named article, applied heat treatment to different types of steel. The surface hardening of the gear material was carried out and the tensile properties were determined experimentally [16]. The main mechanical properties of gear material is listed in Table 6.1. N3 indicates low alloy steel 20MnCr5 as a base materials and obtained gas nitriting a carburizing steel grade.

Table 6.1 Main data of the test gear specimen family (tensile test data)

Family (Code)	Base steel (Grade)	R_m (MPa)	R_s (MPa)	A (%)	Heat treatment (Type)
N3	20MnCr5	1412	1118	11	34 h gas nitriting

The main geometric properties of gear samples are listed in Table 6.2. The gear geometry was selected particularly for this experimental research program in order to be the character of gears for industrial practice and to meet the geometric needs of reference test gears defined in the standard ISO 6336-5:2003 [51]. The test gears, modeled with a full-body gear blank on account of avoiding any effect finally induced by small rim thickness, had a face width of 30 mm, a 4 mm module, and had 28 teeth. All the gear samples were produced according to these geometric properties with the aim of quantifying the effects on the bending fatigue strength of varied base materials and thermo-chemical surface treatments.

Table 6.2 Main geometric characteristics of test gear specimens

Description	Symbol	Unit	Value
Number of teeth	z	(-)	28
Module	m	mm	4
Pressure angle	α	º	20
Helix angle	β	º	0
Profile shift coefficient	x	(-)	0
Reference diameter	d	mm	112.00
Base diameter	d_b	mm	105.25
Tip radius	d_a	mm	120.00
Root diameter	d_f	mm	101.91
Face width	b	mm	30.00

The tests were performed at the laboratories of the Department of Mechanical Engineering of Politecnico di Milano by utilizing Schenck resonance pulsator with a load capacity of 60 kN. The two contact anvils indicate in Figure 6.1, specially designed to carry out tests on gear samples, take place the standard test fixture of this test rig originally sophisticated for compression/tension fatigue tests on cylindrical samples.

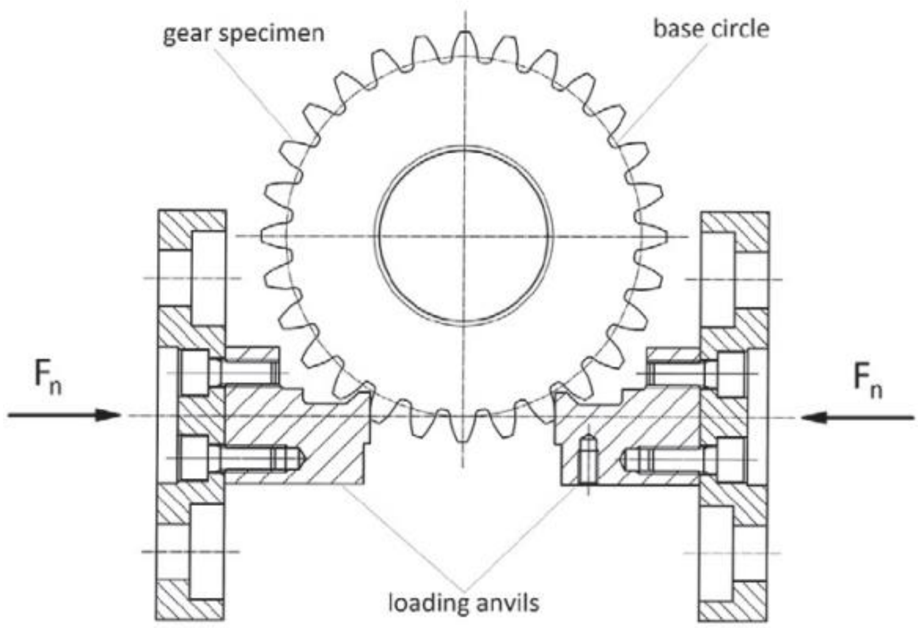

Figure 6.1 Gear specimen mounted in the clamping system [16].

After the first up-and-down series, the tests were conducted in the finite life range in order to approximation the S-N diagrams in this region. For each material group, three load levels, above the load-interval operate to state the fatigue limit, were used. The raw data acquired are shown in Figure 6.2 in terms of tooth root stresses σ_F (suitable to the maximum test load applied F_n) the opposite the number of cycles to failure N.

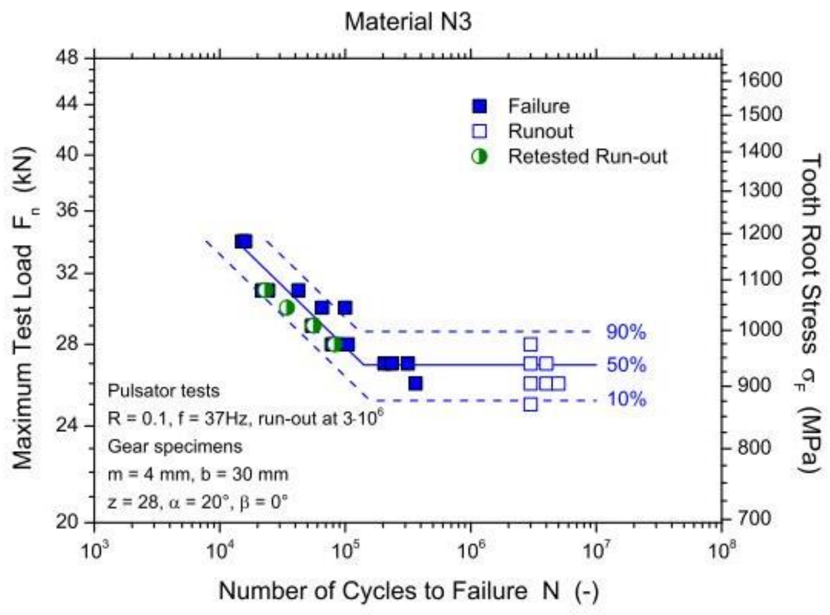

Figure 6.2 Result of tests on nitrided gear (N3) and corresponding S-N curves for different failure probabilities (10%, 50% and 90%)

The bending fatigue strength of nitrided gear steel was characterized by means of Single Tooth Bending Fatigue Tests. The aim of the study was determining the influence of the combination of gear steels and thermo-chemical treatments only. That is why all the gear samples were produced according to the same geometric model.

In this study, the values obtained from the S-N graph are taken by means of the scales used in the graph and given as Table 6.3. In this table, the stresses opposite to the number of cycle data's were transferred to ANSYS Workbench. The gear model specified in the study was formed according to the stated specifications in a homemade software [39-40]. Boundary conditions were created in ANSYS Workbench within the conditions specified in the experimental study. The results obtained by applying the load values specified in the experimental study in ANSYS Workbench are given in

Table 6.3. Stress values obtained in the experimental study and related life cycle numbers and FEA results are very similar.

Table 6.3 Experimental and FEM Comparison of the Stress- number of cycle

Force (N)	Number Of Cycle Literature	Experimental Stress (MPa)	Number Of Cycle	Equivalent (Von-Mises) Stress (MPa)	Maximum Principle Stress (MPa)
34000	17000	1190	16587	1164	1191.6
31000	41500	1065	40352	1064.4	1085
30000	60000	1030	58660	1032	1050.7
28000	100000	965	102860	963.45	980.63
27000	200000	930	203250	929.13	945.61
25500	350000	900	395250	885.2	900.83
24500	3000000	860	3000000	841.79	857.59

S-N curves generated by both experimental data and FEA data are given in Figures 6.3 and 6.4.

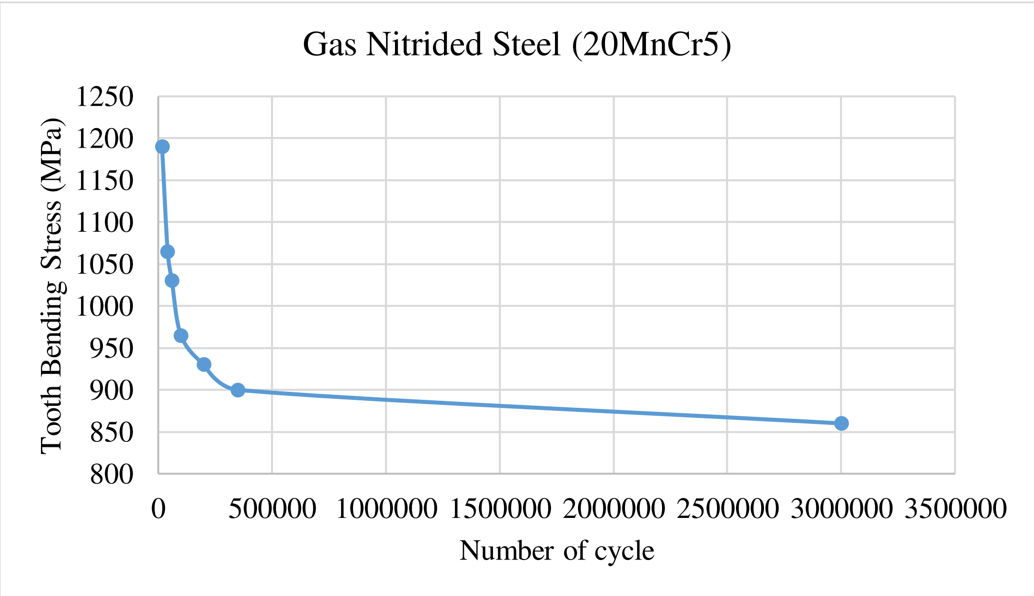

Figure 6.3 S-N curve generated from experimental study data

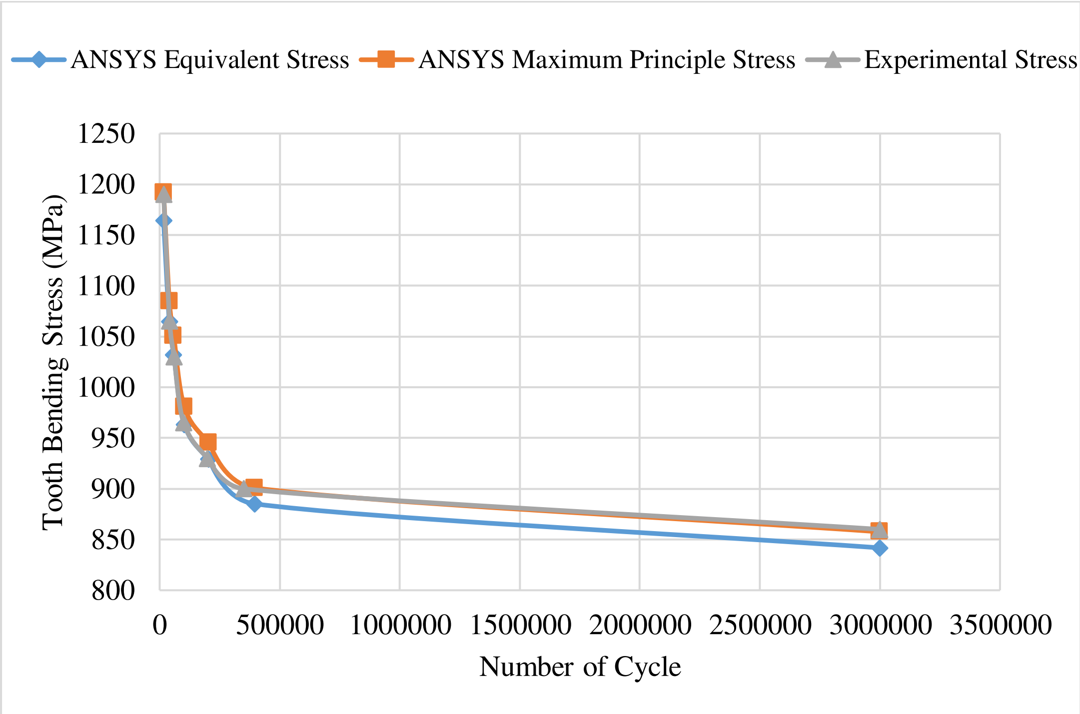

Figure 6.4 S-N curve generated from FEA and experimental data

In this part of the study, tooth root fatigue lives are discussed. The critical section in the tooth root region is easily determined in the analysis with the finite element method. Various models installed in finite elements such as load, rim thickness, number of teeth, pressure angle, module, addendum, tool tip radius and face width are analyzed. As a result of the solution, the change of stresses in the critical section and the related bending fatigue life data are obtained and the graphs are drawn.

As a result of the examination of the models in the literature [42, 43], the following issues have been considered in the installation of gear models. For bending fatigue life analysis, only pinion is modeled and the effects are simulated by tooth force. In many similar studies, the models are created according to force applied to single tooth. In singular application of the load, the effect of local agglomeration around the point of application of the load is neglected according to the SAINT-VENANT principle. According to this principle, the effect of regional behavior results from the application of boundary conditions is rapidly damped at a reasonable distance [44, 45]. In this regard, local concentration does not affect the stress value in the root region, which is sufficiently far from the point of application. In many studies, this situation has not been explained in detail, but it has been observed by researchers.

6.1 Effect of Force

As seen in Table 6.4, the applied loads increased the stress values and consequently the number of cycle decreased. When we evaluate these results together, the fatigue graph obtained is given in Figure 6.5. The load value 2000 N and lower values applied in the gear models are in the infinite life area.

Table 6.4 Tooth bending stress and number of cycle for applied force

Case 1(Load)						
Applied Force (N)	1000	2000	3000	4268	6000	8000
Equivalent (Von-Mises) Stress (MPa)	52.105	103.08	156.33	222.18	312.57	412.76
Number of Cycle	1000000	1000000	630320	83292	14389	3637

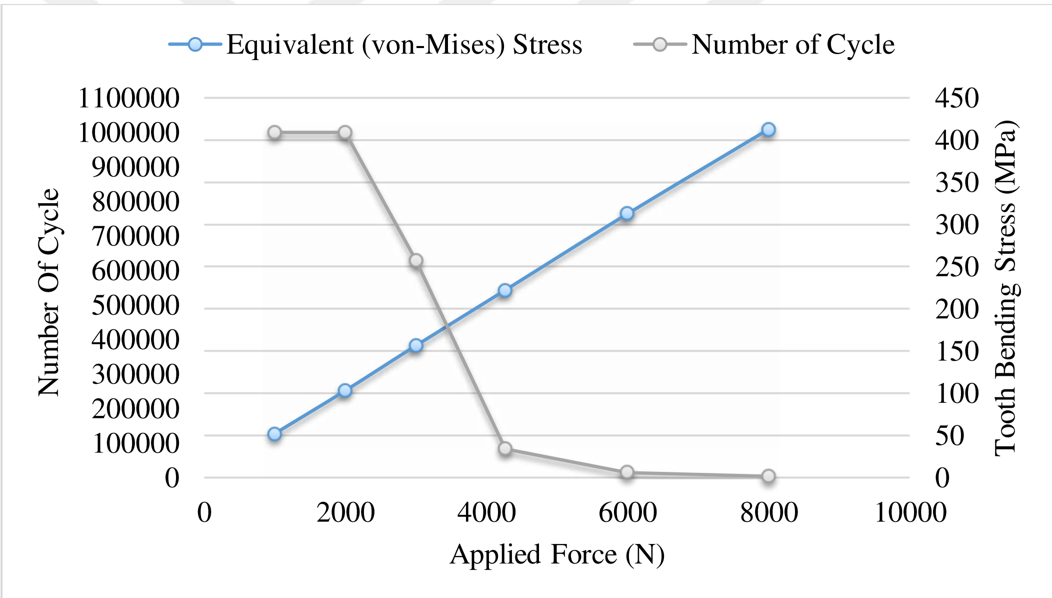

Figure 6.5 Tooth root stress and bending fatigue cycle for different forces

These FEA test results were archived after all the parameters optimized. According to gear standard and to the relevant literature on the topic a semi linear relationship in a semi logarithmic scale between the tooth root stress and the number of cycle to archived as seen Figure 6.6.

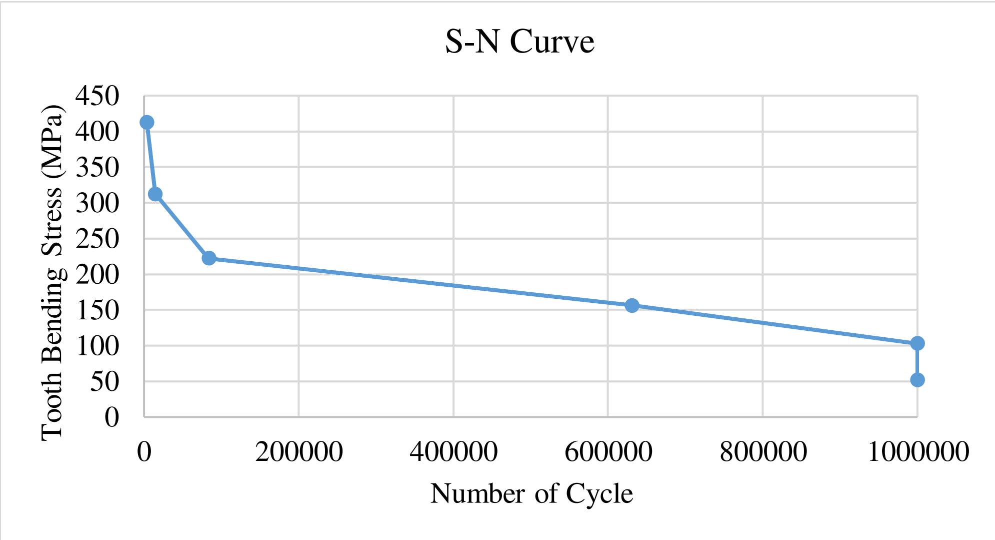

Figure 6.6 S-N curve for structural steel

6.2 Effect of Teeth Number

When we look at the Table 6.5 regarding the results of this study, it is understood that the number of teeth in the gears is an effective parameter on the bending fatigue life. The detailed information can be understood from Figure 6.7.

Table 6.5 Tooth bending stress and number of cycle for different teeth number

Case 2(Load 4268)						
Teeth Number	20	40	60	80	100	120
Equivalent (von-Mises) Stress (MPa)	222.18	195.34	172.98	172.72	168.91	168.50
Number of Cycle	83292	149930	308250	312880	337360	375210

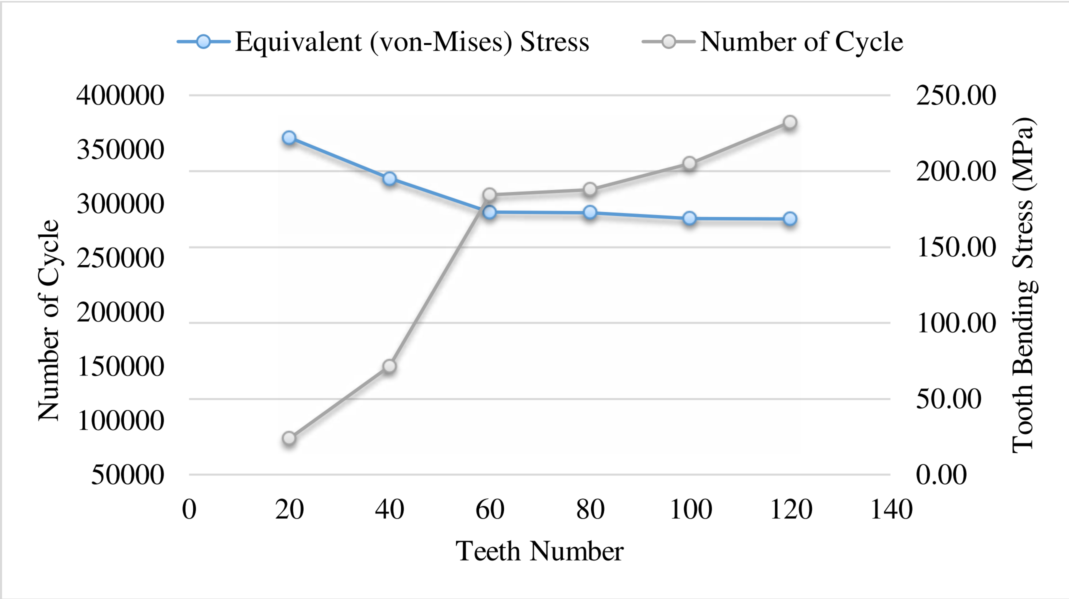

Figure 6.7 Tooth root stress and bending fatigue cycle for different tooth numbers

6.3 Effect of Pressure Angle

When the pressure angle values were analyzed, it was observed that tooth root stresses decreased with increasing pressure angle and fatigue lives increased significantly as seen in Figure 6.8. The FEA results given Table 6.6

Table 6.6 Tooth bending stress and number of cycle for different pressure angles

Case 3 (Load 4268)				
Pressure Angle (Degree)	18	20	22.5	25
Equivalent (von-Mises) Stress (MPa)	230.67	222.18	218.43	205.03
Number of Cycle	71388	83292	89586	118960

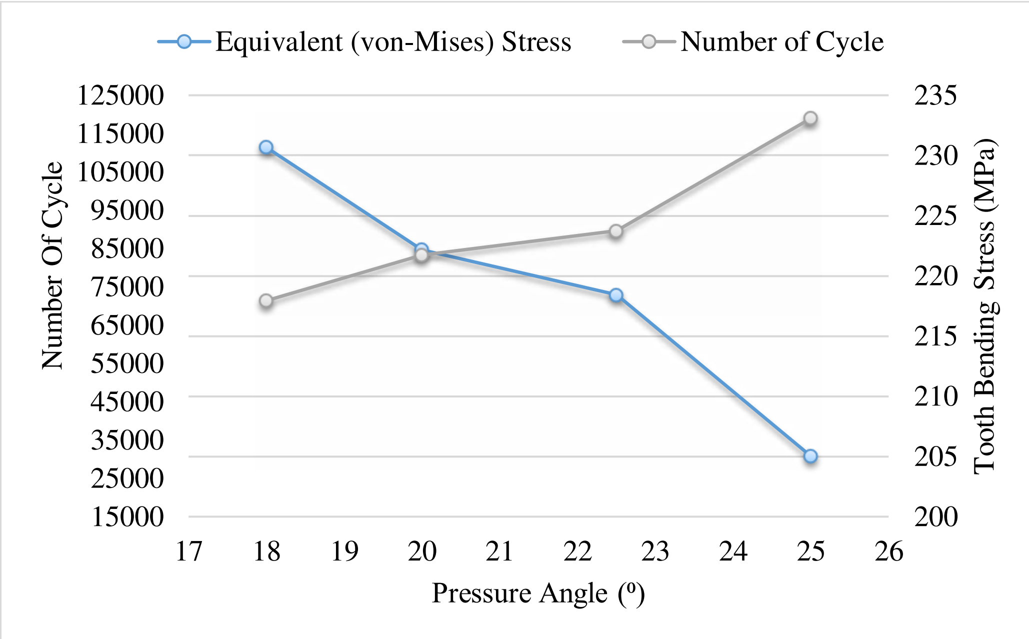

Figure 6.8 Tooth root stress and bending fatigue cycle for different pressure angles

6.4 Effect of Module

As can be seen in Figure 6.9, the module is a highly effective parameter in gear root stresses as well as bending strength. As the gear module increased, root stresses decreased and consequently fatigue life increased as shown in Table 6.7. Mendi et al. [46] created the Borland Delphi 6.0 platform to use the genetic algorithm. They also carried out the choose of ideal module for spur gears as well as made optimization for bevel gears by choosing the ideal shaft diameter, module and rolling bearings [47].

Table 6.7 Tooth bending stress and number of cycle for various modules

Case 4 (Load 4268)						
Module (mm)	1	2	3	4	5	6
Equivalent (von-Mises) Stress (MPa)	526.32	311.02	222.18	171.88	144.38	121.1
Number of Cycle	1059	14783	83292	323720	1000000	1000000

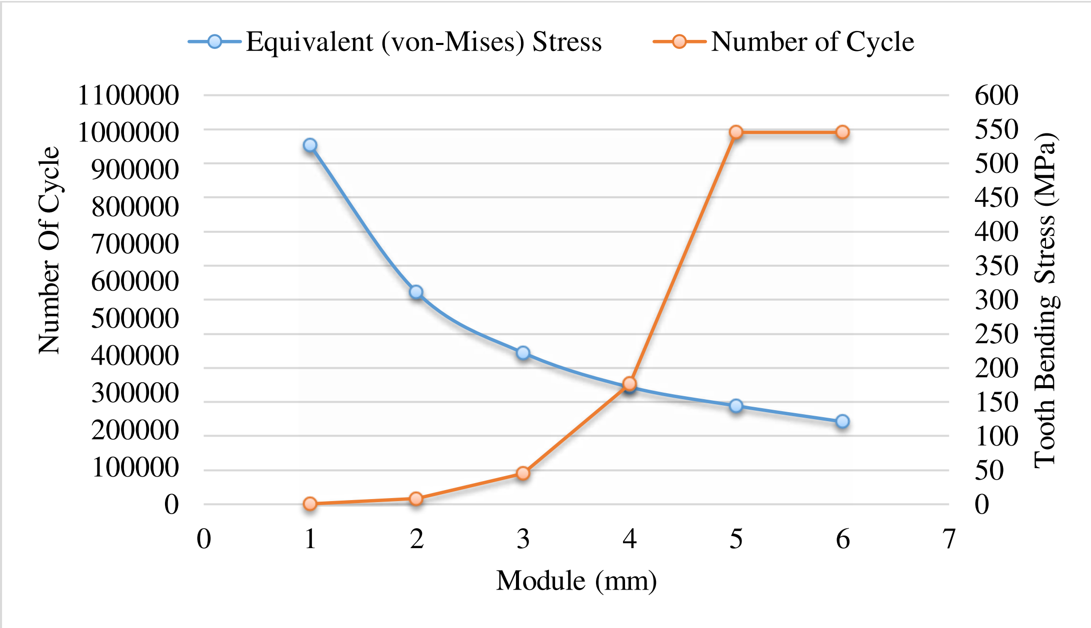

Figure 6.9 Tooth root stress and bending fatigue cycle for different modules

6.5 Effect of Addendum

In this case, the analysis results exhibited very different behavior as can be seen in Figure 6.10. Increasing the addendum up to 1.3*m the stress values decreased that's why number of cycle increased. In this case maximum principle stress values decreased also addendum 1.3*m unlike equivalent stress values given Table 6.8.

Table 6.8 Tooth bending stress and number of cycle for different addendum values

Case 5 (Load 4268)				
Addendum (mm)	1	1.1	1.2	1.3
Dedendum(mm)	1.4	1.4	1.4	1.4
Equivalent (von-Mises) Stress (MPa)	242.56	232.44	219.34	224.53
Maximum Principle Stress (MPa)	256.97	249.02	234.31	233.31
Number of Cycle	52529	69312	87892	79957

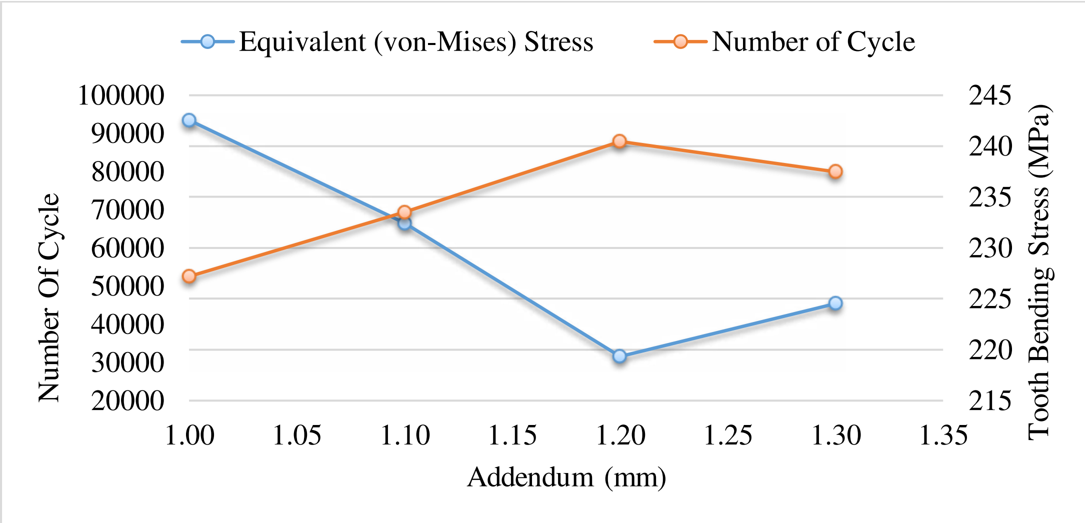

Figure 6.10 Tooth root stress and bending fatigue cycle for different addendum values

6.6 Effect of Tool Tip Radius Coefficient

In this section, five different tool tip radius coefficient (0.1, 0.2, 0.3, 0.38, and 0.47) were studied as seen Table 6.9. The stress values showed much variation in different models, but it was seen in figure 6.11 that number of cycle increased with the increment of the tool tip radius coefficient.

Table 6.9 Tooth bending stress and number of cycle for various tool tip radius coefficients

Case 6 (Load 4268)					
Tool Tip Radius Coefficient	0.1	0.2	0.3	0.38	0.47
Equivalent (von-Mises) Stress (MPa)	253.85	230.16	222.18	219.44	206.65
Number Of Cycle	46626	71880	83292	87798	114780

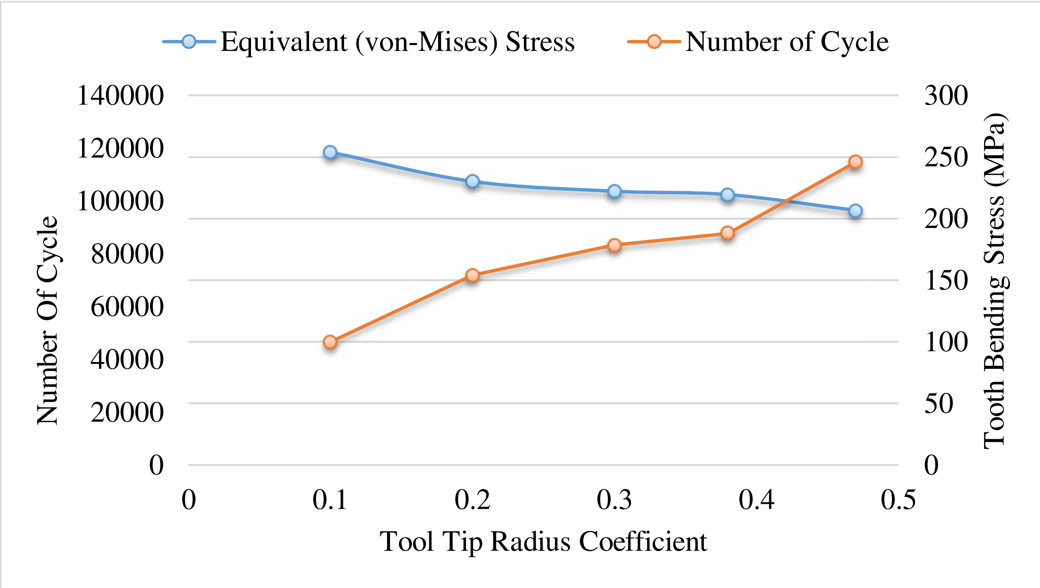

Figure 6.11 Tooth root stress and bending fatigue cycle for various tool tip radius coefficients

6.7 Effect of Rim Thickness

In this case, gear tooth models with various rim thicknesses (1.0*h, 1.5*h, 2.0*h,) were analyzed. It was seen in Figure 6.12 that at lowest bending stresses occurred in 2.5*m models. As can be seen from the graph, there was no linear connection in the variation of rim thickness with bending stresses as given table 6.10. Critical rim thickness and the effect of rim thickness on crack propagation direction were the subject of many studies [48, 49].

Table 6.10 Tooth bending stress and number of cycle for different rim thickness

Case 7 (Load 4268)			
Rim Thickness (mm)	1.0*h	1.5*h	2.0*h
Equivalent (von-Mises) Stress (MPa)	231.88	223.38	222.18
Number Of Cycle	69888	81651	83292

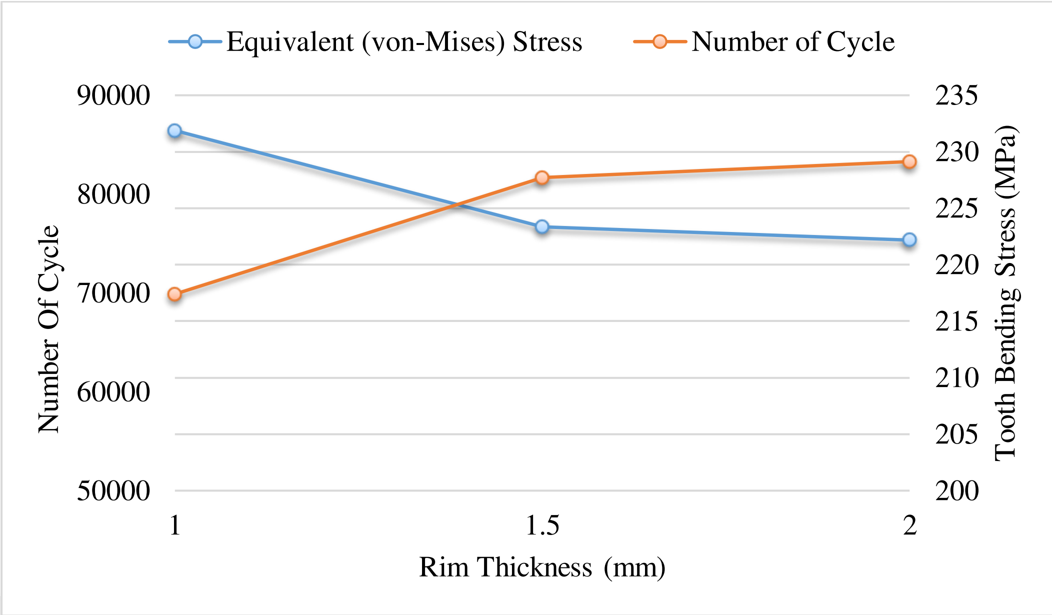

Figure 6.12 Tooth root stress and bending fatigue cycle for different rim thicknesses

6.8 Effect of Face Width

Tooth root stress and bending fatigue cycle for different face width values of (10, 20, 30, 40, 50, 60) was shown in Figure 6.13. With the change of face width, the bending stress formed in spur gears showed inverse proportionality between them, as the face width decreased with increased bending stresses as given Table 6.11.

Table 6.11 Tooth bending stress and number of cycle for different face width values

Case 8 (Load 4268)						
Face Width (mm)	10	20	30	40	50	60
Equivalent (von-Mises) Stress (MPa)	465.43	222.18	141.5	101.36	77.666	62.13
Number of Cycle	1787	83292	1000000	1000000	1000000	1000000

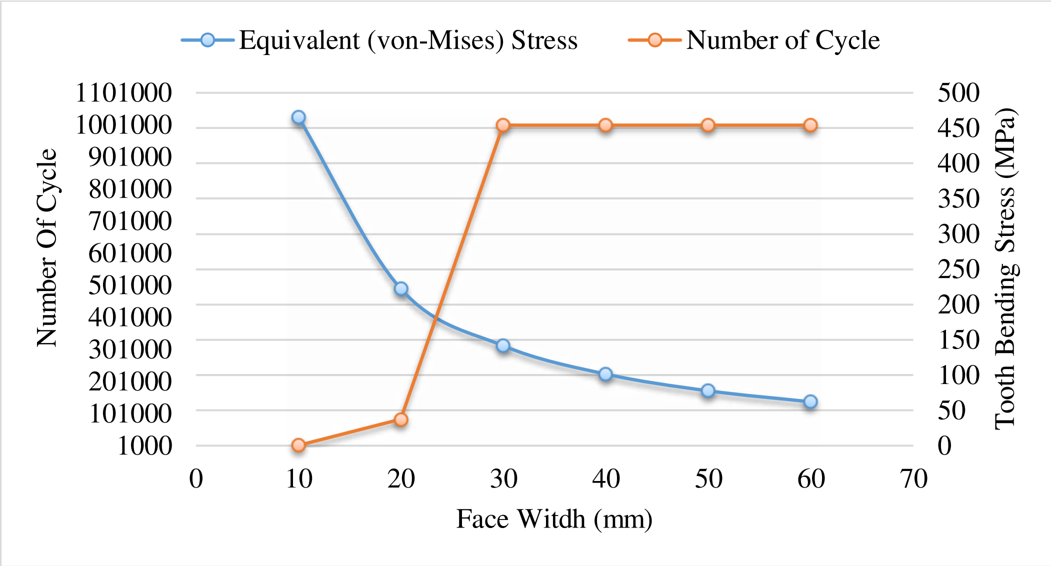

Figure 6.13 Tooth root stress and bending fatigue cycle for different face width values

CHAPTER 7

CONCLUSIONS AND RECOMMENDATIONS FOR FUTURE WORKS

7.1 Conclusions

The finite element method is used in many fields due to its flexibility and ease in modeling. That is why it is preferred in stress and bending fatigue analysis of gears as it is used in many fields. In this study, the method is indicated in the establishment of a finite element model, which accurately represent the stress intensity, and bending fatigue life in the root region, which is a characteristic feature of gearing problems. Complex tooth geometry is expressed based on hierarchical modeling. In the finite element method, the examination of the models, obtained in various modules with various boundary conditions provides information about increase in the fatigue life of the gear wheels. In this respect, the finite element method is a reliable method, which results in a short time.

In the study, gear wheels developed according to experience and gears models were created precisely in the finite element software. The tooth curve was formed according to involute profile and the trochoid form.

By evaluating these analyzes to determine the stress and bending fatigue lives of pairs of different spur gears, the following points can be concluded:

- FEM provides an excellent opportunity to calculate the reliable stress value on tooth root and the number of bending fatigue cycles that can be used as input in extended simulations. Static FEM analysis results are consistent with many studies in the literature.

- The S-N curve created based on the different load values applied allows us to determine the area of the gear to be used safely for the material used.

- In the gear model that was created with different tooth numbers, stress values decreased while increasing the teeth number that's why bending fatigue strength increased.

- The increase in pressure angle was resulted in significant increment in bending fatigue life cycles.

- In the analysis of gears that was modeled according to different modules, tooth root stresses decreased with increasing module value and consequently the fatigue cycle number increased.

- Increasing tool tip radius coefficient decreased tooth root stress and that seriously increased the number of bending fatigue cycles.

7.2 Future Works

- The finite element analysis presented here can also be developed for different type of gear models (Asymmetric, internal, helical gears, etc).
- These operating gear parameters can be analyzed under dynamic loads with the same condition.
- This FEA results can extent with the different gear parameters.
- Experimental analysis can be perform for all cases studied here and can be good comparison studies; experimental and FEA.

REFERENCES

[1] Bibel, G. D., Reddy, S. K., Savage, M., Handschuh, R. F. (1994). Effects of Rim Thickness on Spur Gear Bending Stress. *Journal of Mechanical Design*, ***116*(4),** 1157-1162

[2] Belsak, A., Flasker, J. (2007). Detecting Cracks in the Tooth Root of Gears. *Engineering Failure Analysis*, ***14*(8)**, 1466-1475.

[3] Jelaska, D. T. (2012*). Gears and Gear Drives*. John Wiley & Sons.

[4] Radzevich, S. P. (2012). *Dudley's Handbook of Practical Gear Design and Manufacture*. CRC Press.

[5] Fernandes, P. J. L. (1996). Tooth Bending Fatigue Failures in Gears. *Engineering Failure Analysis,* **3(3),** 219-225.

[6] Pehan, S., Hellen, T. K., Flasker, J., Glodez, S. (1997). Numerical Methods for Determining Stress Intensity Factors Vs Crack Depth in Gear Tooth Roots. *International Journal of Fatigue,* **19(10),** 677-685.

[7] Kramberger, J., Šraml, M., Potrč, I., Flašker, J. (2004). Numerical Calculation of Bending Fatigue Life Of Thin-Rim Spur Gears. *Engineering fracture mechanics*, ***71*(4-6),** 647-656.

[8] Fadhil, B. M. (2013). Crack Path Prediction of Gear Tooth with Different Pressure Angles -Numerical Study, *International Journal of Mechanical Engineering and Technology (IJMET).* 88-102.

[9] Zhang, X., Li, L., Qi, X., Zheng, J., Zhang, X., Chen, B., Duan, S. (2017). Experimental and Numerical Investigation of Fatigue Crack Growth in the Cracked Gear Tooth. *Fatigue & Fracture of Engineering Materials & Structures*, ***40*(7**), 1037-1047.

[10] Podrug, S., Glodež, S., Jelaska, D. (2011). Numerical Modelling of Crack Growth in a Gear Tooth Root. *Strojniški vestnik-Journal of Mechanical Engineering***, *57*(7-8**),579-586.

[11] Zhou, C., Li, Z., Hu, B., Zhan, H., Han, X. (2017). Analytical Solution to Bending and Contact Strength of Spiral Bevel Gears in Consideration of Friction. *International Journal of Mechanical Sciences*, ***128*, **475-485.

[12] Hotait, M. A., Kahraman, A. (2013). Estimation of Bending Fatigue Life of Hypoid Gears Using a Multiaxial Fatigue Criterion. *Journal of Mechanical Design*, ***135*(10),** 101005.

[13] Kumar, P., Hirani, H., Agrawal, A. (2017). Fatigue Failure Prediction in Spur Gear Pair Using AGMA Approach. *Materials Today: Proceedings*, ***4*(2),** 2470-2477.

[14] Handschuh, R. F., Krantz, T. L., Lerch, B. A., Burke, C. S. (2007, January). Investigation of Low-Cycle Bending Fatigue of AISI 9310 Steel Spur Gears. In *ASME 2007 International Design Engineering Technical Conferences and Computers and Information in Engineering Conference* (pp. 871-877). American Society of Mechanical Engineers.

[15] Gasparini, G., Mariani, U., Gorla, C., Filippini, M., Rosa, F. (2008). Bending Fatigue Tests of Helicopter Case Carburized Gears: Influence of Material, Design and Manufacturing Parameters. *In American Gear Manufacturers Association (AGMA) Fall Technical Meeting* (pp. 131-142).

[16] Conrado, E., Gorla, C., Davoli, P., Boniardi, M. (2017). A Comparison of Bending Fatigue Strength of Carburized and Nitrided Gears for Industrial Applications. *Engineering Failure Analysis*, ***78*, **41-54.

[17] Gorla, C., Rosa, F., Conrado, E., Concli, F. (2017). Bending Fatigue Strength of Case Carburized and Nitrided Gear Steels for Aeronautical Applications. *International Journal of Applied Engineering Research,* **12(21),** pp11306-11322

[18] Glodež, S., Pehan, S., Flašker, J. (1998). Experimental Results of the Fatigue Crack Growth in a Gear Tooth Root. *International Journal of Fatigue*, ***20*(9),** 669-675.

[19] Kramberger, J., Šraml, M., Glodež, S., Flašker, J., Potrč, I. (2004). Computational Model for the Analysis of Bending Fatigue in Gears. *Computers & structures*, ***82*(23-26),** 2261-2269.

[20] Jyothirmai, S., Ramesh, R., Swarnalatha, T., Renuka, D. (2014). A Finite Element Approach to Bending, Contact and Fatigue Stress Distribution in Helical Gear Systems. *Procedia materials science*, **6**, 907-918.

[21] Lewicki, D. G., Handschuh, R. F., Spievak, L. E., Wawrzynek, P. A., Ingraffea, A. R. (2001). Consideration of Moving Tooth Load in Gear Crack Propagation Predictions. *Journal of mechanical design*, ***123*(1),** 118-124.

[22] Vučković, K., Galić, I., Božić, Ž., Glodež, S. (2018). Effect of Friction in A Single-Tooth Fatigue Test. *International Journal of Fatigue*, ***114*,** 148-158.

[23] Deng, S., Hua, L., Han, X. H., Huang, S. (2013). Finite Element Analysis of Contact Fatigue and Bending Fatigue of a Theoretical Assembling Straight Bevel Gear Pair. *Journal of Central South University*, ***20*(2),** 279-292.

[24] Curà, F., Mura, A., Rosso, C. (2017). Influence of High Speed on Crack Propagation Path in Thin Rim Gears. *Fatigue & Fracture of Engineering Materials & Structures*, ***40*(1),** 120-129.

[25] Zhang, D., Liu, S., Liu, B., Hong, J. (2013). Investigation on Bending Fatigue Failure of a Micro-Gear through Finite Element Analysis. *Engineering Failure Analysis*, ***31***, 225-235.

[26] Kramberger, J., Potrc, I., Flašker, J. (2002). Prediction of 3-D Crack Growth in Thin Rim-Gears. In *DS 30: Proceedings of DESIGN 2002, the 7th International Design Conference, Dubrovnik* (pp. 1193-1198).

[27] Ghaffari, M. A., Pahl, E., Xiao, S. (2015). Three Dimensional Fatigue Crack Initiation and Propagation Analysis Of A Gear Tooth Under Various Load Conditions And Fatigue Life Extension With Boron/Epoxy Patches. *Engineering Fracture Mechanics*, ***135*,** 126-146.

[28] Amiri Rad, A., Forouzan, M. R., Sadeghi D. A. (2014). Three-Dimensional Fatigue Crack Growth Modelling In a Helical Gear Using Extended Finite Element Method. *Fatigue & Fracture of Engineering Materials & Structures*, ***37*(6)**, 581-591.

[29] AGMA, AGMA Technical Committee. (1995). Appearance of Gear Teeth: Terminology of Wear and Failure. *American Gear Manufacturers Association*, ***40*.**

[30] Errichello, R. (1992). Friction, Lubrication, and Wear of Gears. *Materials Park, OH: ASM International, 1992,* 535-545.

[31] Davis, J. R. (Ed.). (2005). *Gear materials, properties, and manufacture*. ASM International.

[32] Akhoroz, E. (1999). *ANSYS programı ile dizayn optimizasyonu* (Doctoral dissertation).

[33] OLGIERT, C. Z. (1971). *The finite element method in engineering science*. McGraw-Hill.

[34] Kurtay, T., 1987,"Finite Element Method", Y. Lisans Ders Notları, İ.T.Ü., Makine Fakültesi, İstanbul.

[35] Fetvacı, C. (2001). *Düz Dişli Çarkların Sonlu Elemanlar Metodu İle Modellenmesi Ve Gerilmelerin İncelenmesi* (Doctoral dissertation).

[36] Erkoç, C. N. (2000). *Autocad ve ANSYS Yazılımlarını Kullanarak Mil Tasarımı* (Doctoral dissertation).

[37] Erdem, S. S. (1996). *Dişli Çarklarda Diş Üzerinde ANSYS Sonlu Elemanlar Paket Programıyla Gerilme Analizi* (Doctoral dissertation).

[38] Yıldız, S. (2005). Dişli Çarkların Bilgisayar Destekli Analizi.

[39] Şahin, B. (2015). Development Of User Friendly Interface Software For Design And Analysis Of Parallel Axes External Gears Including Quasi-Static Transmission Error Calculations, Master Thesis, University of Gaziantep.

[40] Sahin, B., Akpolat, A., Yildirim, O., Uctu, O., Ersoz, A. (2014). Development of a User Friendly Interface for Design and Analysis of Parallel Axes Gears Based on International Standards Including Quasi Static Transmission Error Curves. In *International Gear Conference, Lyon* (pp. 395-405).

[41] Akkurt, M., 1982, "*Makine Elemanları – Güç ve Hareket İletim Elemanlari*", Birsen Yayınları, Cilt III, İstanbul

[42] Chabert, G., Tran, T. D., Mathis, R. (1974). An Evaluation of Stresses and Deflection of Spur Gear Teeth under Strain. *Journal of Engineering for Industry*, ***96*(1)**, 85-93.

[43] Wilcox, L., Coleman, W. (1973). Application of Finite Elements to the Analysis of Gear Tooth Stresses. *Journal of Engineering for Industry*, ***95*(4),** 1139-1148.

[44] Budynas, R. G. (1999). *Advanced Strength and Applied Stress Analysis*. McGraw-Hill.

[45] Mottram, J. T., Shaw, C. T. (1996). *Using Finite Elements in Mechanical Design*. London: McGraw-Hill.

[46] Mendi, F., Başkal, T., Boran, K., Boran, F. E. (2010). Optimization of Module, Shaft Diameter and Rolling Bearing for Spur Gear through Genetic Algorithm. *Expert Systems with Applications*, ***37*(12),** 8058-8064.

[47] Mendi, F., Baskal, T., Külekci, M. K. (2012). Application of Genetic Algorithm (GA) for Optimum Design of Module, Shaft Diameter and Bearing for Bevel Gearbox. *Materials Testing*, ***54*(6),** 431-436.

[48] Bibel, G. D., Reddy, S. K., Savage, M., Handschuh, R. F. (1994). Effects of Rim Thickness on Spur Gear Bending Stress. *Journal of Mechanical Design*, **116(4)**, 1157-1162.

[49] Lewicki, D. G., Ballarini, R. (1997). Effect of Rim Thickness on Gear Crack Propagation Path. *Journal of Mechanical Design*, **119(1),** 88-95.

[50] ISO 6336-5:2003(E), *Calculation of Load Capacity of Spur and Helical Gears - Part 5: Strength and Quality of Materials*, 2003.

[51] ISO 6336-3:2006(E), *Calculation of Load Capacity of Spur and Helical Gears - Part 3: Calculation of Tooth Bending Strength*, 2006.